GENOME-WIDE PHARMACOLOGICAL MODULATION OF CAP-DEPENDENT TRANSLATIONAL CONTROL

A DISSERATION
SUBMITTED TO THE FACULTY OF
THE UNIVERSITY OF MINNESOTA
BY

JEFFREY JOSEPH BRAZIUNAS

IN PARTIAL FULFILLMENT OF THE REQUIREMENTS
FOR THE DEGREE OF
DOCTOR OF PHILOSOPHY

ADVISOR: PETER B BITTERMAN, MD

DECEMBER 2013

Acknowledgements

Completing my doctorate degree would not have been possible without the personal and professional support of a great many people, some of whom I would like to acknowledge here, and greatly thank for their perpetual support and encouragement over the past six years.

First I must thank my advisor, Dr. Peter B Bitterman. As I experienced the culture of other labs during rotations I was struck by the vibe you have cultivated in your lab. I never considered heading into lab "work", as I thoroughly enjoyed my time there. Your positive upbeat attitude is absolutely infectious, and definitely helped me through some of the tougher times as your door was always open. I hope to emulate your charisma as someone who can command a room with mere presence, and nary a word. Through your steady tutelage I have learned the art of grant and manuscript writing and I believe that you are unmatched in formulating *and conveying* complex concepts; whether they are scientific, cultural, or simply mundane. I consider my selection of Peter to be my advisor as the best decision I made in graduate school, and heartily recommend his lab to incoming graduate students. Thank you for accepting me into your lab, and mentoring me all the way to today, and tomorrow.

To the members of the Bitterman / Polunovsky lab: First off Dr. Matthew Parker, who brought knowledge of physics and computational biology without which this project

would not have been possible. In fact, he should be considered a co-first author on the work presented in chapter 2. I also enjoyed many discussions of fantasy (and “real” life) football with Matt and Mark Peterson, who served as the lab father, so to speak. Mark, you have meticulously taught me so many transferrable lab skills (well maybe not make your own Westerns), and I thank you for your patience in mentoring me. Oh, and for getting me hooked on this fine wine stuff too… Dr. Jose Gomez and Jeremy Herrera – I must thank you for many weekend media changes and your constant support and encouragement as we all traveled down this graduate student road together.

Dr. Karen Smith – thank you for helping me out with a construct whenever I needed it. Your molecular biology knowledge is absolutely amazing and you sped my work immensely. Dr. Vitaly Polunovsky, Dr. Svetlana Avdulov, and Dr. Alexey Benyumov – thank you for your assistance in shaping my research through much needed stern critiques in many a lab meeting. Thank you all!

To former graduate students: Dr. Yong Kim and Dr. Mike Underwood: You laid the foundation for much of my work (especially chapter 3), and I wouldn’t have been successful without your encouragement and assistance in my early studies.

I would also like to acknowledge the members of my dissertation committee: Peter Bitterman MD, Carston R Wagner PhD, Douglas Yee MD, and the chair Hiroshi Hiasa,

PhD. Your continued input and collaboration have helped mold this thesis into its successful form today.

The pharmacology program has also greatly shaped my understanding of science and is now the unfortunate reason I must explain the difference between pharmacology and pharmacy at least a few times a year. I want to especially thank Dr. Jonathan Marchant, who responded to my constant stream of e-mails as I pestered him with questions about the University of Minnesota's Pharmacology program. I am immensely grateful for his generosity, as I cannot imagine being more pleased with my decision to apply and attend here. I also want to thank everyone in the office and elsewhere in the department who helped guide me along my path to defending this thesis.

Finally I absolutely must acknowledge the love and support of my family, especially my wife. Without her constant patience and understanding I never would have succeeded in this endeavor. After a hard day in the lab after yet another unsuccessful experiment I always cheered up after arriving home to her smiling visage. Of course having an amazing home-cooked meal waiting for me when I arrived home (at whatever time that happened to be – sorry for that!) was a definite plus! Now that we have completed this doctoral journey together, I realize how absolutely blessed we have been surrounded by such wonderful colleagues, family, and friends. Thank you all!

Dedication

This thesis is dedicated to my parents as their steady love and encouragement all through my long and winding road has allowed me to flourish personally and professionally.

With Love,

Your Son

Abstract

The first step of cap-dependent translation is mediated by the mRNA cap-binding protein eukaryotic initiation factor 4E (eIF4E). Although involved in translating nearly all cellular transcripts, mRNAs vary widely in their translational response to eIF4E activity changes. Prior studies of mRNA structure revealed several features governing eIF4E responsiveness; however, most of this knowledge is based on comparison of two levels of eIF4E activity with unclear physiological relevance. To identify mRNA structural features that govern genome-wide ribosome recruitment across a full range of physiological eIF4E activities, we precisely modulated eIF4E activity using an eIF4E-inducible system together with 4Ei-1, an inhibitor of the eIF4E-5'mRNA cap association. We identified genes that were more (4E hypersensitive) or less (4E hyposensitive) responsive to eIF4E activity changes than average. Distinct characteristics associated with each class: 4E hypersensitive genes had longer 5'UTRs with higher GC content, longer 3'UTRs with lower GC content; more AU-rich elements and a higher density of unique microRNA targets sites than typical genes. Importantly, these structural characteristics predicted the translational response across the dose range of 4Ei-1. Gene ontology analysis showed an association between 4E hypersensitive genes and proliferation; and cell cycle experiments with 4Ei-1 validated this result. A search for the outcome and mechanism of this proliferative gene activation in a physiological setting revealed that abrupt gain of eIF4E function in quiescent cells first triggers G_0 exit and

then cell cycle transit at least partially by increasing ribosome recruitment to cyclins C and D1. Whereas cyclin C is not necessary for this effect; cyclin D1 is indispensable, although not sufficient. Our findings provide important insights into mRNA properties of eIF4E-modulated translational control.

Table of Contents

List of Tables

Page

List of Figures

Page

Chapter 1 THESIS INTRODUCTION

Multiple mechanisms regulate eukaryotic gene expression

Eukaryotic gene expression is a multistep progression of transcription, translation, and eventual degradation of messenger RNAs and proteins. This progression is coordinated by several regulatory nodes arrayed in a series. Genomic, transcriptional, and posttranslational regulatory mechanisms are well established. However, it is now increasingly recognized that gene expression is also subject to translational control. Highlighting this trend, a recent comprehensive analysis of mammalian gene expression published in *Nature* concluded that "*the cellular abundance of proteins is predominately controlled at the level of translation*" (1).

As with all other major cellular processes, this process of converting mRNA into protein is regulated at multiple stages. These include translation initiation, elongation, termination, and mRNA turnover/stability. This thesis provides important insights into the structural and functional mRNA properties of translation controlled at the level of initiation by eukaryotic initiation factor 4E (eIF4E).

Cap-dependent translation

In eukaryotes, translational occurs almost exclusively through two mechanisms termed cap-dependent and cap-independent translation, although some mRNAs blur these

boundaries (2). Although a small subset of mRNAs can be translated in a cap-independent method through direct contact of the translational machinery with their internal ribosome entry site (IRES), under most physiological conditions the vast majority of mRNAs are translated utilizing cap-dependent translation. The “cap” refers to the 5’ mRNA structure m^7GpppN, where m^7G is 7-methylguanosine and N is the first nucleotide of mRNA (3). This cap is crucial for the efficient translation of the majority of cellular mRNAs and is required for cap-dependent translation initiation (4).

Translation initiation is a key regulatory hub

Initiation of cap-dependent translation functions as a key regulatory hub in the gene expression pathway. Translation rates are modulated by a variety of environmental signals including growth factors, nutrient availability, and stress (5, 6). These modulations lead to outcomes ranging from apoptosis to cell cycle progression and cell growth (5, 7). Because of the profound effects that translation can have on cellular functions, translation is tightly controlled primarily at the level of initiation (8).

eIF4E binds to the m^7G 5’-cap of mRNA

Availability of active eukaryotic initiation factor 4E (eIF4E) is believed to be rate limiting for cap-dependent translation (9). eIF4E is an evolutionary conserved 25kDa polypeptide which specifically recognizes and directly binds to the 5’ mRNA cap (10). The mechanism

of binding occurs either through a one or two step process, which seems to depend on temperature and the relative availability of eIF4E and cap (11, 12). In either model, the binding of the cap structure to eIF4E is the defining event in cap-dependent translation and therefore represents a target for pharmacological intervention in translational control (13, 14).

eIF4E as discussed in this thesis is more preciously termed eIF4E1, and is the most characterized member of the eIF4E protein family. Other members include eIF4E1b, eIF4E2 (also known as 4EHP), and eIF4E3 (15). As these three eIF4E proteins exhibit as much as 200-fold weaker affinities for the mRNA cap; they are functionally distinct from eIF4E1 in gene regulation, oncogenic capacity, and binding partner specificity (16-18).

Assembly and function of the eIF4F complex

eIF4E1 (hereafter termed eIF4E or 4E), is a member of the heterotrimeric initiation complex eIF4F which also includes the scaffolding protein eIF4G and the RNA helicase eIF4A. The eIF4A component of the eIF4F complex functions to unwind secondary structures in the 5' untranslated region (UTR) of mRNA to reveal the initiation codon and facilitate ribosome loading (19). Poly(A) binding protein (PABP) also interacts with the docking protein eIF4G and can mediate the formation of a "closed-loop" circular messenger ribonucleoprotein (mRNP) complex by linking the cap and the poly(A) tail, thereby stimulating translation by enhancing the recycling of ribosomes on the mRNA

(4, 20). A simplified model focusing on eIF4E/eIF4F activity is shown here (Figure 1-1 from (21)), but a more complete overview of the current knowledge of cap-dependent translation initiation and translational control is reviewed in (22). Briefly, the eIF4G component of the eIF4F complex bridges the mRNA to the 40S ribosomal subunit through the eIF3 adapter complex, the largest scaffolding initiation factor which is composed of 13 subunits. At this stage the 40S subunit is also complexed with eIF3, eIF1A, eIF1, eIF2, and a loaded Met-tRNA to form the 48S complex. Once this complex is bound to mRNA, eIF4A unwinds mRNA secondary structure as the complex scans the 5'UTR of the attached mRNA in the 5' to 3' direction until an initiation codon in the proper sequence context is encountered. When the initiation codon is recognized, eIF5 and eIF5B promote the hydrolysis of eIF2-bound GTP, which results in the displacement of the initiation factors and allows the joining of a 60S ribosomal subunit. This changes the conformation of the attached ribosome, marks the end of translation initiation and the start of elongation, and allows protein synthesis to continue.

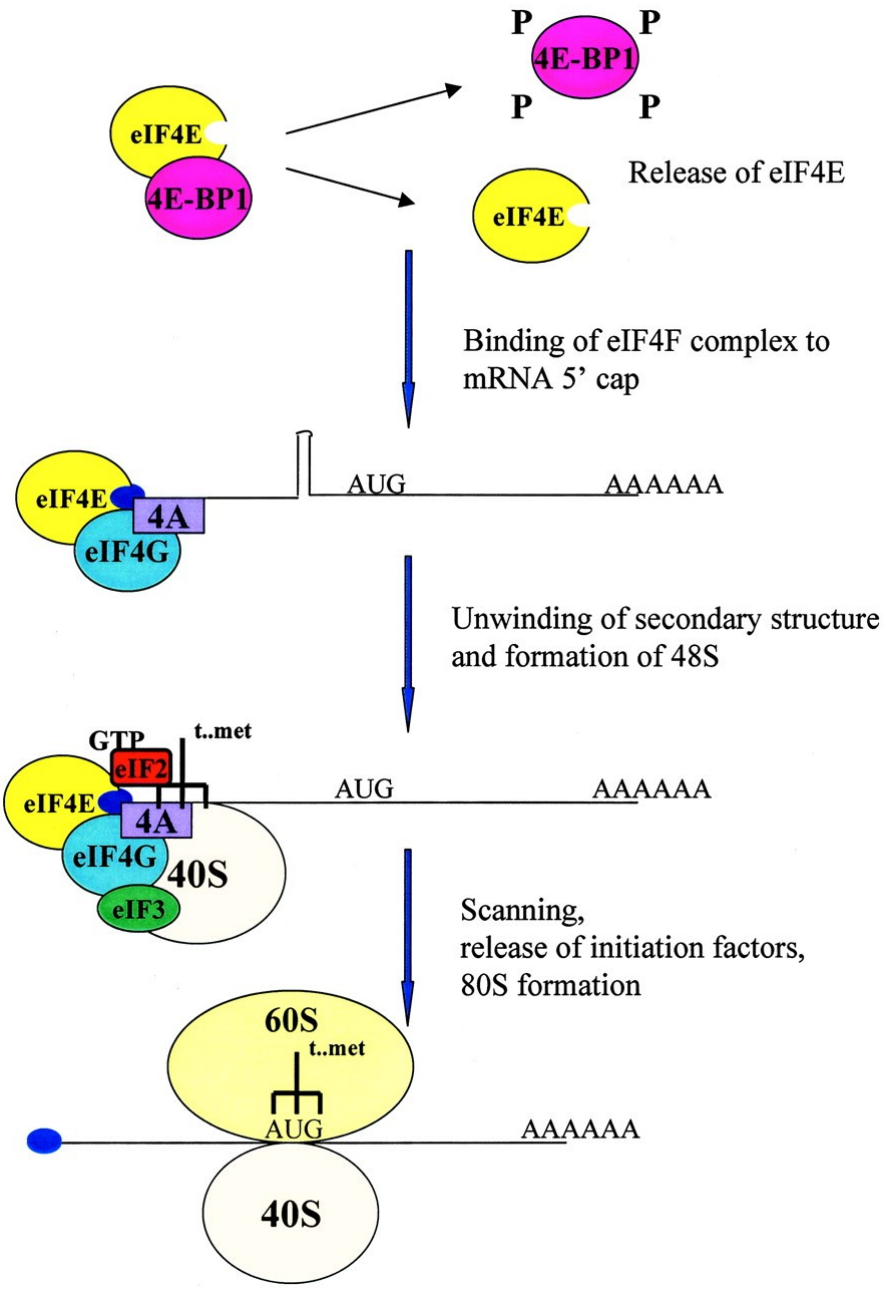

Figure 1-1 Cap-Dependent Translation Overview

Shown is a simplistic model overview of cap-dependent translation. Note that PABP, which circularizes the mRNA by binding to the poly(A)-tail and the mRNA cap, is not shown. *This figure has been reprinted with kind permission from the American Association for Cancer Research.*

Cap-independent translation - IRES

The most common form of cap-independent translation is mediated by an internal RNA structure called an internal ribosome entry site (IRES), which recruits the ribosome independent of both the cap and the eIF4F complex and allows translation to proceed (23). IRES-mediated translation is used by some viruses but also exists on ~100 eukaryotic cellular mRNAs, functioning in times of stress or in development when cap-dependent translation is minimized (24). Although there are recent reports linking IRES-mediated translation with cancer (25-27), deregulation of cap-dependent translation has a more established role in cancer.

Translational control is corrupted in cancer

The regulation and control of translation factors is critical in cancer genesis and development. Aberrant eIF4E overexpression causes resistance to apoptosis (28), increased proliferation (29) and transformation (30-32) in multiple cell lines including NIH3T3 fibroblasts. Consistent with regulation of these key cancer hallmarks, increased eIF4E activity has been detected in a multitude of human malignancies including lung, breast, colon, bladder, prostate and gastrointestinal cancers; head and neck squamous cell carcinoma, fibrosis, lymphomas, leukemias and neuroblastomas, where high eIF4E activity correlates with disease progression and poor clinical outcome (33, 34). This

suggests that eIF4E functions as an oncogene by specifically modulating the translation of key proteins which are beneficial for the cancer phenotype.

eIF4E selectively targets a subset of mRNAs

Although eIF4E is necessary for efficient translation of almost all cellular mRNAs, changes in eIF4E activity in the physiological range only modestly affect the translation of most mRNAs (33) while having a major effect on a subset of mRNAs designated 4E-sensitive (35). Initial studies characterized this subset as containing long, highly structured and complex 5' UTRs with relatively high G+C base pair content (hereafter called GC content), rendering these transcripts strongly dependent on the unwinding activity of the eIF4A helicase (36), as genes with relatively long and structured 5'UTRs are translated less efficiently (37). This has been corroborated by several single-gene and mechanistic studies where long and highly structured 5'UTRs mediated 4E-sensitive translation. mRNAs with relatively long and structured 5'-UTRs which are sensitive to eIF4E include ornithine decarboxylase (38), ornithine aminotransferase (39), cyclin D1 (40), 3-hydroxy-3-methylglutaryl coenzyme A (HMG-CoA) reductase (41), ribonucleotide reductase (42), and vascular endothelial growth factor (VEGF) (43). These key translationally regulated genes are then capable of altering the cellular phenotype.

Regulation of eIF4E activity

Due to the oncogenic capacity of eIF4E, its physiological activity is tightly regulated. The cells "eIF4E activity level" can be defined as the sum effect on translation initiation of eIF4E's: total protein abundance, percentage of that eIF4E functionally available after accounting for regulatory binding to eIF4E regulatory proteins, phosphorylation state, and subcellular localization.

4E-BPs and the mTOR pathway

The activity of eIF4F is negatively regulated by the eIF4E-binding proteins (4E-BPs), a family of translation repressor proteins which compete with eIF4G for a common binding site on eIF4E (44) and thereby prevents formation of the eIF4F complex. The 4E-BPs are themselves regulated by intracellular signaling including the mTOR pathway (45). The mTOR (mammalian target of rapamycin) kinase is the catalytic subunit of two molecular complexes: mTORC1 and mTORC2. The mTOR pathway regulates cell growth and division by simultaneously sensing energy, nutrients, and stress and is critically involved in tumorigenesis (Figure 1-2 from (46)). mTORC1 indirectly regulates protein synthesis by phosphorylating the 4E-BPs leading to their release from eIF4E which is then free to form the eIF4F complex and initiate translation. mTORC1 and to a lesser extent mTORC2 can also be inhibited by the compound rapamycin (47, 48).

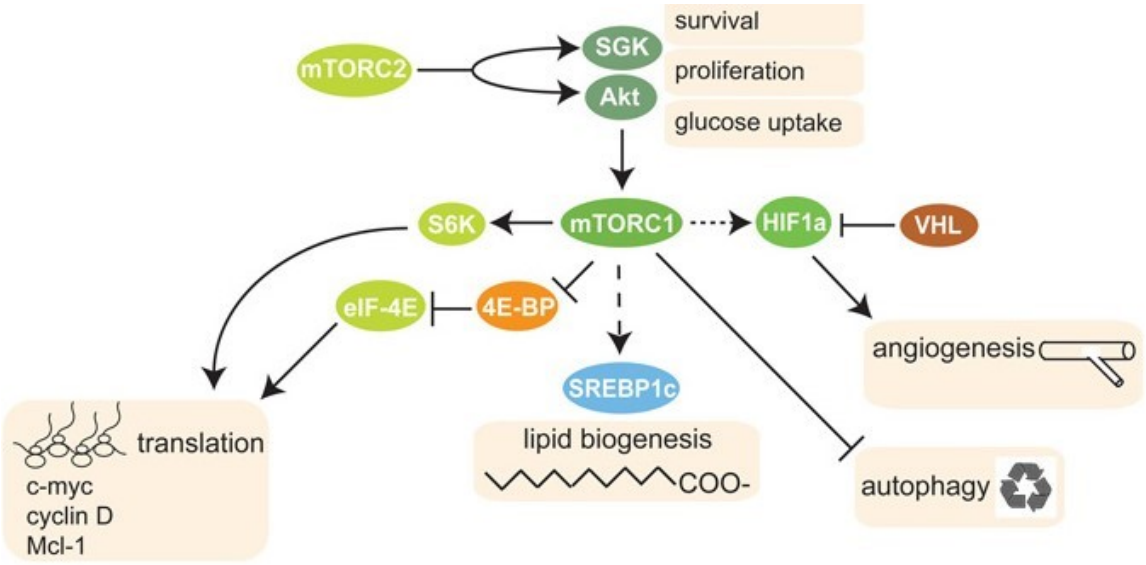

Figure 1-2 mTOR-regulated processes are involved in cancer.

mTOR complex 1 (mTORC1) favors tumor genesis and maintenance of the cancer phenotype by driving the translation of oncogenes by relieving 4E-BP1-mediated inhibition of eIF4E via phosphorylation of the 4E-BPs, by inhibiting autophagy, by upregulating hypoxia-inducible factor 1α (HIF1α) to increase angiogenesis, and by enhancing the accumulation of lipids by activating the transcription factor sterol regulatory element binding protein 1c (SREBP1c). mTORC2 also plays a part in tumorigenesis by activating Akt and other AGC family proteins, such as serum- and glucocorticoid-regulated kinase (SGK), thereby promoting cellular proliferation and survival. Furthermore, by promoting Akt-mediated glucose uptake and utilization, mTORC2 fuels the increased metabolism rate of cancer cells. *This figure has been reprinted with kind permission from Nature Publishing Group.*

c-Myc

The c-myc (Myc) oncogene is the prototypical member of the Myc/Max/Mad transcription factor network, which regulates 15% of all genes and such divergent cellular functions such as protein biosynthesis, proliferation, apoptosis, differentiation, and energy metabolism (49). Myc can stimulate protein synthesis by up-regulating eIF4F activity (50). Up-regulation occurs as the transcription factor Myc regulates the total cellular abundance of all members of the eIF4F complex; eIF4E (51), eIF4A (52), and eIF4G (52). Together these proteins also exert an oncogenic effect as overexpression of eIF4E and Myc abolishes the apoptotic effect of Myc and pushes cellular proliferation (28, 32). In addition, eIF4E is able to increase Myc expression as Myc is also one of the first identified 4E-sensitve mRNAs (53), or a reduction of eIF4E expression decreases Myc expression (54). This data outlines a positive feed forward loop between increasing Myc and eIF4F expression and provides another potential molecular mechanism for the oncogenic capacity of Myc and eIF4E (55).

Mnks

eIF4E is also regulated by phosphorylation, although exactly how this effects function varies in normal and malignant tissue. Activation of the ERK and p38 MAP kinase pathways elicits phosphorylation of Mnk1, which is recruited by eIF4G, and then activated Mnk1 phosphorylates eIF4E at s209 (56, 57). Mnk2 constitutively

phosphorylates eIF4E and is not inducible under normal physiological conditions (58), although the mTOR inhibitor rapamycin may induce eIF4E phosphorylation through Mnk2a (59). Although eIF4E phosphorylation increases oncogenic transformation and mRNA transport (60), this phosphorylation is not required for cellular proliferation and translation under physiological conditions (61); thereby making the Mnks an attractive target for pharmacological intervention in cancer (62). Even though the direct effect of eIF4E phosphorylation on its cap binding affinity are still being debated (33), and it may play an *in vivo* role by suppressing the innate antiviral response (63); eIF4E phosphorylation does not appear to play a *major* role in the physiological regulation of translational control and development (62).

Summary

Control of cap-dependent translation initiation is a critical hub for regulation of physiological cellular growth and is regularly usurped in cancer. This hub is principally regulated through the pleiotropic functions of the 5' mRNA cap-binding protein eIF4E. eIF4E regulates cell growth on multiple levels and is believed to selectively translationally regulate a subset of mRNAs with long and highly structured 5'UTRs which are also critically involved in oncogenic functions. The regulation of eIF4E is complex and occurs on multiple levels: availability to form the eIF4F complex through inhibitory binding by the 4E-BPs and other regulatory proteins, protein abundance through a feed-forward loop with Myc, and transformative capability through phosphorylation by the Mnks. Therefore the pharmacological targeting of specific eIF4E interactions allows targeting of eIF4E function at multiple levels, and the dose-dependent inhibition of a specific interaction allows a detailed exploration of that function of eIF4E.

Rationale and purpose of study

No previous studies have systematically examined translation genome-wide across the physiological range of eIF4E activity. Consequently, the aims of the study are as follows: (a) categorize genes based upon their translational requirement for eIF4E activity, (b) define the structural characteristics of 4E-sensitive genes, and (c) define a molecular mechanism for eIF4E-induced cell cycle progression.

Chapter 2 : Structural features of eIF4E hypersensitive mRNA translation are revealed by combining induction and chemical antagonism of eIF4E

Introduction

Translational control can be analyzed via microarray-polysomal analysis

Pathological translational control manifests as a genome-wide reorganization of ribosome recruitment to mRNA and has been analyzed primarily in the context of established cancers. With the emergence of genome wide approaches to measure gene expression the hypothesis that long and highly structured 5'UTRs mediates pathological 4E-sensitive translation was tested at a genome wide level. Early such studies used combined polysome-microarray analysis (64) to characterize the genome-wide effects of constitutively overexpressed eIF4E (65, 66), deleted 4E-BP1/2 (67), or induced overexpression of eIF4E (35). None of these studies directly identified a pattern where long 5'UTRs with high GC-content were enriched among genes showing 4E-sensitive translation. However, 4E-sensitive mRNAs did show a microRNA binding bias in their

3’UTRs, and microRNAs are known to influence translation by direct inhibition of the 5’ cap recognition step (68).

Limitations of previous systems

Although prior studies characterized eIF4F sensitive genes in a variety of settings, the applicability of their results is restricted by scope. These studies were limited by potential indirect effects and counter regulation arising from long term culturing with constitutively active eIF4E (66) and/or by modulating eIF4E activity to a single high level which is outside the physiological expression range observed in rapidly proliferating cells (69). Another limitation of these studies is that all of them altered eIF4F activity using a single on/off intervention and did not precisely titrate eIF4E activity or alter its cap binding function. As a result these studies may have identified ample numbers of false positives among the 4E-sensitive genes which may have obscured the association with long and 5’ UTRs and high GC contents. More recently, two studies using the recent ribosome profiling technique to measure translation genome-wide completely challenged the role of the 5’UTR in 4F-sensitive translation when suggesting that inhibition of mTOR using chemical agents suppressed translation of a subset of genes with short 5’UTRs in a 4E-BP dependent manner (70, 71). These studies utilized a single dose of an mTOR inhibitor to depress hyperactivated translation in the context of prostate cancer and cultured cells in full growth media and did not analyze 3’UTR

characteristics. Furthermore, their 5'UTR observations may have been confounded by other mechanisms downstream of mTOR and as a result may not reflect 4E-sensitive translation. It was therefore important to complement this data by directly studying the effect on translation induced by differential eIF4E activity in the physiological range.

Our system mimics physiological fluctuations in eIF4E activity

We reasoned that a more measured approach could be required to understand the biological effects of dynamic changes in physiological eIF4E activity on 4E-sensitive translation. eIF4E abundance is tightly tuned to metabolic needs and fluctuates over the course of a cell cycle: scarce in quiescent cells, rising sharply in response to growth factors and peaking at the late G_1 restriction point (69, 72). We therefore developed a model system allowing precise and rapid control of eIF4E activity within the physiological expression range by concurrently modulating eIF4E activity in quiescent cells using an inducible eIF4E protein expression system and the eIF4E inhibitor 4Ei-1. The stable, nontoxic tryptamine phosphoramidate prodrug 4Ei-1, which was used over a wide concentration range to allow studies of dose-dependent regulation, is activated intracellularly by histidine triad nucleotide binding protein 1 (HINT1). The resulting active compound 7-benzyl guanosine monophosphate (7-BnGMP) competitively and directly inhibits the association of eIF4E with the 5'-mRNA cap in a dose-dependent manner (73). Using this dual-mechanism system, we studied ribosome recruitment to

mRNA genome-wide as a function of eIF4E activity and identified structural characteristics of the 5'UTRs and 3'UTRs of 4E-sensitive transcripts.

Summary

We modulated eIF4E activity at two levels: total protein abundance and the percentage of that eIF4E available to bind the 5'mRNA cap after accounting for binding to the 5'mRNA cap analogue 7-BnGMP. We identified genes that were more (4E hypersensitive) or less (4E hyposensitive) responsive to eIF4E activity changes than average. Here we show that structural characteristics of 4E hypersensitive (previously termed 4E-sensitive) transcripts (relative to typical genes) indeed include greater length and higher GC content of the 5' UTR. In addition 4E-hypersensitive genes have longer 3'UTRs with lower GC content and higher microRNA target site density. Moreover, in accordance with the established role of eIF4E activity in cell cycle progression, analysis of eIF4E hypersensitive mRNAs revealed enrichment for proliferation related genes and functional studies showed 4Ei-1 inhibited cell cycle transit in a dose-dependent manner. Thus 4E-sensitive translation depends on structural features of the 3' and 5' UTRs and does not associate with short 5' UTRs.

Results

An in vitro model for precise modulation of eIF4E activity.

To allow studies on how precisely tuned eIF4E activity impacts ribosome recruitment, we developed an inducible system in which expression of the rate limiting component of eIF4F, eIF4E, is induced with the progesterone antagonist mifepristone (MIF). To facilitate its detection, the induced eIF4E was tagged with hemagglutinin (HA-eIF4E). A 2-fold increase in eIF4E approximates the maximum induction observed in rapidly proliferating cells (69), and a relevant model system should therefore show a similar dynamic range. We utilized quiescent cells that are contact inhibited and serum deprived as a model to minimize variations in eIF4E activity induced by fluctuations in intracellular signaling (e.g. caused by differences in confluence) (28). After screening a panel of clonal cell lines we selected one cell line (designated “4E-inducible”) as suitable for these studies as it showed no detectable baseline expression of ectopic HA-eIF4E while total eIF4E (endogenous + ectopic) was increased ~2-fold in response to low dose mifepristone (625 pM, to minimize off target effects) without downward compensation of endogenous eIF4E protein levels over the time period studied (Figure 2-1A). To account for mifepristone effects not related to eIF4E induction, another clonal cell line was selected for use as non-inducible control cells (designated “non-inducible”) as the cell line did not express HA-eIF4E after mifepristone treatment despite exhibiting the

antibiotic resistance of the GeneSwitch expression system plasmids (Figure 2-1A). Induction of the ectopic eIF4E gene in 4E-inducible cells was rapid, with a time dependent increase in HA-eIF4E mRNA apparent within 1h (Figure 2-1B). This was paralleled by a progressive increase in the ribosome recruitment of HA-eIF4E mRNA (Figure 2-1C). To validate that ectopic HA-eIF4E is functional we utilized a reporter mRNA construct in which translation of Renilla luciferase is cap-dependent (74) and observed a 63% increase in renilla luciferase after 24 hours (data not shown). To further validate that HA-eIF4E is functional we assessed its effects on ribosome loading by comparing polysome-profiles. After rendering 4E-inducible and non-inducible cells quiescent by serum deprivation we treated cells with mifepristone for 4h, a time point chosen to induce eIF4E expression 2-fold while minimizing counter-regulation (66). After treatment, equal amounts of ribosome-associated RNA were stabilized and stratified by ultracentrifugation through a sucrose gradient. Transcripts associated with ≥4 ribosomes were pooled and defined as translationally active polysome-associated RNA (Figure 2-1D). We observed high quality polysome-associated RNA under all conditions in both cell lines indicating the absence of non-specific toxicity [RNA Integrity Number (RIN) for all samples was ≥ 7.1; average = 9.2, SD = 0.7]. In contrast to control cells, 4E-inducible cells showed an increase in ribosome loading after mifepristone treatment, as indicated by the increased area under the absorbance plot in the region designated polysome-associated RNA (Figure 2-1D). Note that this comparison must be made

relative to the polysome peaks with 2-3 ribosomes, as the monosome peak is off-scale due to translational repression caused by serum deprivation. Thus 4E-inducible cells can rapidly increase levels of active HA-eIF4E protein, which in turn results in increased global translation.

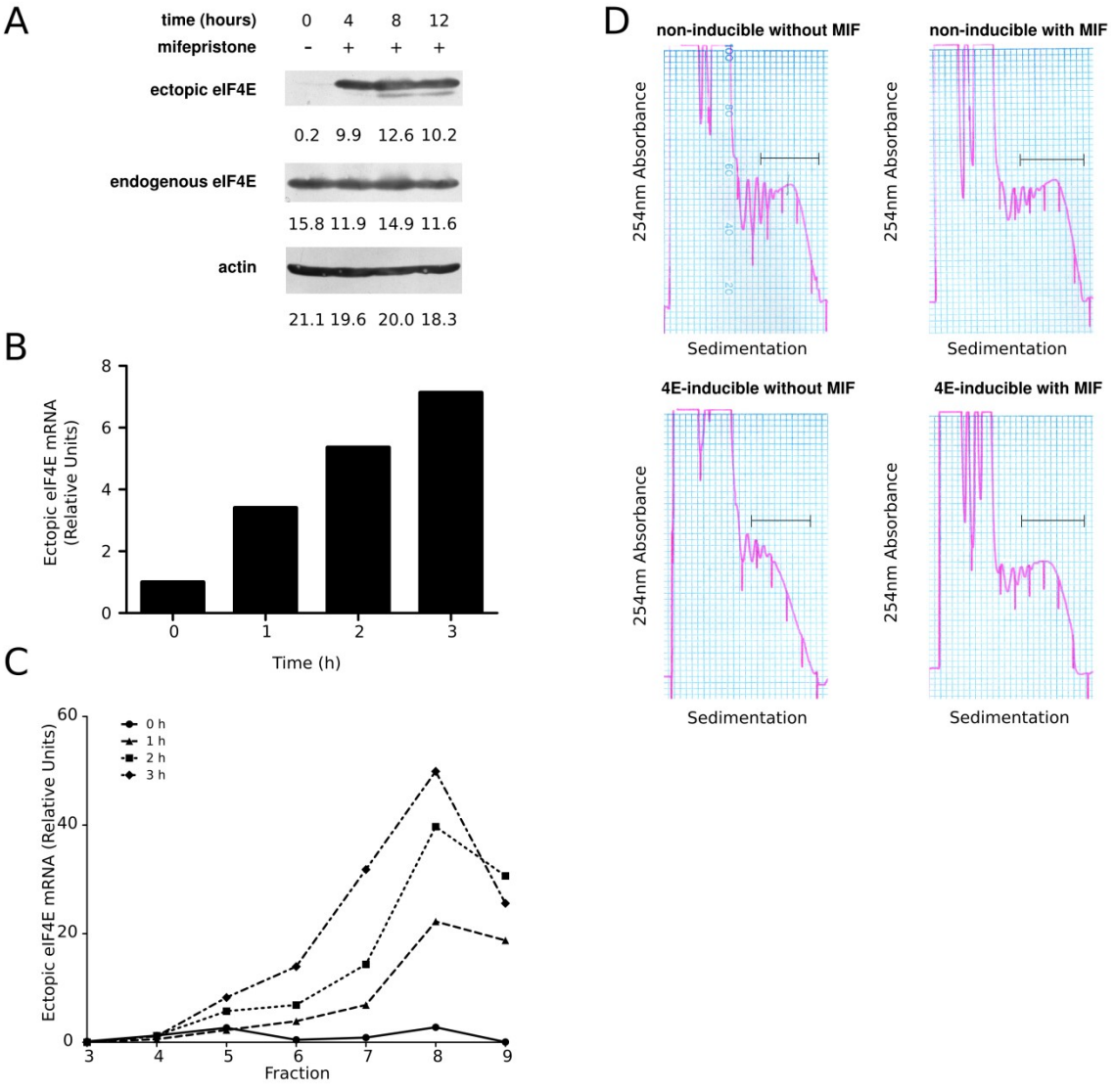

Figure 2-1 An in vitro model for precise modulation of eIF4E activity

(A) Time course of quiescent NIH 3T3 cells harboring an inducible eIF4E construct ("4E-inducible" cells) after incubation with the inducing agent mifepristone (MIF, 625 pM) for the indicated time period. Cells were lysed and both ectopic (HA-tagged) and endogenous eIF4E were quantified by immunoblot. Actin is shown as a loading control. Numbers are relative optical density (OD). **(B)** Time course of total cellular ectopic HA-eIF4E mRNA expression. Quiescent cells were incubated with mifepristone (625pM) for up to 3 h, RNA purified and subjected to Q-PCR analysis. Data from the total mRNA fraction was normalized to a 0 h (baseline) value of 1.0. **(C)** Polysomal mRNA analysis of ectopic eIF4E expression. mRNA from mifepristone treated 4E-inducible cells was stratified on a sucrose gradient and fractionated into 8 increasingly translationally active fractions, numbered 3 (lightest, fewest ribosomes bound) to 10 (heaviest, most ribosomes bound). mRNA was quantified by Q-PCR as a function of time after induction. **(D)** Polysome tracings from 4E-inducible and non-inducible cells. RNA was collected from quiesced 4E-inducible and non-inducible cells treated for 4 h ± mifepristone. Shown is UV absorbance (254 nm) of cellular RNA stratified by ultracentrifugation on a sucrose gradient. Transcripts associated with ≥4 ribosomes are designated as heavily translated mRNA, hereafter defined as polysome-associated RNA, indicated by the bar. Shown are representative tracings of 1-3 independent replicates of each treatment condition.

To allow precise tuning of eIF4E activity within the 2-fold dynamic range we initially considered identifying a panel of cell lines with different maxima for eIF4E induction. However, such an approach would be limited by the possibility of non eIF4E-related differences between the clones. Instead we focused on a more robust approach where eIF4E activity is also modulated by a chemical inhibitor in the 4E-inducible cell line described above. To assess this potential of precisely tuning eIF4E activity using chemical agents we treated quiescent cells with an eIF4E inhibitor, 4Ei-1; concurrent

with induction of ectopic eIF4E expression. 4Ei-1 is rapidly bio-activated to the eIF4E cap binding inhibitor, 7-BnGMP, within 5 minutes (75). Consistent with its role as a translational repressor (73), 4Ei-1 elicited a dose-dependent (up to 200 μM) decrease in polysome-associated RNA (Figure 2-2A). The effect was not caused by general toxicity because total cellular RNA levels remained relatively constant across the entire dose-range (Figure 2-2A). Further corroborating a specific effect of 4Ei-1 on translation, 4Ei-1 treatment reduced cap-dependent translation in a dose-dependent manner in a cell-free translation assay (Figure 2-2B). The stability of total cellular mRNA levels together with the presence of high quality intact polysomes in the presence of 4Ei-1 (Figure 2-3A) indicates that a non-specific toxic effect of 4Ei-1 on gene expression is unlikely. Thus this model system which combines robust and rapid increased expression of eIF4E with precise tuning of eIF4E activity using chemical inhibitors allows detailed studies of how eIF4E activity effects translation across the entire physiological expression range.

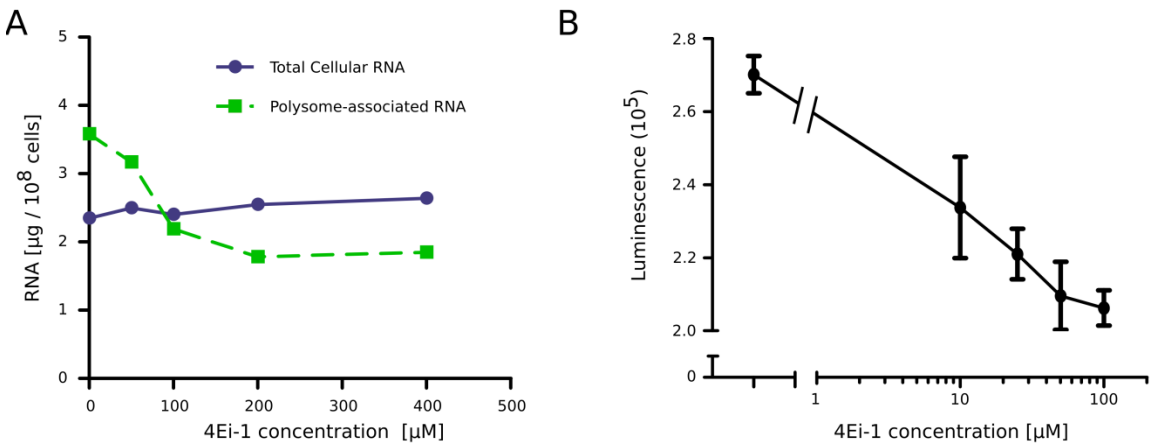

Figure 2-2 4Ei-1 decreases global translational activity.

(A) Total cellular RNA and polysome-associated RNA as a function of 4Ei-1 concentration. Shown are the amounts of polysome-associated and total cellular RNA (normalized to cell number) calculated using UV absorbance at 260 nm. Data shown are from a representative replicate of one set of polysome preparations across the dose range of 4Ei-1. **(B)** Cap dependent translational activity of reticulocyte lysate incubated with 0 to 100 µM 4Ei-1. Renilla luciferase activity was measured in a Lumat luminometer with the Promega Dual-Luciferase Reporter System. Error bars indicate ± SD of quadruplicate samples from a single experiment. Results shown are representative of 3 experiments.

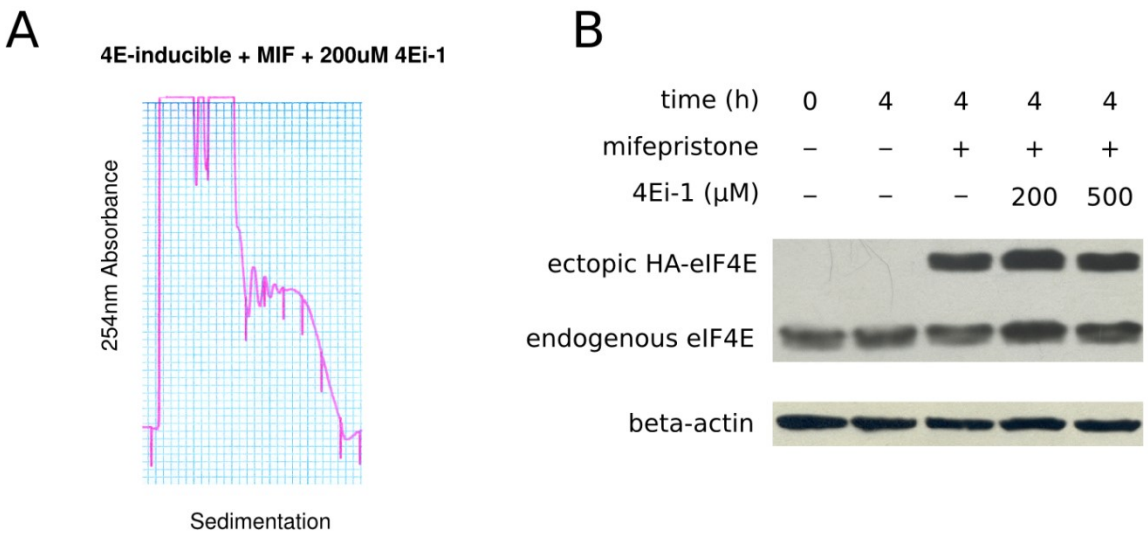

Figure 2-3 4Ei-1 treatment after eIF4E induction does not alter eIF4E protein levels or affect polysome quality

(A) Polysome tracing from 4E-inducible cells. RNA was collected from quiesced 4E-inducible cells treated for 4 h with mifepristone + 200 μM 4Ei-1. Tracing shown is representative of 3 independent replicates. **(B)** Representative Western blot of a time course of quiescent 4E-inducible cells treated either with: mifepristone, mifepristone + 200 μM 4Ei-1, mifepristone + 500 μM 4Ei-1, or untreated control. Cells were lysed and both ectopic (HA-tagged) and endogenous eIF4E was quantified by immunoblot. Actin is shown as a loading control. Shown is a representative example of 2 independent replicates.

4Ei-1 is bio-converted into 7-BnGMP

4Ei-1 was bioactivated into 7-BnGMP in 4E-inducible cells (Figure 2-4B). Of note is that the 4Ei-1 standards prepared in Hepes showed slight degradation into 7-BnGMP or batch impurity, but the 7-BnGMP observed was only about 1% of the 4Ei-1 detected (Figure 2-4B,C). This 1% degradation was also seen in the cell-free media and therefore represents the 7-BnGMP baseline levels in the media treated with 4Ei-1. However, a 35-fold enrichment of 7-BnGMP was seen in the cell-experienced media treated with 500µM 4Ei-1 in DMEM, and a 70-fold enrichment was seen in the cell-experienced media treated with 500µM 4Ei-1 in defined media; indicating that the cells were actively bio-converting 4Ei-1 into 7-BnGMP. Interestingly, the baseline level of 7-BnGMP was also high in the cell-free media sample with 10% FBS, indicating active conversion of 4Ei-1 into 7-BnGMP in the serum. Further analysis of this serum-mediated conversion will be complicated because the internal standard used to quantitate 4Ei-1 and 7-BnGMP was decreased by 23-52% exclusively in the serum-containing samples. Accumulation of intracellular 7-BnGMP and 4Ei-1 was increased in a dose-dependent manner by verapamil (Figure 2-4D, E), which blocks L-type calcium channels (76). To investigate the possibility that cellular bioconversion was not occurring but 4Ei-1 was degrading into 7-BnGMP in the cell-experienced media due to a drop in pH caused by cellular biochemical processes, the pH of media treated for 4 hours was tested (Figure 2-4F). The pH of cell-free and cell-experienced media was not significantly different, indicating that the cells

were likely bioconverting 4Ei-1 into 7-BnGMP and actively exporting it in a Ca^{2+} dependent manner.

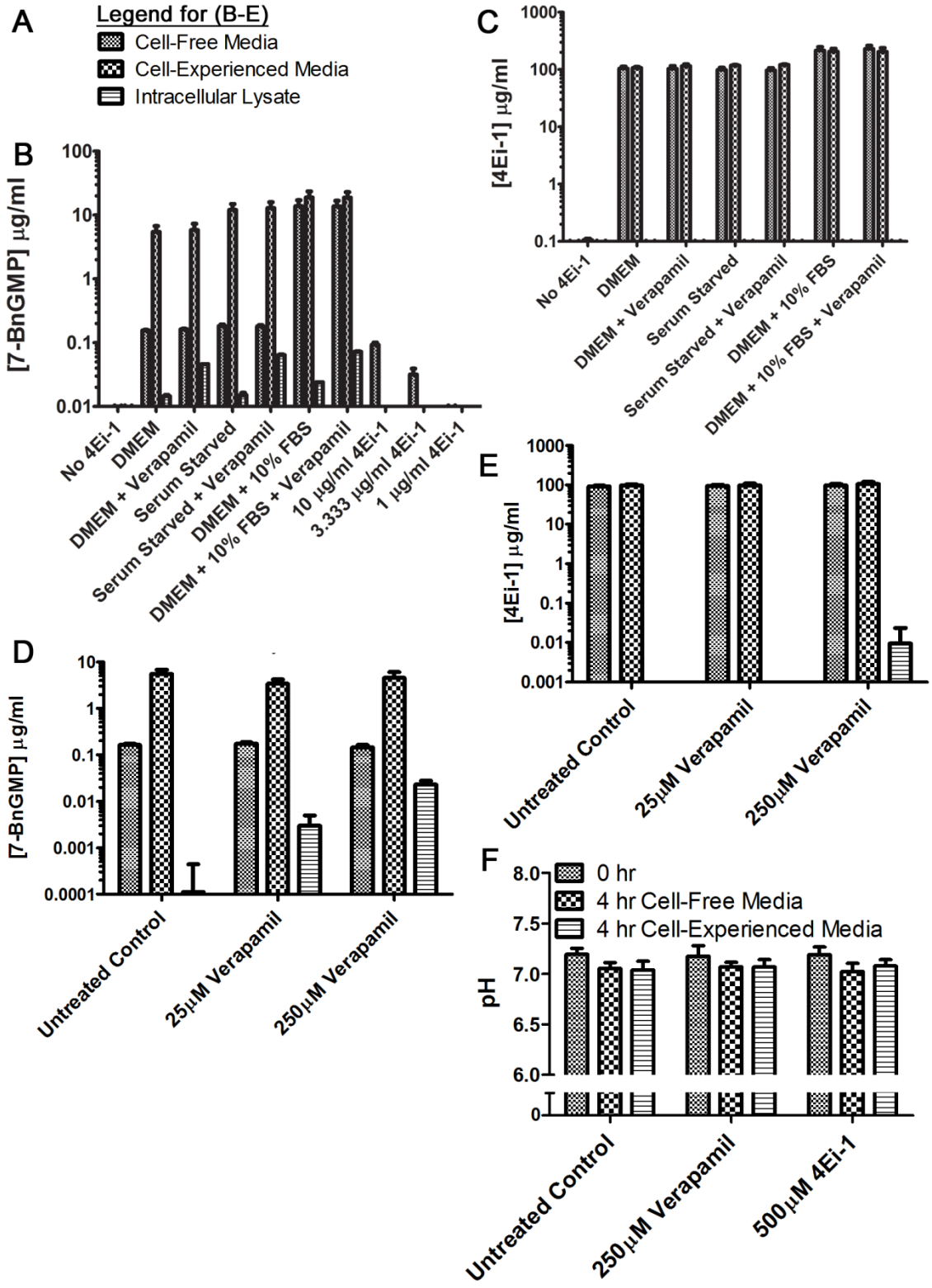
A
Legend for (B-E)
Cell-Free Media
Cell-Experienced Media
Intracellular Lysate
B
[7-BnGMP] µg/ml
100
10
1
0.1
0.01
No 4Ei-1
DMEM
DMEM + Verapamil
Serum Starved
Serum Starved + Verapamil
DMEM + 10% FBS
DMEM + 10% FBS + Verapamil
10 µg/ml 4Ei-1
3.333 µg/ml 4Ei-1
1 µg/ml 4Ei-1
C
[4Ei-1] µg/ml
1000
100
10
1
0.1
No 4Ei-1
DMEM
DMEM + Verapamil
Serum Starved
Serum Starved + Verapamil
DMEM + 10% FBS
DMEM + 10% FBS + Verapamil
D
[7-BnGMP] µg/ml
10
1
0.1
0.01
0.001
0.0001
Untreated Control
25µM Verapamil
250µM Verapamil
E
[4Ei-1] µg/ml
1000
100
10
1
0.1
0.01
0.001
Untreated Control
25µM Verapamil
250µM Verapamil
F
0 hr
4 hr Cell-Free Media
4 hr Cell-Experienced Media
pH
8.0
7.5
7.0
6.5
6.0
0
Untreated Control
250µM Verapamil
500µM 4Ei-1

Figure 2-4 4Ei-1 is bio-converted into 7-BnGMP

(A-C) 4E-inducible cells were plated at high density (serum starved samples were serum deprived with defined media for 24 hours prior to treatment) and then incubated at 37°C for 4 hours with 500µM 4Ei-1 and as indicated. (DMEM = Dulbecco's Modified Eagle Medium, FBS = Fetal Bovine Serum, Verapamil = 100 µM.) Cells were lysed, and incubation (cell-experienced and cell-free) media was collected. All samples were run through an Acquity UPLC system and analyzed for 4Ei-1 and 7-BnGMP content on an electrospray triple-quadrupole mass spectrometer (Waters TQ Detector). The 10, 3.333, and 1 µg/ml 4Ei-1 samples indicate technical standards prepared in Hepes buffer. Error bars indicate triplicate biological replicates each analyzed with triplicate technical LCMS reads. **(D-E)** Samples were treated with mifepristone, 500 µM 4Ei-1, and [0-250 µM] verapamil. All samples analyzed using methods above. **(F)** pH level of media treated as indicated and either kept in a 37°C water bath (untreated control), or incubated for 4 hrs at 37°C and 5% CO_2 either with or without cells. Error bars indicate triplicate biological samples each read three times using a Corning Pinnacle 530 pH meter.

Genome-wide translational analysis identifies differentially responding genes in response to precisely tuned eIF4E activity.

To define the relative translational sensitivity of individual transcripts to precisely tuned eIF4E activity in the physiological range we compared genome-wide expression patterns across six different eIF4E-activity levels from a starting population of quiescent cells (Figure 2-5A). We orthogonally modulated eIF4E activity with a dual system: mifepristone induction of the 4E-inducible cell line to increase eIF4E protein level and activity and a dose range of 4Ei-1 to competitively inhibit eIF4E activity without altering eIF4E protein expression (Figure 2-4B). As the concentration of polysome-associated

RNA did not significantly change with 4Ei-1 concentrations above 200 μM (See Figure 2-2A), a dose range of 4Ei-1 from 0 to 200 μM was chosen. Several controls were used including treatment with a 4Ei-1 analog, 4Ei-4 (has a 10-fold lower affinity for eIF4E as compared to 4Ei-1 (77)), at the highest used concentration to exclude drug class effects unrelated to eIF4E-5'mRNA cap antagonism; and non-inducible cells to exclude effects on translation caused by mifepristone. Due to the disparate mechanisms of action, an off-target effect from the 4Ei-1 drug treatment is unlikely to also be a non-eIF4E related effect of mifepristone treatment and we therefore did not examine this interaction. Both total cellular RNA and polysome-associated RNA were isolated from each condition (Figure 2-5A) and subsequently probed with DNA-microarrays.

Since eIF4E affects gene expression primarily at the level of ribosome recruitment and not at the level of total cellular abundance (35, 66), we focused on the relationship between eIF4E activity and translation. However, polysome-associated RNA levels do not measure effects on translation directly. If transcript abundance increases, there can be an increase in the abundance of that transcript in the polysome pool without any change in translational activity in accordance with the laws of mass action. Therefore, to specifically estimate translation, the polysome-associated RNA level for each gene in each sample was corrected for the total cellular RNA level of that gene in each sample using ANOTA (see Methods).

We first compared the translation of 4E-inducible cells treated with mifepristone for 4h (therefore expressing eIF4E 2-fold above baseline) and treated ± 200 μM 4Ei-1 (with or without eIF4E inhibition). Consistent with the ability of 4Ei-1 to modulate translation through control of eIF4E activity, we found significant changes in translation indicated by an enrichment of genes with low p-values (Figure 2-5B). As expected when modulating eIF4E activity, the differential expression was more pronounced at the level of translation than at the level of total cellular RNA abundance (Figure 2-5C).

Whereas previous genome-wide studies limited their analyses to overexpressed *versus* "normal" eIF4E, our approach provides us the possibility to identify genes whose translation are modulated by 4Ei-1 mediated inhibition of eIF4E activity and altered by increased eIF4E protein levels. This also allows elimination of genes showing non-specific effects under each condition. We identified genes as significantly changed ($p < 0.05$ in two separate tests) if they altered translation after 200 μM 4Ei-1 treatment and also when eIF4E protein level is modulated using mifepristone. In accordance with increased (induced eIF4E expression vs uninduced) and suppressed (4Ei-1 treatment vs no treatment) eIF4E activity, genes that are truly under eIF4E control when treated with 4Ei-1 should modulate translation in the opposite direction when ectopic eIF4E is expressed. Indeed the majority of the genes (188/225) showed the expected inverse regulation pattern (Figure 2-5E). We expected that most of these 188 genes (significantly translationally altered by eIF4E activity) would parallel the activity of eIF4E

(i.e. suppressed translation by 4Ei-1 treatment and activated translation by increased eIF4E expression). In contrast to this assumption, but similar to several previous studies examining the effect of modulated eIF4F levels (35, 66, 70), we not only observed genes whose translation paralleled eIF4E activity (hereafter referred to as 4E hypersensitive, 111 genes, Table 2-1) but also those that showed the opposite translation pattern (hereafter referred to as 4E hyposensitive, 77 genes, Table 2-2) (Figure 2-5D). Moreover, because equal amounts of total cellular and polysome-associated RNA were labeled and probed with the DNA-microarray for each sample, any global decrease in RNA expression is normalized and not observable when comparing the resulting relative microarray expression data. Therefore a "typical" gene which exhibited decreased translation mirroring the global decrease in translation after 4Ei-1 treatment, is found to be unchanged when comparing the equally loaded but differentially treated samples (Figure 2-5D, labeled "typical"). As a result the absolute effect on suppressed translation is underestimated with this approach which is designed to identify those genes showing larger translational effects than the typical gene.

A

Cell Line	Mifepristone	4Ei-1	4Ei-4	Replicates
4E-Inducible	-	-	-	3
4E-Inducible	+	-	-	3
4E-Inducible	+	10 μM	-	3
4E-Inducible	+	50 μM	-	3
4E-Inducible	+	100 μM	-	3
4E-Inducible	+	200 μM	-	3
4E-Inducible	+	-	200 μM	3
non-inducible	-	-	-	1
non-inducible	+	-	-	3

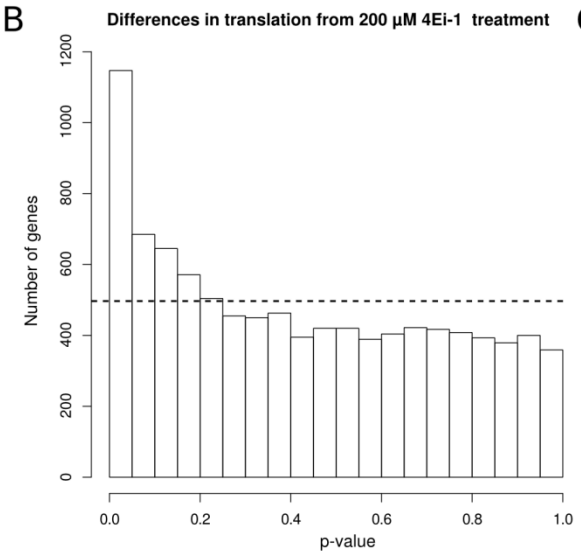

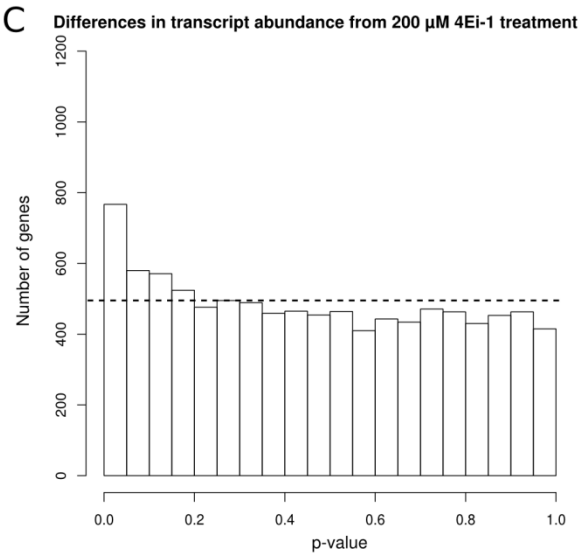

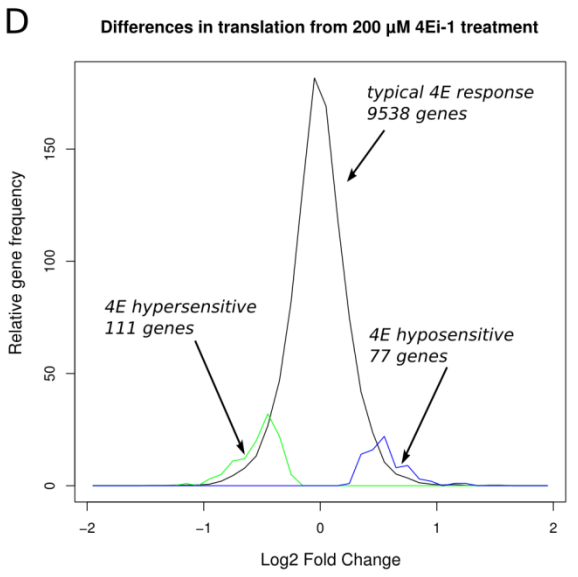

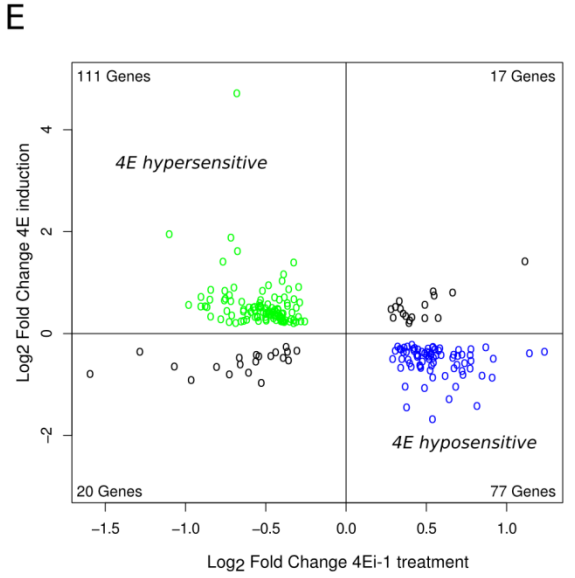

Figure 2-5 Genome-wide translational analysis identifies differentially responding genes in response to precisely tuned eIF4E activity.

(A) Genome-wide study design. Total cellular and polysome-associated samples were collected for each replicate and a "translational" module was generated which corrected polysome-associated expression levels for mRNA abundance (see Methods). The 4E-inducible cell line is the experimental cell line with the non-inducible cell line acting as a mifepristone control, and 4Ei-4 as a control for non-specific drug class effects of 4Ei-1. Equal amounts of RNA from each sample were analyzed by microarray. **(B)** Gene-by-gene p-value histogram comparing the translational modules of 4E-inducible cells treated with mifepristone to 4E-inducible cells treated with both mifepristone and 200 μM 4Ei-1. The dotted line indicates the null distribution. **(C)** Same analysis for total cellular RNA abundance. **(D)** Density plot of translational log2 fold changes elicited by 200 μM 4Ei-1 and mifepristone compared to mifepristone alone in 4E-inducible cells. The black line represents genes not significantly altered by 4E induction and 4Ei-1 treatment when comparing equally loaded microarrays, which normalizes the 4Ei-1 mediated decrease in overall polysome-associated RNA. These genes were defined as having a "typical" response to eIF4E modulation. The green line represents 4E hypersensitive genes and the blue line represents 4E hyposensitive genes (relative gene numbers for these sets 10x relative to typical genes). **(E)** Scatter plot of those genes identified as both: responsive to 4Ei-1 and responsive to 4E induction ($p < 0.05$ in both comparisons). The x-axis is log2 fold change due to 200μM 4Ei-1 treatment in induced cells; the y-axis is log2 fold change due to mifepristone induction when compared to uninduced cells. The blue (4E hyposensitive) and green (4E hypersensitive) dots represent genes which display concordant behavior when treated with 4Ei-1 and induced with mifepristone.

As the main goal of this study was to discover the chemical and biological characteristics of eIF4E responsive genes and because of the relatively permissive FDR threshold, we focused on identifying these two gene sets and not on identifying and characterizing the response of a particular gene to eIF4E. However, this unsupervised analysis did identify VEGF, a validated, eIF4E-responsive gene (43, 78).

Translation of 4E hyposensitive and 4E hypersensitive genes is 4Ei-1 dose-dependent.

Next we assessed the effect of precisely tuned eIF4E activity on the translation of the identified 4E-hyper or –hypo sensitive genes sets by using concentrations of 4Ei-1 between 0 and 200 µM. In theory if the sets are truly 4E-sensitive, as the 4Ei-1 concentration is increased more significant genes will be detected when compared to the no 4Ei-1 baseline. Indeed, the 4E hypersensitive genes showed a dose dependent increase in the number of genes with low p-values (Figure 2-6A, note that all genes at the 200 µM dose exhibit p-values < 0.05 by definition). The 4E hyposensitive genes showed a similar 4Ei-1 dose dependent effect on translation (Figure 2-6B). This dose-regulation relationship could have been caused by an increase in the fold-change differences for translation or a reduction in the experimental variance at higher 4Ei-1 concentrations. To discriminate between the two we directly looked at translation fold-changes. Indeed, such fold-changes are also dose-dependent, as 4E hypersensitive and

4E hyposensitive genes gradually return toward baseline (i.e. the translation in treated cells) with decreasing doses of 4Ei-1 (Figure 2-6C, D). In addition, at 10 μM 4Ei-1, the 4E hyposensitive genes did not exhibit significantly higher expression levels than the untreated control ($p = 0.67$) whereas the 4E hypersensitive genes showed slightly lower expression levels ($p = 7.8 \times 10^{-3}$). To exclude the possibility of a non-specific drug effect, we compared translational fold change in cells treated with 200 μM 4Ei-4. Consistent with an eIF4E-specific effect, 4E hypersensitive and 4E hyposensitive genes were substantially less responsive to 4Ei-4 than to 4Ei-1, indicating that the effect of 4Ei-1 on translational activity was specifically related to its ability to antagonize cap-binding and was unlikely to be a non-specific drug class effect (Figure 2-6C, D). As expected, when comparing all genes, there was very little coherent change across the dose range of 4Ei-1 (Figure 2-6E). Thus, we have identified a set of genes that show true differential eIF4E translational sensitivity in response to precisely tuned eIF4E activity.

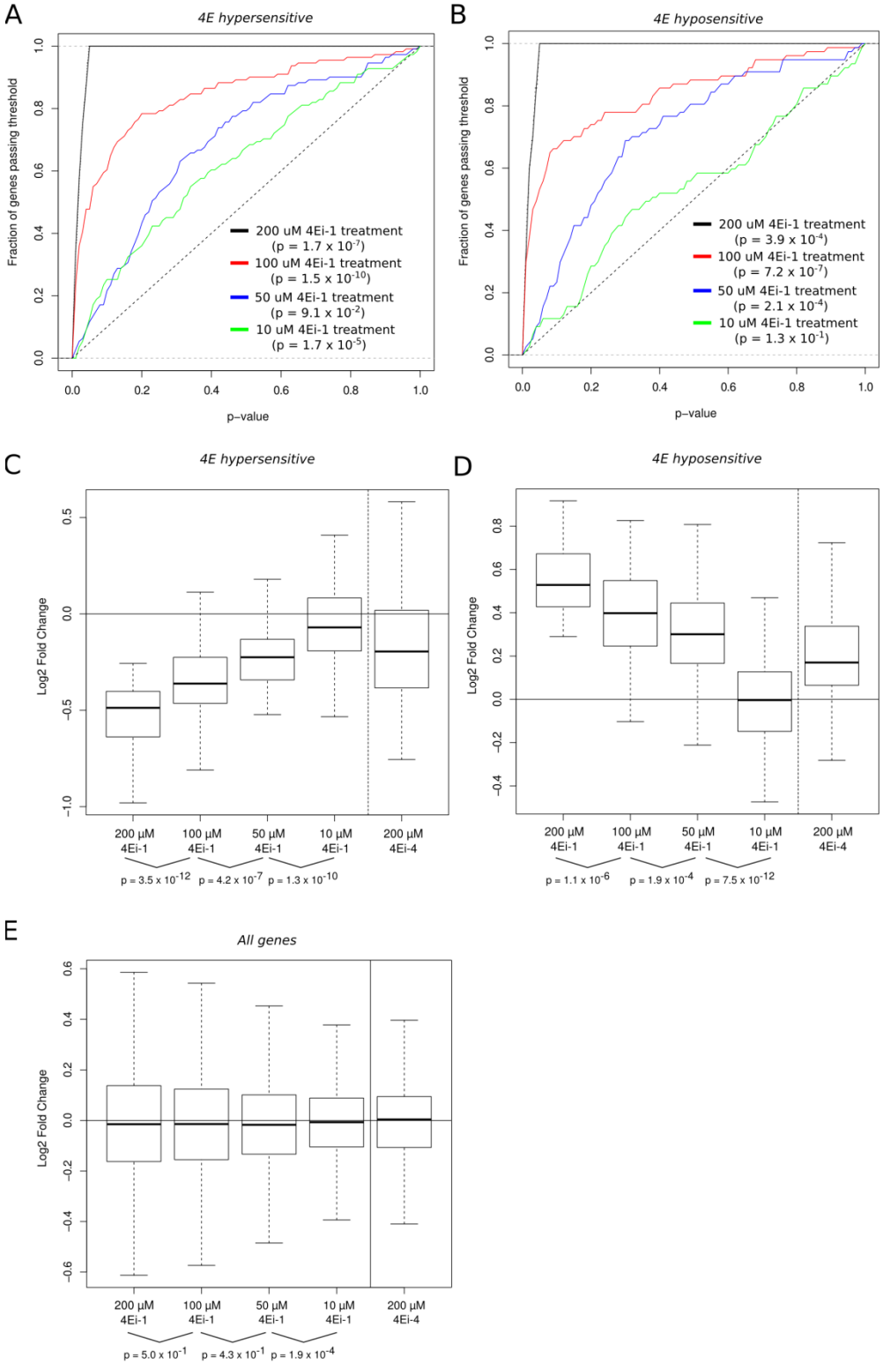
A
4E hypersensitive
Fraction of genes passing threshold
p–value
200 uM 4Ei-1 treatment
(p = 1.7 x 10-7)
100 uM 4Ei-1 treatment
(p = 1.5 x 10-10)
50 uM 4Ei-1 treatment
(p = 9.1 x 10-2)
10 uM 4Ei-1 treatment
(p = 1.7 x 10-5)
B
4E hyposensitive
Fraction of genes passing threshold
p–value
200 uM 4Ei-1 treatment
(p = 3.9 x 10-4)
100 uM 4Ei-1 treatment
(p = 7.2 x 10-7)
50 uM 4Ei-1 treatment
(p = 2.1 x 10-4)
10 uM 4Ei-1 treatment
(p = 1.3 x 10-1)
C
4E hypersensitive
Log2 Fold Change
200 µM 4Ei-1
100 µM 4Ei-1
50 µM 4Ei-1
10 µM 4Ei-1
200 µM 4Ei-4
p = 3.5 x 10-12
p = 4.2 x 10-7
p = 1.3 x 10-10
D
4E hyposensitive
Log2 Fold Change
200 µM 4Ei-1
100 µM 4Ei-1
50 µM 4Ei-1
10 µM 4Ei-1
200 µM 4Ei-4
p = 1.1 x 10-6
p = 1.9 x 10-4
p = 7.5 x 10-12
E
All genes
Log2 Fold Change
200 µM 4Ei-1
100 µM 4Ei-1
50 µM 4Ei-1
10 µM 4Ei-1
200 µM 4Ei-4
p = 5.0 x 10-1
p = 4.3 x 10-1
p = 1.9 x 10-4

Figure 2-6 Translation of 4E hyposensitive and 4E hypersensitive genes is 4Ei-1 dose-dependent.

(A) Fraction of 4E hypersensitive genes (y-axis) passing a given p-value threshold (x-axis) comparing induced cells in the absence of 4Ei-1 to induced cells treated with: 200 µM 4Ei-1 (black line), 100 µM 4Ei-1 (red line), 50 µM 4Ei-1 (blue line) or 10 µM 4Ei-1 (green line). The dotted line represents the theoretical null distribution. P-values are calculated from Wilcoxon signed ranked test and compare the indicated dose with the previous concentration (e.g. the 10 µM line is the comparison of 10 µM to the theoretical null distribution). **(B)** The same analysis is shown for 4E hyposensitive genes. **(C)** Translational log2 fold changes induced by [0 – 200] µM 4Ei-1 or 200 µM 4Ei-4 on the 4E hypersensitive genes. The p-values shown compare each dose with the next lowest concentration (paired Wilcoxon signed ranked test used). **(D)** The same analysis is shown for 4E hyposensitive genes. **(E)** The same analysis for all 7,201 genes detected in our system.

4E hyposensitive and 4E hypersensitive genes have distinct sequence characteristics.

To elucidate the structural features that distinguish transcripts within the 4E hypersensitive and 4E hyposensitive gene lists, we analyzed the 5’ and 3’ UTRs of both sets for length and GC content, and 3’ UTRs for microRNA binding sites. In contrast to the most recent reports suggesting that 4F-sensitive mRNAs have short 5’UTRs (70, 71), this analysis revealed that 4E hypersensitive genes had longer 5’UTRs compared to the typical responding genes, and the same held true when comparing the typical genes to 4E hyposensitive genes (Figure 2-7A). A similar pattern was observed for 5’UTR GC content (Figure 2-7B). Moreover, 4E hypersensitive genes displayed increased 3’UTR

length (Figure 2-7C), but *decreased* GC content in their 3'UTRs (Figure 2-7D), contrary to what was seen in their 5' UTRs. When examining microRNA target number in the 3'UTRs, we found that 4E hypersensitive genes exhibited increased numbers of unique microRNA target sites compared to typical genes (Figure 2-7E); even after correction for 3'UTR length (Figure 2-7F). These findings reestablish the importance of structural features within the 5' UTR for 4E sensitive translation.

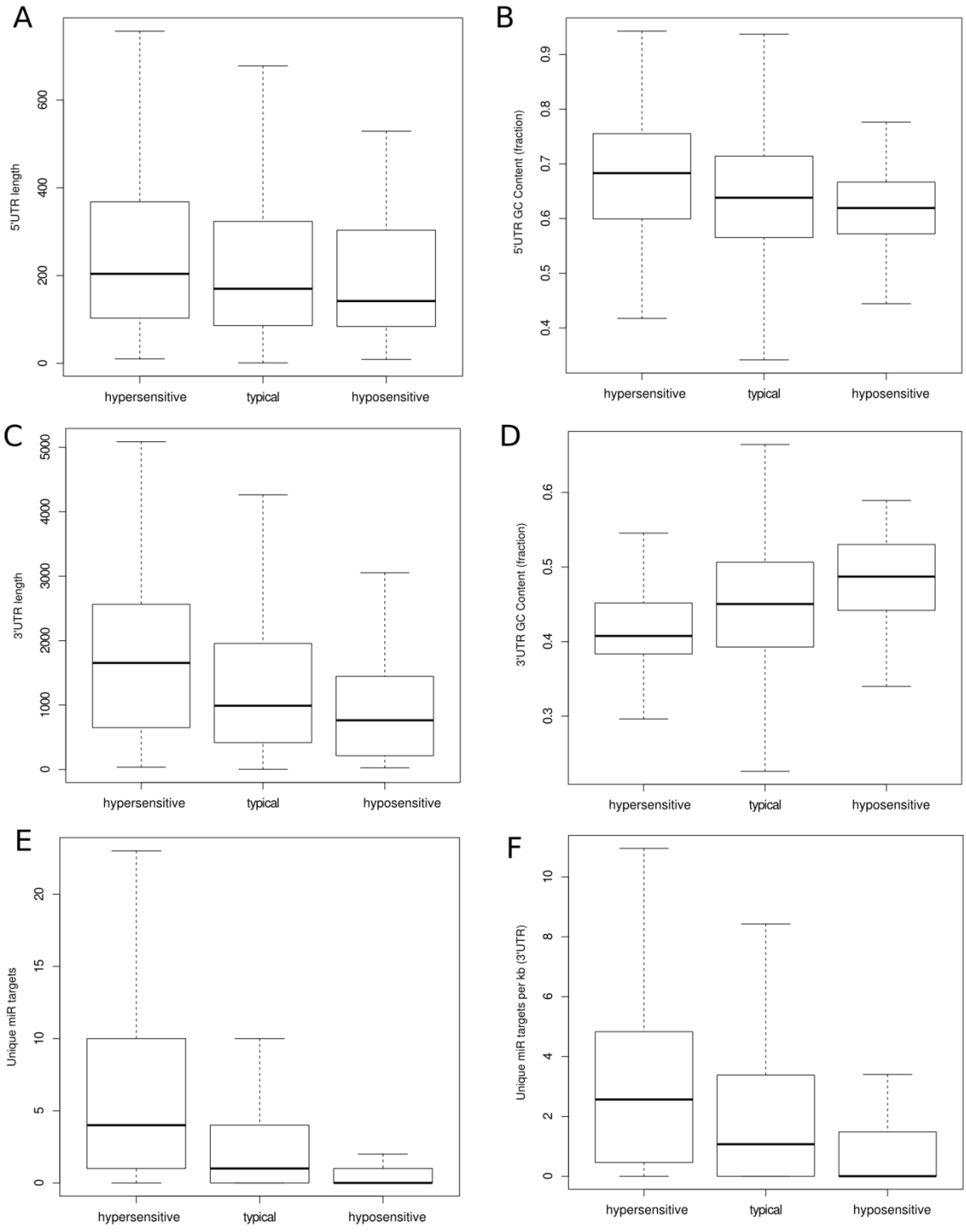
A
5'UTR length
0
200
400
600
hypersensitive
typical
hyposensitive
B
5'UTR GC Content (fraction)
0.4
0.5
0.6
0.7
0.8
0.9
hypersensitive
typical
hyposensitive
C
3'UTR length
0
1000
2000
3000
4000
5000
hypersensitive
typical
hyposensitive
D
3'UTR GC Content (fraction)
0.3
0.4
0.5
0.6
hypersensitive
typical
hyposensitive
E
Unique miR targets
0
5
10
15
20
hypersensitive
typical
hyposensitive
F
Unique miR targets per kb (3'UTR)
0
2
4
6
8
10
hypersensitive
typical
hyposensitive

Figure 2-7 4E hyposensitive and 4E hypersensitive genes have distinct sequence characteristics.

Shown are sequence characteristics of 4E hypersensitive genes and 4E hyposensitive genes compared to typical genes. P-values were calculated using the Mann-Whitney U test. **(A)** 4E hypersensitive genes have longer 5'UTRs ($p = 2.7 \times 10^{-2}$) and 4E hyposensitive genes trend toward shorter 5'UTRs ($p = 2.0 \times 10^{-1}$). **(B)** 4E hypersensitive genes trend toward higher GC content in their 5'UTRs ($p = 1.2 \times 10^{-1}$) and 4E hyposensitive genes have lower GC content ($p = 4.9 \times 10^{-2}$). **(C)** 4E hypersensitive genes have longer 3'UTRs ($p = 5.5 \times 10^{-6}$) and 4E hyposensitive genes have shorter 3'UTRs ($p = 1.2 \times 10^{-2}$). **(D)** 4E hypersensitive genes have lower 3'UTR GC content ($p = 4.2 \times 10^{-7}$) and 4E hyposensitive genes have higher 3'UTR GC content ($p = 2.6 \times 10^{-4}$). **(E)** 4E hypersensitive genes have more unique microRNA target sites (1.0×10^{-7}); 4E hyposensitive genes have fewer microRNA target sites ($p = 1.8 \times 10^{-3}$). **(F)** After correcting for the 3'UTR length, the 3'UTRs of 4E hypersensitive genes are more densely populated with microRNA target sites ($p = 1.7 \times 10^{-4}$) and the 3'UTRs of 4E hyposensitive genes are more sparsely populated with microRNA target sites ($p = 9.2 \times 10^{-3}$).

Characteristics associated with eIF4E hypersensitivity predict the genome-wide translational response across the physiological eIF4E activity range.

In the previous section we identified the features of eIF4E hypersensitive genes: longer 5'UTRs with higher GC content, longer 3'UTRs with lower GC content and more unique microRNA targets even after correction for 3'UTR length. To assess whether these features are sufficient to explain 4E-hypersensitive translation across the 4Ei-1 dose range we removed the identified 4E hypo- and hyper-sensitive genes and analyzed these

features to see if they predicted the translational response. To that end, we divided the 7,201 genes we detected into deciles based on the criteria analyzed. Note that each decile contains many more genes than the 4E hypersensitive gene list (111 genes). Although there was substantial variation, we found that transcripts in the highest decile of 5' UTR length (> 403 nt), on average showed a decrease in translational fold-change with increasing doses of 4Ei-1 (Figure 2-8A). Similarly, transcripts in the highest decile of 5' UTR GC content (> 77%) showed a decrease in translational fold-change with increasing doses of 4Ei-1 (Figure 2-8B). This dose dependence was also true for the 3'UTR features. Transcripts in the highest decile of 3' UTR length (> 2898 nt) showed a decrease in translational fold-change with increasing doses of 4Ei-1 (Figure 2-8C); and transcripts in the *lowest* decile of 3' UTR GC content (< 35%) showed a decrease in translational fold-change with increasing doses of 4Ei-1 (Figure 2-8D). We also examined the relationship between microRNAs and eIF4E sensitivity and found that transcripts with greater than 10 unique microRNA target family seed regions in their 3'UTR showed a decrease in translational fold-change with increasing doses of 4Ei-1 (Figure 2-8E). All these findings are consistent with the observed sequence characteristics of 4E hyper- and hypo-sensitive genes.

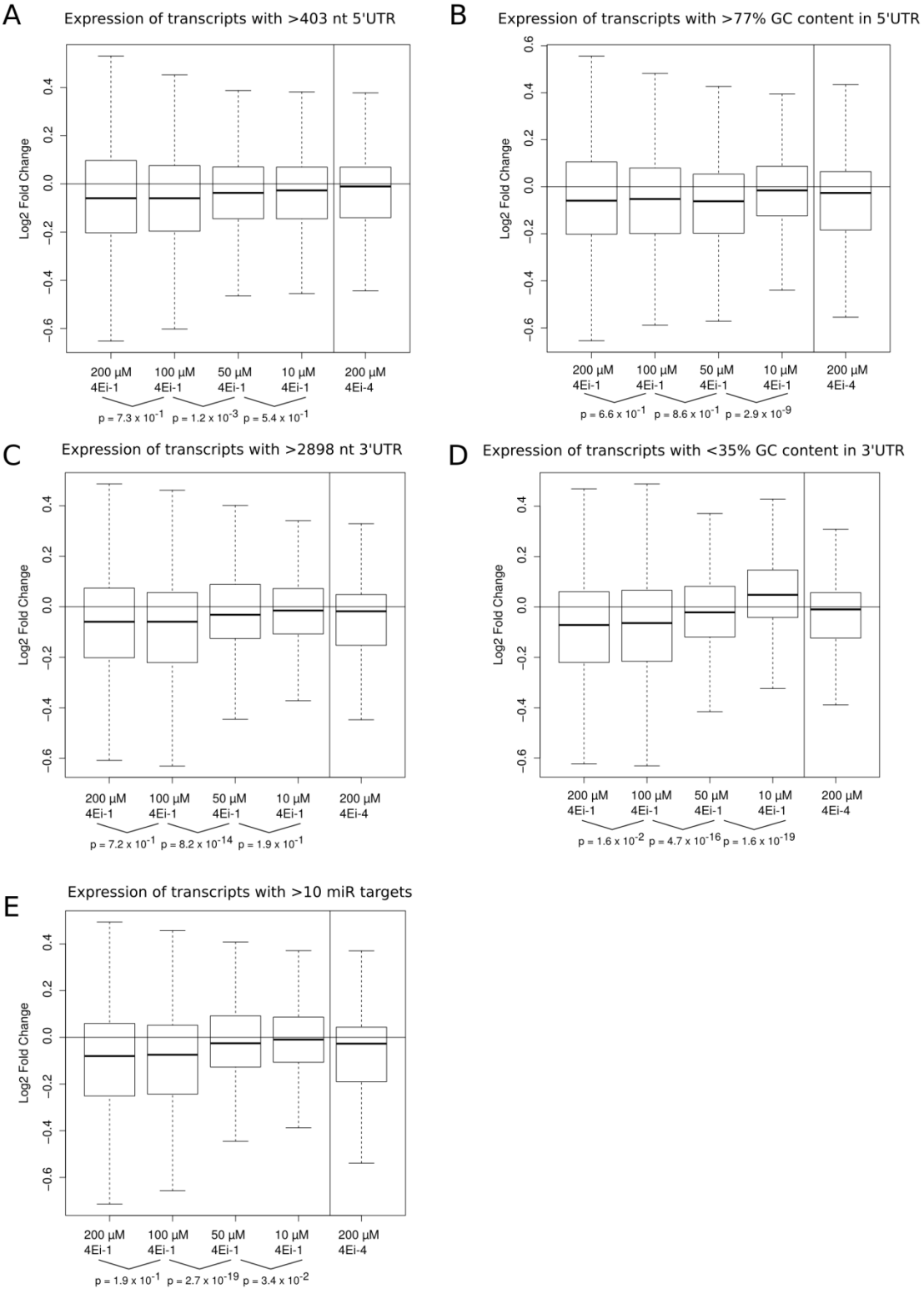
A
Expression of transcripts with >403 nt 5'UTR
Log2 Fold Change
200 µM 4Ei-1
100 µM 4Ei-1
50 µM 4Ei-1
10 µM 4Ei-1
200 µM 4Ei-4
p = 7.3 x 10-1
p = 1.2 x 10-3
p = 5.4 x 10-1
B
Expression of transcripts with >77% GC content in 5'UTR
p = 6.6 x 10-1
p = 8.6 x 10-1
p = 2.9 x 10-9
C
Expression of transcripts with >2898 nt 3'UTR
p = 7.2 x 10-1
p = 8.2 x 10-14
p = 1.9 x 10-1
D
Expression of transcripts with <35% GC content in 3'UTR
p = 1.6 x 10-2
p = 4.7 x 10-16
p = 1.6 x 10-19
E
Expression of transcripts with >10 miR targets
p = 1.9 x 10-1
p = 2.7 x 10-19
p = 3.4 x 10-2

Figure 2-8 Characteristics associated with eIF4E hypersensitivity predict the genome-wide translational response across the physiological eIF4E activity range.

For each structural characteristic of 4E hypersensitive genes identified in Figure 2-7, after removing the 4E hypersensitive and 4E hyposensitive gene sets the set of transcripts in the top decile of each characteristic was collected from among the 7,201 genes detected in our system. For each gene set, 4E hypersensitivity was evident when cells were treated with 200 μM of 4Ei-1 (p-value in legend indicates comparison of genes in top decile in specified category to all other genes), and expression reverted toward baseline with decreasing dosage of 4Ei-1. Gene sets tested were: **(A)** transcripts with >403 nt in their 5'UTR ($p = 1.1 \times 10^{-8}$), **(B)** transcripts with >77% GC content in their 5'UTR ($p = 1.8 \times 10^{-7}$), **(C)** transcripts with >2898 nt in their 3'UTR ($p = 6.3 \times 10^{-11}$), **(D)** transcripts with <35% GC content in their 3'UTR ($p = 5.5 \times 10^{-18}$), and **(E)** transcripts with >10 unique microRNA targets ($p = 2.0 \times 10^{-19}$).

To investigate the role of specific sequence-based 3'UTR characteristics on the 4Ei-1 translational response, we analyzed the 3'UTRs of all detected genes for AU-rich and GU-rich elements. AU-rich elements are cis-acting short sequences that mediate recognition of an array of RNA-binding proteins and affect mRNA stability and translation (79). Another mechanism of 3'UTR regulated stability is found on transcripts containing the consensus GU-rich sequence of "UGUUUGUUUGU" (80) and GU-rich repeats (81), both of which elicit rapid CELF1-mediated mRNA decay. We found that genes with either AU-rich ($p = 1.4 \times 10^{-15}$) or GU-rich sequences ($p = 0.014$) exhibited a decrease in translational fold change with increasing doses of 4Ei-1 (Figure 2-9A, B), supporting the link between 3'UTR mediated translational suppression and 4E hypersensitivity, especially for AU-rich elements.

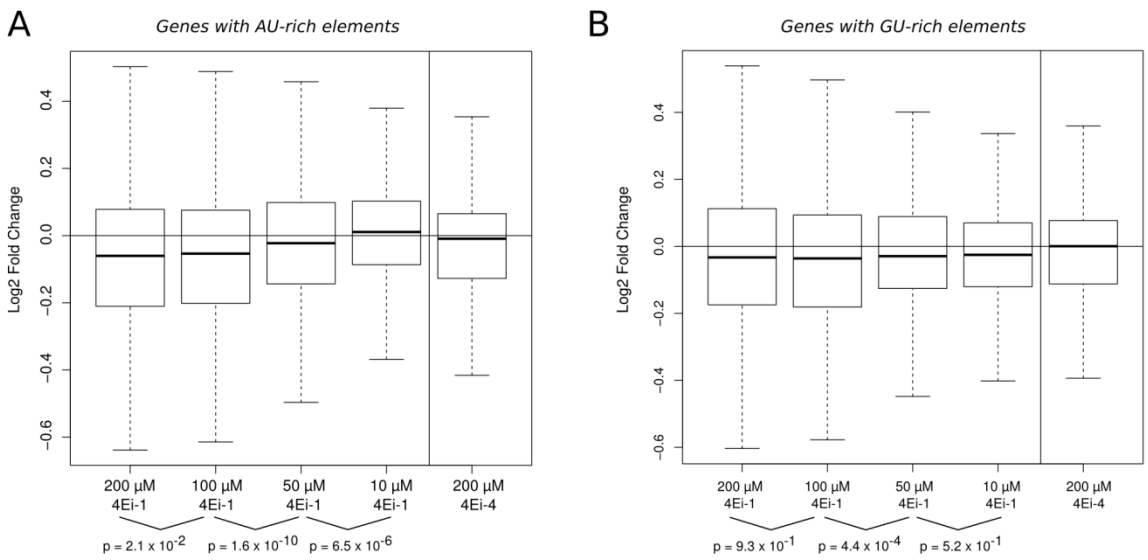

Figure 2-9 4Ei-1 treatment decreases the translation of genes with AU-rich sequences and GU-rich sequences.

(A) Translational log2 fold changes induced by [0 – 200] µM 4Ei-1 or 200 µM 4Ei-4 on genes with AU-rich elements. The p-values shown in the figure compare each dose with the next lowest concentration (paired Wilcoxon signed ranked test used). 4Ei-1 sensitivity was especially evident when cells were treated with 200 µM of 4Ei-1 ($p = 1.4 \times 10^{-15}$ comparing genes with AU-rich elements to genes without them) **(B)** Same translational log2 fold change with GU-rich elements ($p = 0.014$).

eIF4E hypersensitive genes are associated with cell proliferation.

To identify cellular functions associated with 4E hypersensitive and 4E hyposensitive genes, we used Gene Ontology annotations to determine ontologies that were over-represented in our 4E hypersensitive and 4E hyposensitive gene lists (FDR < 0.1) (Figure 2-10A). Among the significant ontologies, “regulation of proliferation” was

overrepresented in the 4E hypersensitive gene list; a result in accord with reports that 4E-hypersensitive mRNAs commonly encode proto-oncogenic, proliferation, and survival promoting proteins (82). To probe proliferation functionally, we induced eIF4E and performed cell cycle analysis across the 4Ei-1 dose range. After eIF4E induction, we observed a 5-fold increase in the proportion of cells in S phase or G_2/M (Figure 2-10B), although the absolute numbers of the induced cycling cells were small. 4Ei-1 significantly decreased the percentage of cycling cells in a dose dependent manner ($p < 0.0001$ at 80, 200, and 500 µM 4Ei-1; $p < 0.01$ at 12 µM 4Ei-1). Of note, 4Ei-1 treatment of uninduced cells did not significantly decrease the basal level of cell cycle transit (two-tailed unpaired t-test, $p = 0.19$) (Figure 2-10B), and mifepristone treatment of non-inducible cells had no impact on cell cycle distribution (Figure 2-11). Therefore, in accord with enrichment of the "regulation of proliferation" ontology, eIF4E induction drives a small proportion of quiescent fibroblasts into the cell cycle and 4Ei-1 attenuates this effect.

A

Gene ontologies associated with eIF4E hypersensitive genes

	p-value	FDR	GO Term
GO:0007010	5.0×10^{-4}	0.0995	cytoskeleton organization
GO:0045944	9.7×10^{-4}	0.0995	positive regulation of transcription from RNA polymerase II promoter
GO:0045893	1.6×10^{-3}	0.0995	positive regulation of transcription, DNA-dependent
GO:0042127	2.3×10^{-3}	0.0995	regulation of cell proliferation

Gene ontologies associated with eIF4E hyposensitive genes

	p-value	FDR	GO Term
GO:0008152	5.7×10^{-4}	0.0975	metabolic process
GO:0005681	8.6×10^{-4}	0.0975	spliceosomal complex
GO:0071013	1.2×10^{-3}	0.0975	catalytic step 2 spliceosome

B

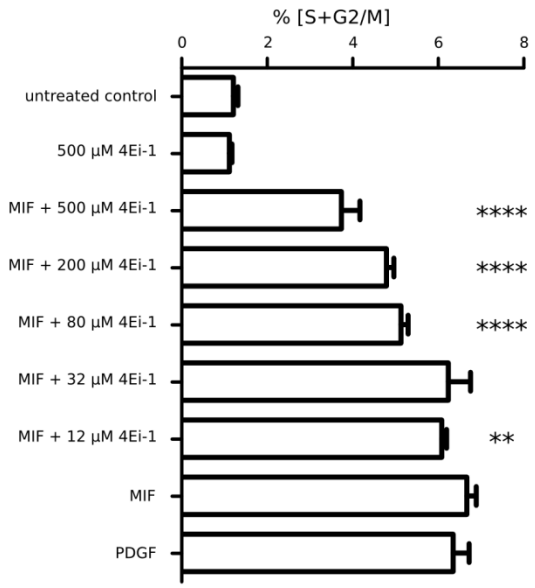

Figure 2-10 eIF4E hypersensitive genes are associated with cell proliferation.

(A) Gene ontologies that are over-represented in the 4E hypersensitive and 4E hyposensitive genes (FDR < 0.1, calculated using Fisher's exact test). **(B)** Cell cycle transit of quiescent 4E-inducible cells pre-treated for 4 h with the indicated concentrations of 4Ei-1 with treatment continued for 24 h as indicated. DNA content was quantified by flow cytometry using Hoechst 33258. Shown is the percent of cells in S+G_2/M and is a representative replicate of 3 independent experiments. Error bars indicate ±*SD* of quadruplicate samples from a single experiment. Serum deprived cells in defined media were used as an untreated negative control and 1 nM PDGF as a positive control. **** = p <0.0001 versus MIF induction alone. ** = p <0.01 versus MIF induction alone.

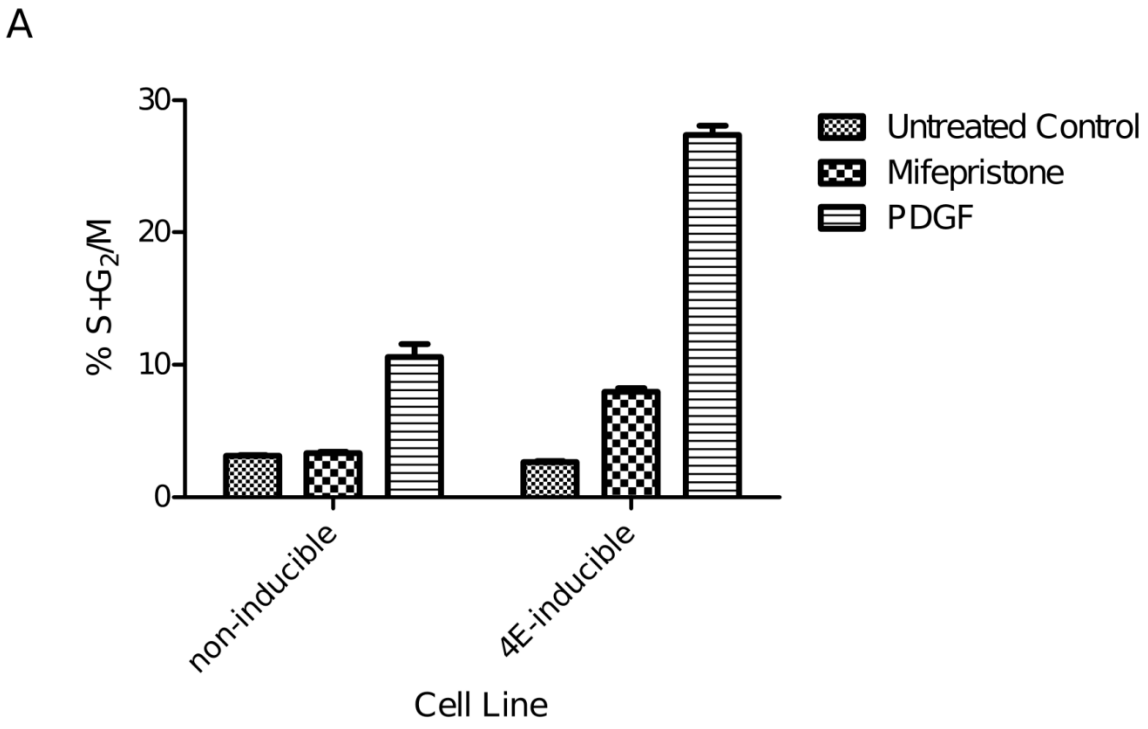

Figure 2-11 Mifepristone treatment has no effect on cell cycle transit in non-inducible cells.

Cell cycle transit of quiescent non-inducible and 4E-inducible cells treated for 24 h as indicated. DNA content was quantified by flow cytometry using Hoechst 33258. Shown is the percent of cells in S+G2/M, and is a representative replicate of 3 independent experiments. Error bars indicate ±SD of quadruplicate samples from a single experiment. Serum deprived cells in defined media were used as an untreated control and 1 nM PDGF as a positive control.

Table 2-1 List of 4E Hypersensitive Genes

Gene ID	Gene Symbol	Gene Name
68497	1110018G07Rik	RIKEN cDNA 1110018G07 gene
11477	Acvr1	activin A receptor, type 1
66549	Aggf1	angiogenic factor with G patch and FHA domains 1
98404	AI597479	expressed sequence AI597479
23802	Amfr	autocrine motility factor receptor
245886	Ankrd27	ankyrin repeat domain 27 (VPS9 domain)
11773	Ap2m1	adaptor protein complex AP-2, mu1
320982	Arl4c	ADP-ribosylation factor-like 4C
65105	Arl6ip4	ADP-ribosylation factor-like 6 interacting protein 4
76976	Arxes2	adipocyte-related X-chromosome expressed sequence 2
12069	Bex2	brain expressed X-linked 2
12166	Bmpr1a	bone morphogenetic protein receptor, type 1A
12328	Caml	calcium modulating ligand
12340	Capza1	capping protein (actin filament) muscle Z-line, alpha 1
12389	Cav1	caveolin 1, caveolae protein
67282	Ccdc53	coiled-coil domain containing 53
227210	Ccnyl1	cyclin Y-like 1
12696	Cirbp	cold inducible RNA binding protein
12753	Clock	circadian locomotor output cycles kaput
98417	Cnih4	cornichon homolog 4 (Drosophila)
12816	Col12a1	collagen, type XII, alpha 1
67876	Coq10b	coenzyme Q10 homolog B (S. cerevisiae)
12859	Cox5b	cytochrome c oxidase, subunit Vb
70425	Csnk1g3	casein kinase 1, gamma 3
217615	Ctage5	CTAGE family, member 5
99375	Cul4a	cullin 4A
22428	Dctn6	dynactin 6
19347	Dennd5a	DENN/MADD domain containing 5A
386655	Eid2	EP300 interacting inhibitor of differentiation 2
14042	Ext1	exostoses (multiple) 1
14062	F2r	coagulation factor II (thrombin) receptor
226016	Fam108b	family with sequence similarity 108, member B
399558	Flrt2	fibronectin leucine rich transmembrane protein 2
71375	Foxn3	forkhead box N3
14573	Gdnf	glial cell line derived neurotrophic factor
629364	Gm16372	actin related protein 2/3 complex, subunit 5 pseudogene
638695	Gm7247	predicted gene 7247
14874	Gstz1	glutathione transferase zeta 1 (maleylacetoacetate isomerase)
14913	Guca1a	guanylate cyclase activator 1a (retina)
50708	Hist1h1c	histone cluster 1, H1c
98758	Hnrnpf	heterogeneous nuclear ribonucleoprotein F
17082	Il1rl1	interleukin 1 receptor-like 1
16179	Irak1	interleukin-1 receptor-associated kinase 1
74158	Josd1	Josephin domain containing 1
107351	Kank1	KN motif and ankyrin repeat domains 1
16600	Klf4	Kruppel-like factor 4 (gut)
77889	Lbh	limb-bud and heart
218454	Lhfpl2	lipoma HMGIC fusion partner-like 2

29806	Limd1	LIM domains containing 1
16974	Lrp6	low density lipoprotein receptor-related protein 6
226778	Mark1	MAP/microtubule affinity-regulating kinase 1
69790	Med30	mediator complex subunit 30
66213	Med7	mediator complex subunit 7
56615	Mgst1	microsomal glutathione S-transferase 1
381269	Mreg	melanoregulin
66448	Mrpl20	mitochondrial ribosomal protein L20
50529	Mrps7	mitchondrial ribosomal protein S7
74026	Msl1	male-specific lethal 1 homolog (Drosophila)
67154	Mtdh	metadherin
100044124	NA	NA
100044475	NA	NA
100044862	NA	NA
100046953	NA	NA
100047184	NA	NA
100047670	NA	NA
100048622	NA	NA
633016	NA	NA
76522	Naa38	N(alpha)-acetyltransferase 38, NatC auxiliary subunit
17973	Nck1	non-catalytic region of tyrosine kinase adaptor protein 1
66866	Nhlrc2	NHL repeat containing 2
20409	Ostf1	osteoclast stimulating factor 1
76073	Pcgf5	polycomb group ring finger 5
14755	Pigq	phosphatidylinositol glycan anchor biosynthesis, class Q
72084	Pigx	phosphatidylinositol glycan anchor biosynthesis, class X
18764	Pkd2	polycystic kidney disease 2
71801	Plekhf2	pleckstrin homology domain containing, family F member 2
19053	Ppp2cb	protein phosphatase 2 (formerly 2A), catalytic subunit, beta isoform
103554	Psme4	proteasome (prosome, macropain) activator subunit 4
28193	Reep3	receptor accessory protein 3
73296	Rhobtb3	Rho-related BTB domain containing 3
69581	Rhou	ras homolog gene family, member U
59044	Rnf130	ring finger protein 130
19822	Rnf4	ring finger protein 4
78294	Rps27a	ribosomal protein S27A
20104	Rps6	ribosomal protein S6
20168	Rtn3	reticulon 3
50724	Sap30l	SAP30-like
107767	Scamp1	secretory carrier membrane protein 1
58172	Sertad2	SERTA domain containing 2
107723	Slc12a6	solute carrier family 12, member 6
69048	Slc30a5	solute carrier family 30 (zinc transporter), member 5
268996	Ss18	synovial sarcoma translocation, Chromosome 18
226551	Suco	SUN domain containing ossification factor
24071	Synj2bp	synaptojanin 2 binding protein
83671	Sytl2	synaptotagmin-like 2
21813	Tgfbr2	transforming growth factor, beta receptor II
72098	Tmem68	transmembrane protein 68
74493	Tnks2	tankyrase, TRF1-interacting ankyrin-rel. ADP-ribose polymerase 2
21983	Tpbg	trophoblast glycoprotein

22031	Traf3	TNF receptor-associated factor 3
68842	Tulp4	tubby like protein 4
65960	Twsg1	twisted gastrulation homolog 1 (Drosophila)
53330	Vamp4	vesicle-associated membrane protein 4
22339	Vegfa	vascular endothelial growth factor A
232023	Vopp1	vesicular, overexpressed in cancer, prosurvival protein 1
66840	Wdr45l	Wdr45 like
215280	Wipf1	WAS/WASL interacting protein family, member 1
22418	Wnt5a	wingless-related MMTV integration site 5A
383295	Ypel5	yippee-like 5 (Drosophila)
142682	Zcchc14	zinc finger, CCHC domain containing 14
170737	Znrf1	zinc and ring finger 1

4E hypersensitive genes are defined as genes which have a p-value < 0.05 and a decrease in relative expression when comparing 4E-inducible cells treated only with mifepristone to 4E-inducible cells treated with both mifepristone and 200 μM 4Ei-1, as well as an increase in expression ($p < 0.05$) when comparing untreated 4E-inducible cells to 4E-inducible cells treated only with mifepristone.

Table 2-2 List of 4E Hyposensitive Genes

Gene ID	Gene Symbol	Gene Name
234734	Aars	alanyl-tRNA synthetase
27406	Abcf3	ATP-binding cassette, sub-family F (GCN20), member 3
11370	Acadvl	acyl-Coenzyme A dehydrogenase, very long chain
104112	Acly	ATP citrate lyase
329910	Acot11	acyl-CoA thioesterase 11
27360	Add3	adducin 3 (gamma)
11669	Aldh2	aldehyde dehydrogenase 2, mitochondrial
214579	Aldh5a1	aldhehyde dehydrogenase family 5, subfamily A1
235606	Apeh	acylpeptide hydrolase
16801	Arhgef1	Rho guanine nucleotide exchange factor (GEF) 1
102098	Arhgef18	rho/rac guanine nucleotide exchange factor (GEF) 18
210004	B3gntl1	UDP-GlcNAc:betaGal beta-1,3-N-acetylglucosaminyltransferase-like 1
224727	Bag6	BCL2-associated athanogene 6
239368	BC030476	cDNA sequence BC030476
12036	Bcat2	branched chain aminotransferase 2, mitochondrial
140721	Caskin2	CASK-interacting protein 2
67179	Ccdc25	coiled-coil domain containing 25
386463	Cdsn	corneodesmosin
83429	Ctns	cystinosis, nephropathic
218581	Depdc1b	DEP domain containing 1B
66233	Dmap1	DNA methyltransferase 1-associated protein 1
13433	Dnmt1	DNA methyltransferase (cytosine-5) 1
70601	Ecd	ecdysoneless homolog (Drosophila)
110147	Ehmt2	euchromatic histone lysine N-methyltransferase 2
13667	Eif2b4	eukaryotic translation initiation factor 2B, subunit 4 delta
77938	Fam53b	family with sequence similarity 53, member B
12091	Glb1	galactosidase, beta 1
277333	Gm5069	glyceraldehyde-3-phosphate dehydrogenase pseudogene
384710	Gm5340	acidic ribosomal phosphoprotein P0 pseudogene
666036	Gm7901	3-phosphoglycerate dehydrogenase pseudogene
76238	Grhpr	glyoxylate reductase/hydroxypyruvate reductase
433943	Gstm2-ps1	glutathione S-transferase mu 2 (muscle), pseudogene 1
98053	Gtf2f1	general transcription factor IIF, polypeptide 1
72748	Hdhd3	haloacid dehalogenase-like hydrolase domain containing 3
78908	Igsf3	immunoglobulin superfamily, member 3
210146	Irgq	immunity-related GTPase family, Q
193796	Kdm4b	lysine (K)-specific demethylase 4B
16211	Kpnb1	karyopherin (importin) beta 1
235497	Leo1	Leo1, Paf1/RNA polymerase II complex component, homolog (S. cerevisiae)
217325	Llgl2	lethal giant larvae homolog 2 (Drosophila)
16905	Lmna	lamin A
17688	Msh6	mutS homolog 6 (E. coli)
192156	Mvd	mevalonate (diphospho) decarboxylase
637711	NA	NA

17995	Ndufv1	NADH dehydrogenase (ubiquinone) flavoprotein 1
100608	Noc4l	nucleolar complex associated 4 homolog (S. cerevisiae)
230082	Nol6	nucleolar protein family 6 (RNA-associated)
68323	Nudt22	nudix (nucleoside diphosphate linked moiety X)-type motif 22
18293	Ogdh	oxoglutarate dehydrogenase (lipoamide)
12304	Pdia4	protein disulfide isomerase associated 4
216134	Pdxk	pyridoxal (pyridoxine, vitamin B6) kinase
75273	Pelp1	proline, glutamic acid and leucine rich protein 1
18624	Pepd	peptidase D
18641	Pfkl	phosphofructokinase, liver, B-type
54381	Pgcp	plasma glutamate carboxypeptidase
57435	Plin4	perilipin 4
70428	Polr3b	polymerase (RNA) III (DNA directed) polypeptide B
56031	Ppie	peptidylprolyl isomerase E (cyclophilin E)
19089	Prkcsh	protein kinase C substrate 80K-H
68879	Prpf6	PRP6 pre-mRNA splicing factor 6 homolog (yeast)
19182	Psmc3	proteasome (prosome, macropain) 26S subunit, ATPase 3
19185	Psmd4	proteasome (prosome, macropain) 26S subunit, non-ATPase, 4
97541	Qars	glutaminyl-tRNA synthetase
223864	Rapgef3	Rap guanine nucleotide exchange factor (GEF) 3
68272	Rbm28	RNA binding motif protein 28
20227	Sart1	squamous cell carcinoma antigen recognized by T cells 1
378702	Serf2	small EDRK-rich factor 2
66354	Snw1	SNW domain containing 1
20322	Sord	sorbitol dehydrogenase
108903	Tbcd	tubulin-specific chaperone d
19241	Tmsb4x	thymosin, beta 4, X chromosome
231712	Trafd1	TRAF type zinc finger domain containing 1
15547	Trmt2a	TRM2 tRNA methyltransferase 2 homolog A (S. cerevisiae)
22271	Upp1	uridine phosphorylase 1
22283	Ush2a	Usher syndrome 2A (autosomal recessive, mild)
80743	Vps16	vacuolar protein sorting 16 (yeast)
22594	Xrcc1	X-ray repair complementing defective repair in Chinese hamster cells 1

4E Hyposensitive genes are defined as genes which have a p-value < 0.05 and an increase in relative expression when comparing 4E-inducible cells treated only with mifepristone to 4E-inducible cells treated with both mifepristone and 200 μM 4Ei-1, as well as an decrease in expression ($p < 0.05$) when comparing untreated 4E-inducible cells to 4E-inducible cells treated only with mifepristone.

Discussion

Most genome-wide studies examining eIF4E function have used constitutive over expression to study the long term effects of eIF4E activation and found eIF4E-sensitive genes had longer 5'UTR's. However, recent studies used chemical inhibition of mTOR and found that eIF4F-sensitive genes had shorter 5'UTR's. Here we probe this issue by rapidly increasing global translational activity with eIF4E induction in quiescent cells. In addition, we utilized the eIF4E chemical inhibitor 4Ei-1 to tune eIF4E activity in a dose-dependent fashion, allowing us to examine gene expression across a range of eIF4E activities. Using this novel two-pronged system, we identified both 4E hypersensitive genes (more responsive to eIF4E activity than average) and 4E hyposensitive genes (less responsive to eIF4E activity than average). Both of these gene sets were validated by observing a coherent pattern of 4Ei-1 dose-dependence. We determined the structural characteristics associated with each of these classes: eIF4E hypersensitive genes tended to have longer 5'UTRs with higher GC content, longer 3'UTRs with lower GC content, higher density of unique microRNA target sites, and more AU-rich elements. These mRNA characteristics were also predictive of the translational response of all 7,201 detected genes across the tested dose range of 4Ei-1.

Increased eIF4F activity has been proposed to stimulate the translation of mRNAs with highly structured 5'UTRs through several possible mechanisms including the inability of

these mRNAs to compete for eIF4E, elicit formation of the eIF4F complex, retain the eIF4F complex, recruit ribosomes, or unwind mRNA (or some combination of these properties) compared with mRNAs without highly structured 5'UTRs (36). Our results address this directly at the level of eIF4E by modulating eIF4E abundance and its cap binding function. Increased eIF4E activity has been shown to selectively activate the translation of transcripts with longer 5'UTRs (83). Our finding that 4E hypersensitive genes tend to have increased 5'UTR GC content is in accord with previous studies showing that as the complexity of the 5'UTR is reduced, there is a loss of sensitivity for eIF4E in their translation (84). Consistent with this, in a polyelectrostatic model of protein-mRNA interactions, genes with up-regulated translational efficiencies in the *caf20Δ* (yeast 4E-BP homologue) mutant have high 5'UTR secondary structure and are longer (85). As the 4E-BPs function to negatively regulate eIF4E, this data is in general accord with our result that 4E hypersensitive genes possess higher 5'UTR secondary structure and length. This is in contrast with studies indicating that eIF4E targeted genes contain shorter 5'UTRs (70, 71, 86). Such inconsistencies may arise due to significant differences among experimental systems which reflect true biological differences in the state of the translational pathway under those conditions. In particular, systems featuring inducible eIF4E activity differ from systems with constitutively active eIF4E in which cells have had the opportunity to counter the effects of eIF4E over expression (66, 86). Other than our unique two-pronged system utilizing eIF4E-5'mRNAcap

antagonism, other differences from our system include the use of: human telomerase reverse transcriptase (hTERT) immortalized human mammary epithelial cells (66, 86), non-quiescent cells (66, 86), different number of ribosomes collected as the polysome-associated pool (5, 35), and ribosome profiling (70, 71). It is plausible that in these altered regulatory environment, eIF4E hypersensitive genes may exhibit a distinct set of structural features and these features may be distinct from those regulated directly by mTOR. Interestingly, when we looked at other known 5'UTR regulatory features, such as the 5'-TOP (5'-terminal oligopyrimidine tract) regulatory element (87), and despite recent data identifying TOP or TOP-like motifs as the key and almost ubiquitous regulatory characteristic of mTORC1-regulated mRNAs (70), we found no significant 5'TOP enrichment in our 4E hyposensitive and 4E hypersensitive genes. A likely explanation is that the set of translationally regulated genes is substantially different in these environments: direct downregulation of mTORC1 activity in rapidly proliferating cells in full serum with fully activated eIF4E activity (a status akin to many established cancers (88)) and inhibition of the eIF4E-5'mRNAcap association in quiescent serum deprived cells with low eIF4E activity (a status akin to physiological tissue repair and regeneration and cancer genesis). Thus our study provides additional context and complements established literature.

When probing the 3'UTRs of eIF4E hypersensitive mRNAs, we found that they tended to have longer 3'UTRs with less GC content; again in contrast to observations made in cells

with constitutive eIF4E activation (86). However, as evidenced by the much lower p-values for 3'UTR structural features compared to 5'UTR features, our data reinforced the concept that eIF4E hypersensitive transcripts are more likely to be translationally regulated through their 3'UTRs (86). One interpretation of this result is that increased 3'UTR length and decreased complexity allow increased microRNA regulation of these transcripts, in accord with our result showing increased microRNA target density in 4E hypersensitive transcripts. This parallels data showing that eIF4E is a component of processing-bodies (PB) and stress granules, implying that it plays a role in mRNA sequestration and/or turnover (89, 90). RNAi-mediated knockdown experiments reveal that a subset of P body factors, including eIF4E-T (eIF4E-transporter), LSm1, rck/p54, and Ccr4 are required for the accumulation of eIF4E in P bodies (91). Processing bodies also contain mRNA but lack other pre-initiation factors. Instead, they contain microRNAs and a number of proteins associated with mRNA decay (e.g. DCP1a, DCP2, hedls/GE-1, p54/RCK, argonaute) and transport (e.g. FAST, RAP-55, TTP) allowing shepherding of specific mRNA transcripts between the translation and decay machineries (92). TTP binds to AU-rich elements in the 3'UTR's of mRNA and promotes their degradation (93). eIF4E hypersensitive genes are enriched in AU (i.e. they are low in GC), and we found that genes containing AU-rich elements exhibited a decrease in translation after 4Ei-1 treatment. These data support a model in which eIF4E selects specific mRNAs for translation, degradation, or sequestration based on their 3'UTR sequence

characteristics. Increased eIF4E activity may be able to rescue 4E hypersensitive transcripts from 3'UTR controlled translational suppression which occurs through multiple mechanisms including AU-rich elements, GU-rich elements, or microRNAs. Further analysis of those protein and mRNAs that associate with eIF4E in processing bodies will be necessary to further develop this model.

A goal of our experiments was to elucidate the biological characteristics of 4E hypersensitive genes as a group. To this end, we probed for biological processes associated with eIF4E hypersensitive genes, searching for gene ontologies that were particularly enriched in this gene set. Of particular interest, we identified the gene ontology "regulation of proliferation", a finding we functionally validated by showing that eIF4E induction increases proliferation and 4Ei-1 attenuates this effect. This result aligns with previous data showing that 4Ei-1 suppresses proliferation in $CD4^+$ T-cells (77). In our system, 4Ei-1 was able to affect cell cycle transit at doses as low as 12 μM in contrast to the much higher doses needed to suppress T-cell proliferation. This result indicates that 4Ei-1 is effective at lower doses in our fibroblast system, particularly in the biologically relevant context of quiescence. Multiple genes in the "regulation of proliferation" ontology have previously been validated as translationally regulated genes. These included *Tgfbr2* (transforming growth factor, beta receptor II), a gene we identified as 4E hypersensitive and which has been previously validated as translationally controlled during rat lung development (94). Another gene in the

"regulation of proliferation" ontology is *MIF* (macrophage migration inhibitory factor), a gene we identified as 4Ei-1 hypersensitive and which was previously validated as 4E sensitive after eIF4E induction (35). Our result showing the eIF4E sensitivity of proliferation genes also provides an explanation for why exogenous eIF4E mRNA augments wound healing (95).

This search for biological processes also identified 4E hyposensitive genes as enriched in components of the spliceosomal complex, aligning with previous reports linking spliceosomal function to eIF4G; independent of its association with eIF4E (96). A separate nuclear pool of eIF4G stably associates with spliceosomes *in vitro* and shows close association with spliceosomal snRNPs and splicing factors in vivo (97). This complex may be recruited to pre-mRNAs via its interaction with the nuclear cap-binding complex (CBC) and accompany the mRNA to the cytoplasm, facilitating the switching of CBC for eIF4F (96). Therefore, it is expected that spliceosomal function and the translation of its components should be independent of eIF4E activity. This is in accord with the established precept that the expression of genes associated with homeostatic cellular functions (including the other hyposensitive ontology, "metabolic process") are relatively insulated from changes in eIF4E activity and are translated at relatively constant rates (33).

Our experimental system provides several advantages compared to previous studies. The rapid induction of eIF4E expression after mifepristone treatment is not only faster but produces a more constant protein expression over time than previously published tetracycline-inducible eIF4E 3T3 cells (35). To reduce off-target effects and false positives in our list of hypersensitive and hyposensitive genes, we exploited the fact that induction increases eIF4E activity by altering protein level; whereas 4Ei-1 decreases eIF4E activity by competing for the 5' cap. This enabled us to modulate eIF4E activity in orthogonal ways. Although it has been shown in epithelial cancer cell lines that extended 4Ei-1 treatment (24-72 hrs) is capable of decreasing eIF4E protein levels by initiating eIF4E proteasomal degradation (75), we did not observe this in our cells after 4 hours. Further, the use of a dose-range of 4Ei-1 allowed us to validate the behavior of the hypersensitive and hyposensitive genes lists across a range of eIF4E activity. The two-pronged approach used here could also detect eIF4E hypersensitive genes in other cell types and *in vivo* models. This approach could be expanded to proteins other than eIF4E which have selective small molecule inhibitors available, and a dose range of the inhibitor could be combined with an inducible expression system to powerfully detect genome-wide effects from carefully tuned expression of the translational machinery component of interest.

Materials & Methods

Cell culture

NIH 3T3 cell derivatives were maintained at 37^{o}C, 5% CO_2 in growth medium [Dulbecco's modified Eagle's medium high-glucose (DMEM, Sigma-Aldrich) supplemented with 10% fetal bovine serum (FBS, Sigma-Aldrich), 25mM Hepes, 100 units/ml penicillin, 100 units/ml streptomycin and 125 ng/ml amphotericin (Life Techologies)].

Cell transfection

Cells were seeded into 35 mm wells of 6-well clusters. After 24 h, cells were transfected with 4 µg DNA using Lipofectamine 2000 reagent (Life Technologies) according to the manufacturer's instructions. Cells were incubated in the presence of Lipofectamine 2000 for 6 h, switched to DMEM containing 5% FBS for 24 h, and cultures were continued in growth medium until use.

Inducible eIF4E system

The inducible GeneSwitch system functions by expressing a truncated human progesterone receptor ligand-binding domain which can be bound by mifepristone, triggering a conformational change in the GeneSwitch protein, formation of an active homodimer, transcription of the transgene and production of the protein of interest

(98). GeneSwitch NIH 3T3 cells were purchased from Invitrogen and maintained in growth medium supplemented with hygromycin (50μg/ml) at 37^{o}C, 5% CO_2. Plasmids encoding hemagglutinin (HA)-tagged wild-type eIF4E [pKAS8-3] were linearized by digesting with SspI and transfected into GeneSwitch NIH 3T3 cells in log phase growth. Two days post-transfection, cells were subcultivated and zeocin selection begun (500 μg/ml zeocin). Transfected cells were incubated at 37^{o}C, 5% CO_2 under zeocin selection for 2-3 weeks. Approximately 100 individual foci were isolated and expanded in growth medium under hygromycin and zeocin selection. For each clone, cells were added to 10 cm dishes, cultured overnight, shifted to growth medium with or without the inducer mifepristone (625 pM) for 48 h, and lysed. Clones were screened for background expression of ectopic HA-eIF4E without induction and mifepristone-induced expression of HA-eIF4E by immunoblot. Two clones were utilized for the experiments reported here: 1) “non-inducible” control cells do not express ectopic eIF4E despite exhibiting resistance to hygromycin and zeocin, i.e. the cells contain all of the ectopic GeneSwitch expression system plasmids but do not exhibit exogenous gene expression upon induction; and 2) “4E-inducible” cells express ectopic eIF4E at a level comparable to the endogenous gene, yielding an approximately 2-fold overexpression. For our ectopic eIF4E induction studies, cells were first rendered quiescent in “defined medium” (F-12 supplemented with 25mM Hepes, 0.1 mg/ml bovine serum albumin, 10 mg/ml holo-transferrin, 10^{-8} M selenium, $3*10^{-6}$ M linoleic acid; with 40 ng/ml IGF + 5 ng/ml EGF to

preserve viability; all components from Sigma-Aldrich) for 22 h (99); with cultures continued for the indicated amount of time in defined medium +/- the inducer mifepristone (625pM).

Immunoblot analysis

Cells were lysed with RIPA lysis buffer [1% NP-40, 50 mM Tris pH 7.5, 150 mM NaCl, 1% sodium deoxycholate, 1% SDS (all Sigma-Aldrich)] supplemented with protease inhibitor (Roche) and protein quantified using a BCA protein assay kit (Pierce). Equal amounts of cell lysate protein per lane were subjected to SDS-PAGE and transferred onto nitrocellulose membranes. Antibodies directed against eIF4E (mouse monoclonal antibody, 1:500, BD Transduction Laboratories) and actin (rabbit polyclonal antibody, 1:1500, Sigma-Aldrich) were used to identify these proteins. Signal was detected with secondary antibodies conjugated to horseradish peroxidase (Calbiochem) and developed with chemiluminescent ECL Western Blotting Detection Reagents (GE Healthcare Life Sciences).

Cell based translational activity assay

To quantify the global level of cap-dependent translation, a luciferase reporter system was utilized (74). Cells were transfected with 1 µg of pcDNA3-rLuc-polio-fLuc, and fresh media was added 6 h after transfection. Cells were rinsed with PBS 24 h after

transfection and induced to express ectopic eIF4E with mifepristone (625pM). After 24 h, cells were lysed with passive lysis buffer (Promega) for 15 min, cell debris was pelleted by centrifugation and triplicate supernatant samples were assayed for luciferase activity in a Lumat LB 9507 luminometer (BG&G) using the Promega Dual-Luciferase Reporter System.

In vitro translational activity assay

To verify that 4Ei-1 functioned as a translational repressor, a cell-free luminescence reporter system was utilized. A master mix was created with 1.25 µL 20x buffer and 17 µL rabbit reticulocyte lysate from the Retic Lysate IVT kit (Life Technologies) and 1 µL l-methionine (final concentration 50 µM) and 0.5 µL (1 µg) pcDNA3-rLuc-polio-fLuc mRNA reporter. The master mix was aliquoted into microcentrifuge tubes with 5.25 µL of 4Ei-1 (over a dose range of 0 - 100 µM) and the reaction was allowed to proceed at 30°C for 75 min. 100 µM 7-MeGTP was used as a positive inhibitory control. Five µL of each reaction mix was combined with 100 µL of nuclease-free water. Five µL of this mix was assayed for Renilla luciferase activity in a Lumat LB 9507 luminometer (BG&G) using the Promega Dual-Luciferase Reporter System.

RNA preparation

Total cellular and ribosome-associated RNA were prepared as described previously (65). In order to assess ribosome recruitment to each and every mRNA transcript, cell homogenates were overlaid onto a 5 ml sucrose gradient, stratified by ultracentrifugation and fractionated into ten 0.5 ml fractions, numbered 1 (lightest, no ribosomes bound) to 10 (heaviest, most ribosomes bound). These ten fractions of 0.5 ml were collected into tubes containing 50 µl of 10% SDS.

RNA quantification

To assess the effect of mifepristone induction on ectopic HA-eIF4E's overall transcript abundance and ribosome recruitment, total cellular RNA and fractions 3 to 10 of ribosome-associated RNA were individually purified using Tri-reagent (Sigma-Aldrich) and reverse transcribed to cDNA using the TaqMan reverse transcriptase kit (Roche). Fractions 1 and 2, containing translationally inactive RNA not bound to ribosomes, were not quantified. Quantitative PCR (Q-PCR) was performed using the Roche Light-Cycler 1.5 with SYBR Green dye (Roche). The HA-eIF4E primer used was: 5'-ACGTTCCAGATTACGCTGCT-3' (forward) and 5'-AGAGTGCCCACCTGTTCTGT-3" (reverse). The reaction products were subjected to gel electrophoresis to confirm the presence of a single PCR product of the appropriate length. Data from total cellular RNA was normalized to a 0 h (baseline) value of 1.0.

HPLC-ESI-MS/MS instrumentation

4E-inducible cells were plated at 3 million cells/10cm plate, serum starved for 24 hr, and then treated for 4 hrs with 500µM 4Ei-1 in the media indicated (DMEM = Dulbecco's Modified Eagle Medium, FBS = Fetal Bovine Serum, Serum Starved = defined media). Intracellular lysates were resuspended in 100uL Hepes prior to LC/MS analysis. Cell-experienced media was also collected along with the cells and analyzed via LC/MS. Cell-free control media was also collected which was placed in fresh 10cm dishes and also incubated at 37°C without cells. All samples were then analyzed as performed previously (75).

Media pH test

As 4Ei-1 is less stable at acidic pH, we analyzed the pH of cell-free and cell-experienced media. 3 million cells/10cm plate were played and serum deprived for 22 hrs in defined media and then treated with mifepristone and 250 µM verapamil or 500 µM 4Ei-1 and incubated for 4 hours at 37°C and 5% CO_2. The pH of each media sample was determined using a Corning Pinnacle 530 pH meter.

Quantification of translational activity

To assess genome-wide translational activity, RNA from sucrose-gradient fractions 7 to 10, representing heavily translated mRNA containing 4 or more bound ribosomes per transcript, was pooled and termed polysome-associated RNA. Total cellular RNA and polysome-associated RNA were quantified and quality checked using both the NanoDropND-8000 and Caliper Labchip GX. Samples passing quality thresholds (260/280 ratio > 1.8 and an RNA Integrity Number (RIN) of 7.1 or higher (average = 9.2, SD = 0.7)) were labeled using an Illumina TotalPrep-96 RNA Amplification Kit, hybridized to Illumina murine WG-6 v2.0 expression BeadChips and the resulting signal was captured with an Illumina iSCAN scanner. The data was normalized using robust spline normalization and $\log_2$ transformed in R/Bioconductor. As the large number of samples required the data to be run across multiple chips, technical replicates were included and bead summary data were batch corrected as described previously (100). Probes for which the expression level exceeded all negative controls (detection p-value = 0.0 as defined by the Illumina platform) in 2/3 of total cellular RNA samples were included in downstream analysis. Gene expression levels were mapped from probe levels by selecting the highest expressing probe from each mapped gene. Using these criteria, 7,201 genes were identified. Data integrity was verified by testing 5' to 3' ratios and scaling factors. This dataset has been deposited at the Gene Expression Omnibus (GEO).

Because the amount of each transcript bound to polysomes depends in part upon the abundance of that particular transcript in the cytoplasmic pool, in order to determine whether each gene is regulated specifically at the step of translation, the expression level of the gene in the polysomal RNA sample was corrected for the expression level of that gene in the corresponding total cellular RNA sample. This is often done by considering the ratio [polysomal mRNA] / [total cellular mRNA], termed the translational efficiency (TE) or translational ratio (TR). However, this assumes that an increase in total cellular mRNA levels is noiselessly associated with a corresponding increase in the polysomal mRNA level, an assumption that leads to increased false positives (101). We used a more robust correction, ANalysis Of Translational Activity (ANOTA), in which polysomal RNA is corrected by a linear fit to the total cellular RNA (102):

$$Ex_{polysomal} = \gamma_{total} \cdot Ex_{total} + \gamma_{biological\ variable}$$

where $Ex_{polysomal}$ is the measured expression of a given gene in the polysomal mRNA, Ex_{total} is the measured abundance of a given gene in the total cellular mRNA, γ_{total} is the fitted linear dependence of the polysomal expression on the total cellular expression and $\gamma_{biological\ variable}$ is the change in translation induced by the biological variable in the comparison. The resulting p-values were corrected using RVM adjustment (103).

Categorization of genes by eIF4E sensitivity

We utilized a multi-step approach to stratify the translational activity of genes by eIF4E sensitivity:

Step 1: Identify genes differing ($p < 0.05$; corresponding to an FDR of 0.41) in the comparison of 4E-inducible cells + mifepristone with 4E-inducible cells + mifepristone + 4Ei-1 (200 µM).

Step 2: In order to reduce false positives, we also required a true positive to achieve $p < 0.05$ in the comparison of 4E-inducible cells + mifepristone to 4E-inducible cells - mifepristone. Genes with significantly decreased translational activity from step 1 which also showed increased expression in this comparison were designated “4E hypersensitive genes” (111 genes), and genes with significantly increased translational activity from step 1 which also showed decreased expression after mifepristone treatment compared to no mifepristone treatment were designated “4E hyposensitive genes” (77 genes).

Annotation of RNA features

The 5’ and 3’ UTRs of the UCSC canonical isoform (104, 105) for each gene were annotated in R using the Bioconductor packages GenomicFeatures (106) and TxDb.Mmusculus.UCSC.mm9.knownGene (107). Unique microRNA targets of each gene

were annotated using targetScanMouse via the targetscanMouse.db package in R (108). Genes with AU-rich sequences were annotated using the ARED organism database (109). Genes with GU-rich sequences were defined by searching their canonical isoform for the sequence UGUUUGUUUGU (80) and the defined GU-rich repeat sequence (81).

Gene ontology analysis

In order to identify biological processes associated with the 4E hyposensitive and 4E hypersensitive genes, Fisher's exact test was used on ontologies from the gene ontology consortium (110) to determine those that were over-represented in each group (FDR < 0.1).

Cell cycle analysis

Cells were seeded in growth medium at 33,000 cells/35 mm well of a 6-well cluster. Growth medium was replaced with defined medium on day 7 for 22 h, cells were pre-treated for 4 h with [0 – 500 μM] 4Ei-1 in defined medium and shifted to treatment medium (defined medium + treatment condition) for 24 h. For each sample, the 4 h pretreatment concentration of 4Ei-1 was identical to the 24 h treatment concentration for that sample. Cultured cells were rinsed with PBS, detached with trypsin, washed with PBS + 1% FBS to inactivate trypsin, washed in staining buffer [Hank's balanced salt solution w/ magnesium chloride and calcium chloride (Life Technologies), supplemented

with 1% FBS, 1g/L glucose, and 20 mM Hepes (pH 7.2)] and pelleted by centrifugation. Cells were resuspended in 1 ml staining buffer supplemented with Hoechst (40 μg/ml) and Pyronin Y (1 μg/ml), incubated for 45 min at 37^{o}C, washed in staining buffer and analyzed using an LSR II flow cytometer (Becton Dickinson [BD]). The percentages of cells with G_1 and S+G_2/M DNA content was determined with FlowJo software (version 7.5) using published protocols (111). All statistical values were generated using unpaired two-tailed t-tests, and all error bars indicate standard deviation.

Chapter 3 : eIF4E mediates G_0 exit and cell cycle transit via a Cyclin C-independent mechanism

Introduction

Cell Cycle

The regulation of cellular proliferation is critically important in physiological cell growth and is aberrantly usurped in almost all cancers. Proliferation can only be achieved in mammalian cells after DNA replication in the cell cycle, which is therefore a key regulatory node (Figure 3-1 from (112)).

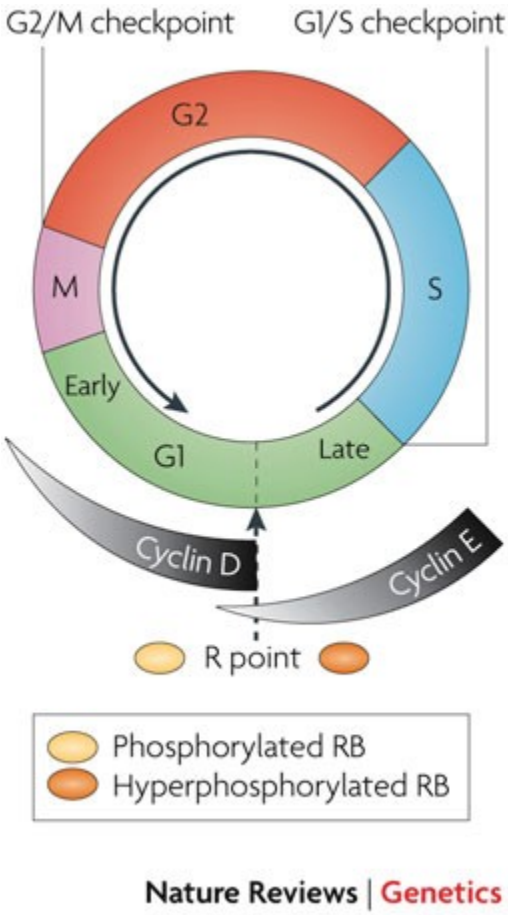

Figure 3-1 The cell cycle

Mammalian cell proliferation occurs through a series of stages that are collectively termed the cell cycle. The cell cycle can be divided into four phases: DNA synthesis (S), mitotic segregation (M), and two intervening gap phases (G1 and G2) preceding S and M phases, respectively. Progression through the cell cycle requires hyperphosphorylation of the retinoblastoma (RB) protein and is highly regulated, particularly at the "checkpoints" from G_1 phase to S phase and from G_2 phase to M phase. These checkpoints are controlled in part by the association of the cyclin family of proteins with cyclin dependent kinases (cdk's) to form an enzymatically active complex, and their antagonist cell cycle inhibitors (CDKIs), discussed below. *This figure has been reprinted with kind permission from Nature Publishing Group.*

Cyclin C is involved in G_0 exit

The regulated balance of cell proliferation and quiescence is critical for tissue homeostasis and organismal health. Cells in a quiescent state are outside of the cell cycle, and are defined as in G_0 phase. During G_0 phase global protein synthesis is largely down-regulated, but a subset of mRNAs is specifically translated to ensure cell survival and responsiveness to proliferative signals (113). These proteins tightly control exit from G_0, and despite the importance of this regulatory node current knowledge is still lacking in this area. One of the mRNAs known to be highly expressed in G_0 is cyclin C (114). Cyclin C mRNA levels also increase specifically only in the G_0 population of quiescent serum pulsed cells (115). Cyclin C (CCNC) was originally found to associate with cyclin-dependent kinase 8 (cdk8) and this complex regulated the efficiency of RNA Polymerase II transcription by phosphorylating its carboxy terminal domain (CTD) in the presence of a CTD-specific kinase (116). However, when cyclin C complexes with cdk3 instead, this complex stimulates retinoblastoma (Rb) phosphorylation at serine 807/811, and this phosphorylation is required for cells to exit G_0 efficiently as it occurs prior to cyclin D1-mediated phosphorylation of Rb (111). Acute inactivation of pRB alone is also sufficient for G_0-arrested cells to reenter the cell cycle (117). This data indicate that RB phosphorylation is critical for G_0 exit, but the molecular trigger and relative significance of cyclin C-induced phosphorylation is unclear.

Cyclin D1 controls the R point through phosphorylation of the retinoblastoma protein

Once a mammalian cell has exited G_0, a combination of intrinsic and extrinsic signals regulate the transition from early to late G_1 phase. This transition is termed the restriction (R) point, and divides the G_1 phase of the cell cycle into the mitogen-dependent early G_1 phase and the mitogen-independent late G_1 phase (118). During normal physiological homeostasis and tissue regeneration, cells must be stimulated by mitogenic signals (i.e. soluble growth factors) to traverse the G_1 phase and enter into the cell cycle. After the R point the cell has committed to enter the cell cycle and mitogenic stimuli are no longer required.

Transit through the R point is largely controlled by cyclin D and the retinoblastoma (Rb) protein. When quiescent cells are exposed to growth factors, cyclin D1 abundance in the cytoplasm increases as it associates with one its partner kinases, cdk4 or cdk6, resulting in their activation (119). The activated cyclin D1-cdk complexes enter the nucleus where they phosphorylate Rb on residue serine-780 (120). Cyclin D1 in turn is rapidly phosphorylated by glycogen synthase kinase-3 beta (GSK3β) on Thr-286, triggering nuclear export and ubiquitin mediated degradation by the 26S proteasome (121).

Once past the R point the mitogen-independent activation of cyclin E-cdk2 complexes elicit further hyperphosphorylation and inactivation of Rb and other family members

(122). This leads to release of E2F family members, which then regulate transcription of genes necessary for S-phase entry and continued cell cycle progression towards the G_2 and M phases of the cell cycle (123).

Cyclin-dependent kinase inhibitors regulate the formation of cyclin-cdk complexes.

Cdk's are activated after binding to their respective cyclin partner, but cdk's can be maintained in an inactive state after binding with cyclin-dependent kinase inhibitors (CDKIs). Two families of CDKIs regulate the transition through G_1 phase. Members of the Ink4 family (p15, p16, p18, p19) are direct inhibitors of the association of the early G_1 cyclin D–cdk4 and cyclin D–cdk6 complexes , and members of the CIP/KIP family (p21CIP, p27KIP1, p57KIP2) are direct inhibitors of the association of the late G_1 cyclin E–cdk2 complexes (124). Therefore high CDKI activity is effective at slowing or blocking S phase entry.

eIF4E is known to translationally regulate key oncogenic proteins

eIF4E is known to translationally regulate the abundance of: key cell cycle drivers including ornithine decarboxylase (38), cyclin D1 (40), fibroblast growth factor 2 (125); and other oncogenic proteins including matrix metallopeptidase 9 (126), the transcription factor c-Myc (53), and the angiogenic vascular endothelial growth factor

(VEGF) (43). These pleiotropic effects of eIF4E on the full range of cancer-related functions have made elucidating the mechanism of eIF4E-mediated transformation a challenge. In addition, the majority of these early studies were limited by potential indirect effects and counter regulation arising from long term cell culturing with constitutively active eIF4E (127). Dissecting the localized roles of eIF4E on individual transcripts has also proven difficult, as eIF4E forms nuclear bodies and regulates the nucleo-cytoplasmic export of key mRNAs in addition to its role in the cytoplasm to initiate translation (78). For example, eIF4E was shown to promote nuclear export of cyclin D1 mRNAs via an element in the 3'UTR but the technology of the time was unable to show that eIF4E selectively increases the translation of cyclin D1 (40, 128). Therefore the molecular mechanisms by which eIF4E impacts cell cycle function are incompletely defined, especially in the physiological context of quiescence and cancer genesis. Here we show that abrupt gain of eIF4E function in quiescent cells triggers G_0 exit and cell cycle transit and increases ribosome recruitment to cyclins C and D1. These data establish an oncogenic mechanism linking increased levels of cellular eIF4E and proliferative autonomy in the absence of growth factors.

Results

Ectopic eIF4E expression elicits G_0 exit and cell cycle transit

To elucidate the molecular mechanisms by which abrupt activation of the cap-dependent translation initiation complex modulates cell cycle kinetics, quiescent 4E-inducible cells were treated with or without the inducer mifepristone, thus increasing eIF4E protein levels from those commonly observed in quiescent cells to levels commonly seen in cancer (88). We then determined cell cycle status by flow cytometric quantification of DNA and RNA content. eIF4E induction elicited a pronounced decrease in the percentage of G_0 cells, from a baseline of 24% G_0 to 7% at 26 hours (Figure 3-2A), thus signifying G_0 exit. eIF4E induction increased cell cycle transit (hereafter defined as cell cycle progression through the R point and into S and G_2 phases) after G_0 exit, as evidenced by a 4-fold increase in the percentage of cells in S and G_2 phase when compared with this baseline (Figure 3-2B). Although this increase was consistent, it was also modest, as no more than 6% of mifepristone-induced cells were observed in S or G_2 phase at any time point. In accord with prior reports, we observed a small, but persistent proportion of cells in S or G_2 phase, even at high density after serum deprivation (129). To exclude a clone-specific effect, we examined 3 additional clones which expressed eIF4E after mifepristone induction and observed similar results (data

not shown). These data establish a direct relationship between eIF4E abundance, translational activation, G_0 exit and cell cycle transit from G_1 phase through M phase.

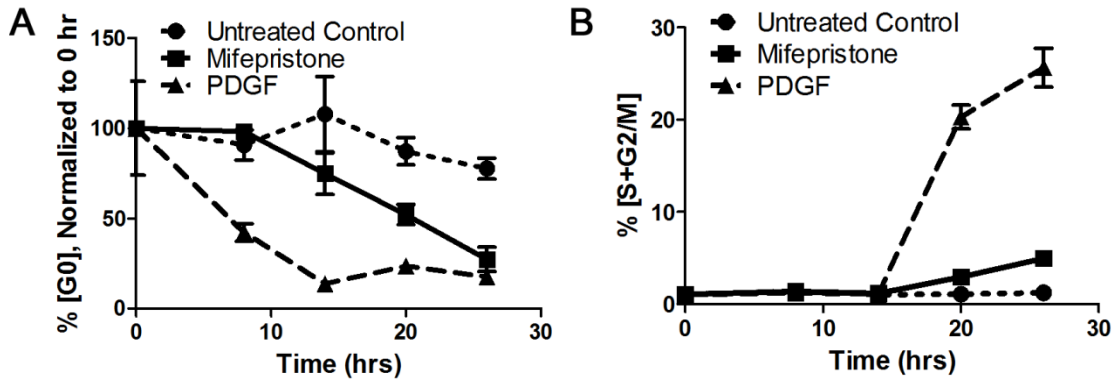

Figure 3-2 Ectopic eIF4E expression elicits G_0 exit and cell cycle transit.

(A) Cell cycle timecourse of quiescent 4E-inducible cells treated as indicated. DNA and RNA content was quantified by flow cytometry using Hoechst 33258 and Pyronin Y, respectively. Shown is the percent of cells in G_0 normalized to the 0 hr timepoint, which showed 23.7% of cells in G_0. The G_0 population was defined as cells with 2n DNA content and RNA content less than cells with 4n DNA content. Shown is a representative replicate of 3 independent experiments, with error bars indicating ±SD of triplicate samples from a single experiment. Serum deprived cells were used as an untreated negative control and 1 nM PDGF (platelet derived growth factor) as a positive control. **(B)** Data obtained concurrent to panel A data. Shown is the percent of cells in $S+G_2/M$ as a function of time.

eIF4E-mediated cyclin C translational activation is not necessary for G_0 exit and cell cycle transit

Cyclin C (*CCNC*), in partner with kinases including cdk2 and cdk3, can mediate G_0 exit (111, 130). We therefore monitored ribosome recruitment to the cyclin C transcript in

response to rapid eIF4E induction. The predominant effect on cyclin C mRNA was an increase in ribosome loading as seen by a shift from lighter to heavier polysomes (Figure 3-3A). To differentiate this shift from the genome-wide translational activation elicited by ectopic eIF4E expression, cytochrome C served as an invariant control (Figure 3-3B) (65). As expected, there was no significant difference between the total cellular mRNA abundance of cyclin C and cytochrome C, and HA-eIF4E continued increasing in the 3 hour time period probed (Figure 3-3C). Therefore cyclin C is translationally activated by eIF4E induction.

Knockdown of cyclin C has previously been shown to delay G_0 exit and S phase entry (111). To examine whether cyclin C was necessary for eIF4E-mediated G_0 exit and cell cycle transit, we transduced 4E-inducible cells with a GFP expressing shRNA construct targeting cyclin C, sorted on GFP expression (Figure 3-3D), and reduced cyclin C mRNA by 54% when compared to the non-silencing (NS) control (Figure 3-3E). Despite this reduction, there was no significant change in eIF4E-mediated G_0 exit (Figure 3-3F), indicating that cyclin C is not necessary for eIF4E-mediated G_0 exit. Although there was a trend towards non-silencing shRNA delaying G_0 exit ($p=0.054$) at 12 hrs, cyclin C knockdown was unable to ablate or delay eIF4E-mediated G_0 exit. As expected, serum deprived cells showed a slight increase in the percentage of G_0 cells over time and PDGF elicited a significant decrease in the percentage of G_0 cells over time (data not shown).

Cyclin C knockdown also had no significant effect on eIF4E-mediated cell cycle transit (Figure 3-3G).

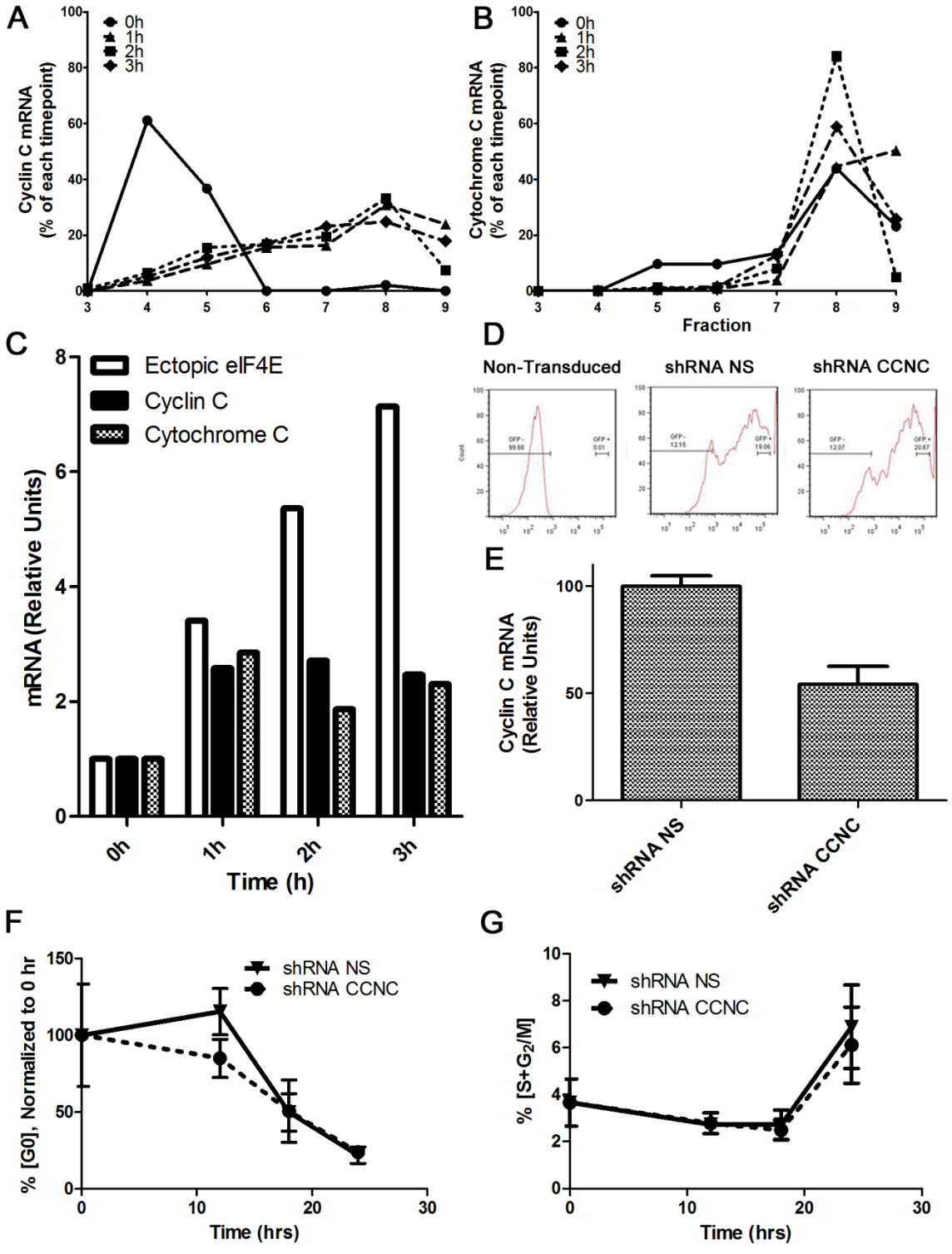
A
Cyclin C mRNA (% of each timepoint)
0h
1h
2h
3h
B
Cytochrome C mRNA (% of each timepoint)
Fraction
C
Ectopic eIF4E
Cyclin C
Cytochrome C
mRNA (Relative Units)
Time (h)
D
Non-Transduced
shRNA NS
shRNA CCNC
E
Cyclin C mRNA (Relative Units)
shRNA NS
shRNA CCNC
F
% [G0], Normalized to 0 hr
shRNA NS
shRNA CCNC
Time (hrs)
G
% [S+G2/M]
shRNA NS
shRNA CCNC
Time (hrs)

Figure 3-3 eIF4E-mediated cyclin C translational activation is not necessary for G0 exit and cell cycle transit

(A) mRNA from mifepristone treated 4E-inducible cells was stratified on a sucrose gradient and fractionated into 8 increasingly translationally active fractions, numbered 3 (lightest, fewest ribosomes bound) to 10 (heaviest, most ribosomes bound). mRNA was quantified by Q-PCR as a function of time after induction. Shown is the relative polysomal transcript abundance of cyclin C mRNA. Each data point is expressed as the percent of that fraction divided by the sum of fractions 3-10 for that timepoint (0, 1, 2 or 3 hrs). **(B)** Same for cytochrome C mRNA. **(C)** Time course of total cellular mRNA expression of HA-eIF4E, cyclin C, and cytochrome C. Quiescent 4E-inducible cells were incubated with mifepristone for up to 3 h, RNA purified and subjected to Q-PCR analysis. Data was normalized to a 0 h (baseline) value of 1.0. **(D-G)** 4E-inducible cells were transduced with a lentiviral shRNA construct expressing GFP which targeted either cyclin C (CCNC) or was non-silencing (NS). Cells were flow sorted for GFP expression **(D)**, and expanded GFP+ cells subjected to Q-PCR analysis of cyclin C. Error bars indicate duplicate Q-PCR samples in a single experiment (**E**). Unsorted cells were also quiesced, mifepristone treated for the indicated time period, and analyzed for cell cycle status. Shown is the percentage of GFP+ cells in G_0 normalized to the 0 hr timepoint **(F)** and GFP+ cells in $S+G_2$ **(G)** as a function of time. DNA and RNA content was quantified as performed previously. Shown is a representative replicate of 3 independent experiments. Error bars indicate quadruplicate samples within 1 individual experiment. The percentage of cells in G_0 is normalized to the GFP+ 0 hr timepoint, which showed 21.8% of cells in the GFP+ population.

Increased cyclin D1 is required but not sufficient for eIF4E-mediated cell cycle transit

We next examined the effect of eIF4E induction on negative and positive regulators of the G_1/S cell cycle checkpoint. To calibrate the response range, we utilized PDGF as a

single trophic agent and serum as a pleiotropic stimulus. Cyclin D1 was the only protein whose expression levels changed among the cell cycle regulators surveyed, increasing 8-fold in abundance (Figure 3-4).

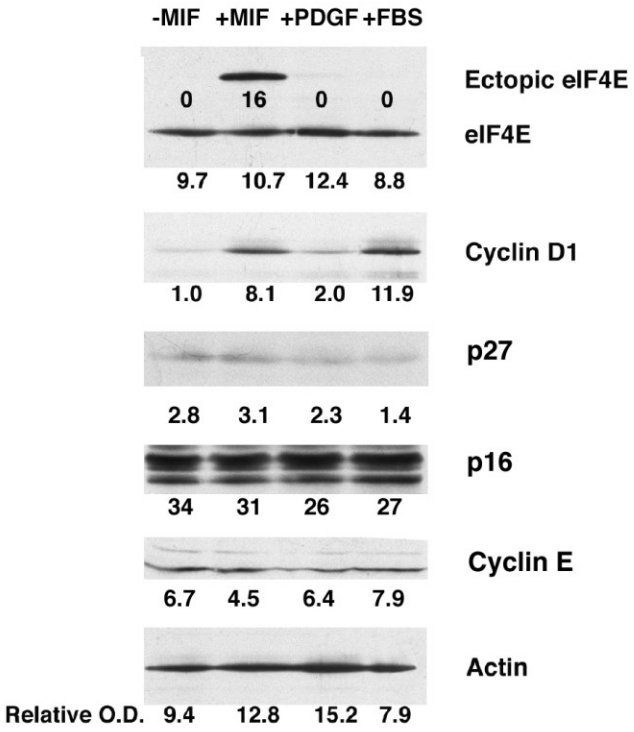

Figure 3-4 Abundance of G_1/S Checkpoint Regulators after eIF4E Induction

Quiescent cells were cultured with or without 625pM mifepristone for 24h, lysed and subjected to immunoblot analysis for a panel of G_1/S checkpoint regulators. 10% fetal bovine serum (FBS) and 50pM PDGF served as positive controls, and actin served as a loading control.

Prior studies indicate that when established NIH3T3 cell lines constitutively over express eIF4E, cyclin D1 abundance is increased through eIF4E facilitated nuclear export of the cyclin D1 mRNA, rather than through increased recruitment of ribosomes (131, 132). To

examine the mechanisms when eIF4E activity is abruptly increased, we monitored cyclin D1 mRNA abundance and its association with ribosomes. The total cellular mRNA abundance of cyclin D1 did not change after eIF4E induction (Figure 3-5A). Instead we observed a rapid translational activation of the cyclin D1 transcript (Figure 3-5B). This increased ribosome recruitment, coupled with increased nuclear export, can promote an increased accumulation of the cyclin D1 protein.

Introduction of cyclin D1 into quiescent primary hepatocytes is sufficient to trigger cell cycle transit (133, 134). Therefore, it was in principle possible that eIF4E mediated cell cycle transit might be mediated solely by the observed increase in cyclin D1. To address this issue, we utilized 3 different shRNA's, each targeting a different region of the cyclin D1 transcript, to achieve a knockdown of cyclin D1 ranging from 64%-85% (Figure 3-5C). There was a concomitant abrogation of eIF4E-mediated cell cycle transit in each case, including modest but reproducible suppression of basal S phase entry in the uninduced state (Figure 3-5D). Thus, eIF4E mediated cell cycle transit cannot be rescued by the pleiotropic effects of eIF4E on global translation; and depends upon the ability of eIF4E to increase cyclin D1.

To examine whether cyclin D1 alone was sufficient to trigger G_0 exit and cell cycle transit, we utilized an adenoviral expression system to ectopically express cyclin D1 (134). Quiescent cells were infected with adenovirus expressing cyclin D1 at a

multiplicity of infection (MOI) of 40 or 175; or induced with mifepristone. Adenovirus expressing beta-galactosidase at a MOI of 40 served as a negative control and 1nM PDGF served as a positive cell cycle control. We achieved comparable levels of cyclin D1 expression between mifepristone induced cells and cyclin D1 adenovirus infected cells at a MOI of 40 (Figure 3-5E). Nonetheless, ectopic cyclin D1 expression was not sufficient to increase the percentage of cells in S and G_2 phase either by itself or in combination with eIF4E induction (Figure 3-5F). A slight statistically significant difference ($p<0.003$) was seen with ectopic cyclin D1 expression in combination with PDGF compared with PDGF alone (52.88% S+G_2/M vs 50.22%). However , the combination of eIF4E induction and PDGF yielded a more striking increase in cell cycle transit (56.15% S+G_2/M vs 50.22%, $p<0.0001$) when compared to PDGF alone, and this increase (5.93%) was comparable to the increase in eIF4E induction alone (5.78%), when compared to control. A similar result was obtained for G_0 exit, as ectopic cyclin D1 was unable to alter the percentage of cells in G_0 either by itself, when paired with mifepristone, or when paired with PDGF (Figure 3-5G). Therefore, cyclin D1 is not sufficient to replace the effect of eIF4E on cell cycle transit and/or G_0 exit.

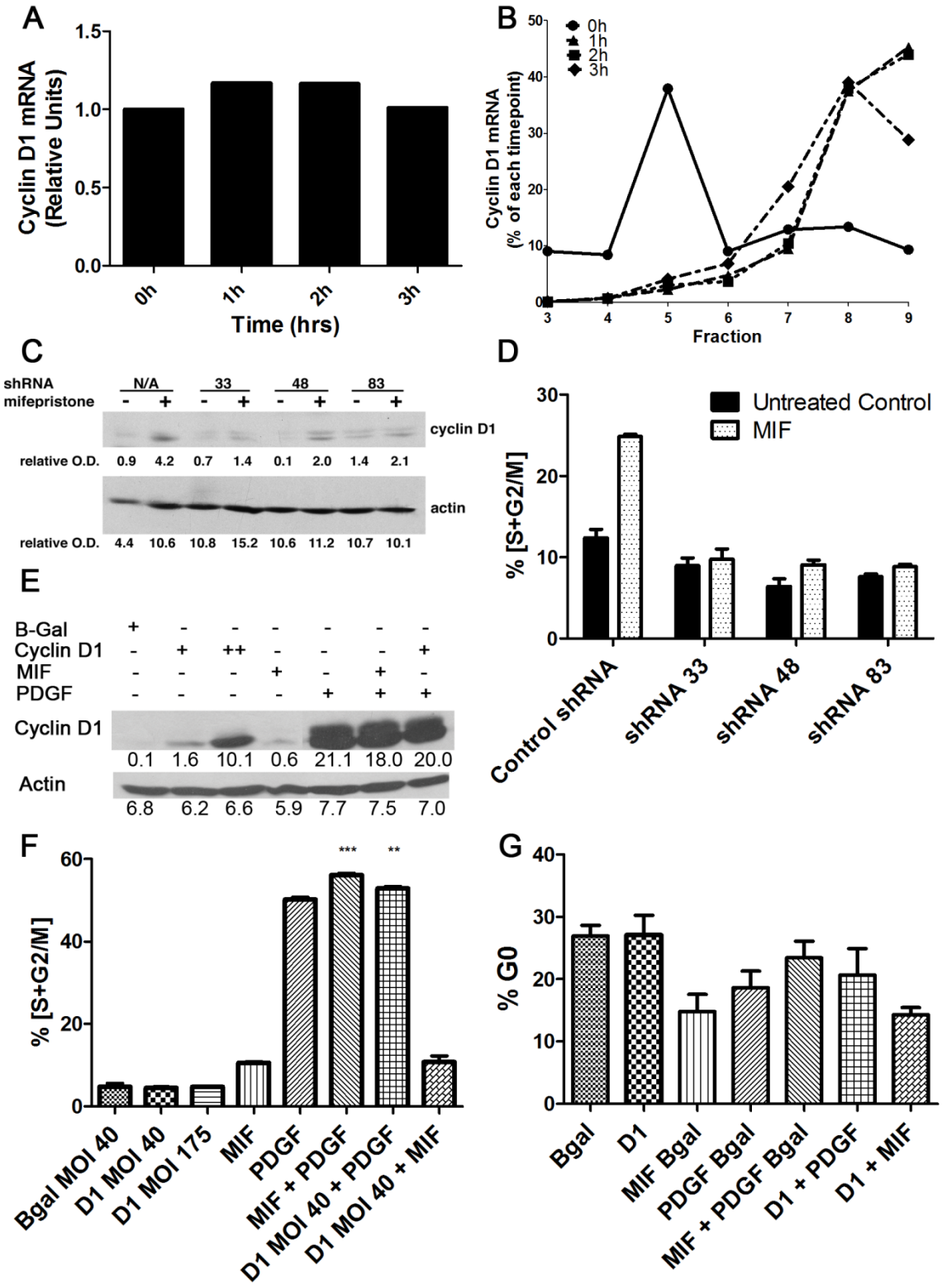
A
Cyclin D1 mRNA (Relative Units)
1.5
1.0
0.5
0.0
0h
1h
2h
3h
Time (hrs)
B
0h
1h
2h
3h
Cyclin D1 mRNA (% of each timepoint)
50
40
30
20
10
0
3
4
5
6
7
8
9
Fraction
C
shRNA
mifepristone
N/A
33
48
83
- + - + - + - +
cyclin D1
relative O.D. 0.9 4.2 0.7 1.4 0.1 2.0 1.4 2.1
actin
relative O.D. 4.4 10.6 10.8 15.2 10.6 11.2 10.7 10.1
D
Untreated Control
MIF
% [S+G2/M]
30
20
10
0
Control shRNA
shRNA 33
shRNA 48
shRNA 83
E
B-Gal + - - - - - -
Cyclin D1 - + ++ - - - +
MIF - - - + - + -
PDGF - - - - + + +
Cyclin D1
0.1 1.6 10.1 0.6 21.1 18.0 20.0
Actin
6.8 6.2 6.6 5.9 7.7 7.5 7.0
F
% [S+G2/M]
60
40
20
0
***
**
Bgal MOI 40
D1 MOI 40
D1 MOI 175
MIF
PDGF
MIF + PDGF
D1 MOI 40 + PDGF
D1 MOI 40 + MIF
G
% G0
40
30
20
10
0
Bgal
D1
MIF Bgal
PDGF Bgal
MIF + PDGF Bgal
D1 + PDGF
D1 + MIF

Figure 3-5 Increased cyclin D1 is required but not sufficient for eIF4E-mediated cell cycle transit

(A) Time course of cytoplasmic cyclin D1 mRNA expression. Quiescent 4E-inducible cells were incubated with mifepristone (625pM) for up to 3 h, RNA purified and subjected to Q-PCR analysis. Data was normalized to a 0 h (baseline) value of 1.0. **(B)** mRNA from mifepristone treated 4E-inducible cells was stratified on a sucrose gradient and quantified by Q-PCR as a function of time after induction. Shown is the relative polysomal transcript abundance of cyclin D1 mRNA. **(C)** 4E-inducible cells were transduced with one of three distinct lentiviral shRNA constructs, each targeting a different region of the cyclin D1 mRNA (designated shRNA 33, 48 or 83). Empty lentiviral vector is used as a control. Quiescent transduced cells were then incubated with or without mifepristone for 24h, lysed and subjected to immunoblot analysis for cytoplasmic cyclin D1. Actin is shown as a loading control. Numbers are relative optical density (OD). **(D)** 4E-inducible cells expressing one of the 3 cyclin D1 shRNA constructs or empty vector (control) were rendered quiescent, incubated for 24h with or without mifepristone, fixed, stained with propidium iodide, and DNA content was quantified by flow cytometry. Shown is the percent of cells in S+G_2/M. **(E)** 4E-inducible cells were transduced with one of two distinct adenoviruses: control virus expressing beta-galactosidase shRNA at a multiplicity of infection (MOI) of 40, or cyclin D1 shRNA at an MOI of 40 (+) or 175 (++). Quiescent cells were cultured for 24h as indicated with or without mifepristone (MIF) and 1nM PDGF, lysed and subjected to immunoblot analysis for cyclin D1. Actin is shown as a loading control. Numbers are relative optical density (OD). **(F)** Concurrent with panel E, treated cells were fixed, stained with propidium iodide, and DNA content was quantified by flow cytometry. Shown is the percent of cells in S+G_2/M. Shown is a representative replicate of 2 independent experiments, with error bars ±SD of triplicate samples from a single experiment. *** = $p < 0.001$ versus PDGF alone. ** = $p < 0.01$ versus PDGF alone. **(G)** Quiescent 4E-inducible cells were treated for 26h as indicated. DNA and RNA content was quantified by flow cytometry using Hoechst 33258 and Pyronin Y, respectively. Shown is the percent of cells in G_0. Shown is a representative replicate of 3 independent experiments, with error bars indicating ±SD of triplicate or quadruplicate samples from a single experiment.

eIF4E-mediated cell cycle transit follows the canonical growth factor pathway

To determine if eIF4E-mediated cell cycle transit followed the canonical growth factor initiated pathway, we traced the fate of cyclin D1 and its partner kinase cdk4 after eIF4E induction. Within 1h of induction, the abundance of ectopic eIF4E and cyclin D1 in the cytoplasm increased sharply, with a concomitant decrease in cdk4 that was even more pronounced at 2h (Figure 3-6A). Within this time frame, we found cyclin D1 associated with cdk4 (Figure 3-6B), and by 8h of induction we observed a 2-fold increase in Rb phosphorylation (Figure 3-6C). These data indicate that eIF4E enables cells to efficiently exit G_0 and initiate cell cycle transit by facilitating transit of the Rb-governed restriction point at the G_1/S phase boundary.

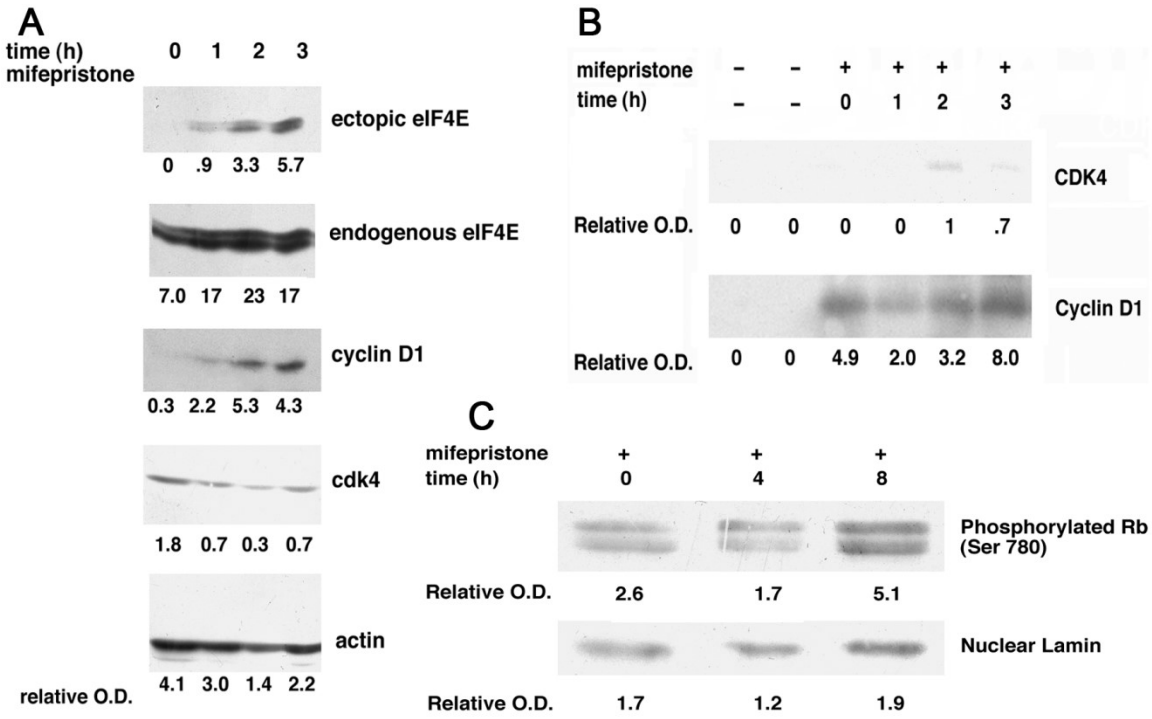

Figure 3-6 eIF4E-mediated cell cycle transit follows the canonical growth factor pathway.

Quiescent 4E-inducible cells were incubated with or without mifepristone for the indicated time interval, lysed, and separated into cytoplasmic or nuclear subcellular fractions. **(A)** Immunoblot analysis for cytoplasmic cdk4, cyclin D1, and eIF4E. Actin is shown as a loading control. Shown is a representative example of triplicate independent replicates. Numbers are relative optical density (OD). **(B)** Nuclear lysates were immunoprecipitated with anti-cyclin D1 antibody. Shown is a representative immunoblot for cdk4 and cyclin D1 of duplicate independent replicates. **(C)** Nuclear lysates were subjected to immunoblot analysis for Ser 780 phosphorylated Rb. Nuclear lamin is used as a loading control. Shown is a representative example of triplicate independent replicates.

Discussion

The eukaryotic translation initiation factor eIF4E exhibits an activity level above the physiological range in many human malignancies and serves as an indicator for poor prognosis (135). Previous investigations of eIF4E overexpression have focused on modeling the effects of high eIF4E activity as seen in *established* human malignancies by utilizing constitutive overexpression of eIF4E. However, data regarding the immediate molecular effects of eIF4E activation in the context of cancer genesis is lacking, even though eIF4E is thought to be an early event on the causal path to neoplastic transformation (31, 136-138). This gap in knowledge leaves uncertain whether disruption of translational control rapidly enables a key property of cancer, autonomous proliferation, or if this is an indirect effect generated from other accumulated mutations as seen in established cancers. Therefore, parsing eIF4E's contribution to promoting autonomous proliferation from other oncogenic alterations would not only provide insight on how deregulation of translation is essential for cancer initiation, but also for development of future targeted therapeutics.

To test whether abruptly increasing eIF4E abundance could confer cells autonomous proliferation, one of the hallmarks of cancer, we utilized an established model cell line in eIF4E research, NIH 3T3 cells, and introduced a mifepristone inducible eIF4E construct, thus allowing quantification of G_0 exit and cell cycle transit after increasing eIF4E

abundance to levels commonly found in early-stage human malignancies. Here we show that abrupt gain of eIF4E function in quiescent cells first triggers G_0 exit and then cell cycle transit by increasing ribosome recruitment to cyclins C and D1. Whereas cyclin C is not necessary for this effect; cyclin D1 is indispensable, although not sufficient. It is also apparent that eIF4Es primary cell cycle effect is pushing cells out of G_0, but the absence of complementary cell cycle transit indicates that a majority of these pushed cells are blocked from entering S phase and progressing through the cell cycle, thus limiting eIF4Es proliferative effect but providing a fertile ground for the cumulative effects of additional mutations. This adds additional mechanisms for eIF4Es potent role as an oncogene and function in cancer genesis while illustrating eIF4Es pleiotropic effects on human malignancy.

The relative importance of cyclin C on G_0 exit and cell cycle progression is still a matter of debate. Based on prior data, we expected cyclin C knockdown to delay G_0 exit and S-phase entry (111). However, although we only achieved a 54% knockdown of cyclin C, quiescent cells with severely decreased levels of cyclin C have been shown to still respond to growth signal induced proliferation by activating other major signaling pathways such as pAKT, pp42/44, and pp70 S6K (130). This may account for the retention of eIF4E-mediated G_0 exit and cell cycle transit we observed after cyclin C knockdown as the pleiotropic effects of eIF4E on cell growth-related factors (35) may be able to compensate for the loss of cyclin C. In addition, we believe the apparent

difference in the 12 hour G_0 timepoint (p=0.054) is not likely due to cyclin C knockdown, as the GFP- control cells (not expressing the shRNA construct) exhibited a similar difference to that observed in the GFP+ cells. Another possibility is that the enhanced eIF4E-mediated translation of cyclin C is able to overcome the relatively small 54% mRNA knockdown of cyclin C. Additional experimentation will be necessary to resolve the role of cyclin C in eIF4E-mediated G_0 exit.

Unfortunately the molecular mechanisms of G_0 exit have not been well defined, and current data suggests that there are multiple mechanisms available to the cell to exit G_0 (111, 139-145), compared to a single method of transiting the R point. This correlates with data indicating that colon adenocarcinomas overexpress multiple cyclins, and that cyclin C was the most commonly overexpressed cyclin and independently associated with an unfavorable prognosis (146). Taken together with our data, this indicates that although cyclin C is an important factor for G_0 exit and tumor maintenance, Cyclin C likely works in concert with multiple other factors and pathways which will need to be thoroughly analyzed using gain and loss of function studies. Unfortunately my attempts to define a panel (CDC6, Ki-67, p130, pRB (S807), CCNC) of protein and/or mRNA markers to preciously delineate G_0 from early G_1 were not successful due to inconsistent immunohistochemistry staining of $G_0/G_1/S/G_2$ sorted cells, and this remains an important research topic.

The importance of cyclin D1 expression in eIF4E-mediated cell cycle transit becomes more apparent after elaborating on the roles of p27 and cyclin E. In quiescent NIH 3T3 cells expressing ectopic cyclin D1, cyclin D1 forms an inactive complex with CDK4 due to simultaneous association with p27; and knockdown of p27 was required for S-phase entry (139). This may explain our observation that ectopically expressed cyclin D1 did not elicit G_0 exit or cell cycle transit by itself or with mifepristone, as mifepristone treatment had no effect on p27 levels. However, cyclin D1 overexpression did increase PDGF-mediated cell cycle transit as PDGF treatment alone decreased p27 levels by ~50%. Our data also indicate that although eIF4E-mediated cell cycle transit follows the canonical growth pathway via Rb phosphorylation; it is p27 independent; as ectopic eIF4E expression does not alter p27 protein levels, although eIF4E may affect p27 function rather than protein level. Further experimentation is needed to determine if knockdown of p27 increases eIF4E-mediated cell cycle transit as the eIF4E-mediated increase in translationally activated cyclin D1 should be more effective at eliciting cell cycle transit without p27 present. If this increase occurs it will be another example of the “fertile ground” eIF4E overexpression generates, by allowing an additive effect to the eIF4E-mediated increase in cell cycle transit, as was seen in induced cells further activated with PDGF. Further emphasizing the importance of cyclin D1 overexpression mediated by eIF4E, we did not detect any modulation in cyclin E activity after eIF4E induction. Increased cyclin E expression renders the cyclin D-cdk4 complex dispensable

for Rb activation and S phase entry (147). Therefore increased eIF4E activity increases cell cycle transit via translational activation of cyclin D1 without directly affecting p27 and cyclin E.

Our study provides novel insights into eIF4Es role as an oncogene. Enforced over expression of eIF4E translationally activates cyclins C and D1, stimulates G_0 exit and cell cycle transit, and thus is capable of bypassing key regulatory steps of the canonical growth factor pathway. However, an unidentified regulatory mechanism prevents the majority of cells which have exited G_0 from entering S phase, and the eventual fate of these cells is unknown. These cells are primed to respond to further oncogenic stimuli, thus allowing the cells to progress further towards a fully oncogenic phenotype. These observations establish eIF4Es potent pleotropic oncogenicity and further emphasize cap-dependent translational control as a crucial target for cancer therapy. Along those lines, second generation antisense oligonucleotides targeting eIF4E are currently undergoing clinical studies (54, 148).

Materials & Methods

Cell culture for inducible eIF4E system

Inducible eIF4E cells were generated as previously described. All experiments were performed with "4E-inducible" cells which express ectopic eIF4E at a level comparable to the endogenous gene, yielding an approximately 2-fold overexpression. 4E-inducible cells were maintained at 37^{o}C, 5% CO_2 in growth medium [Dulbecco's modified Eagle's medium high-glucose (DMEM, Sigma-Aldrich) supplemented with 10% fetal bovine serum (FBS, Sigma-Aldrich), 25mM Hepes, 100 units/ml penicillin, 100 units/ml streptomycin and 125 ng/ml amphotericin (Life Techologies)]. For our ectopic eIF4E induction studies, cells were first rendered quiescent in "defined medium" (F-12 supplemented with 25mM Hepes, 0.1 mg/ml bovine serum albumin, 10 mg/ml holo-transferrin, 10^{-8} M selenium, $3*10^{-6}$ M linoleic acid; with 40 ng/ml IGF + 5 ng/ml EGF to preserve viability; all components from Sigma-Aldrich) for 22 h (99); with cultures continued for the indicated amount of time in defined medium +/- the inducer mifepristone (625pM).

Cell cycle analysis

Cells were seeded in growth medium at 33,000 cells/35 mm well of a 6-well cluster. Growth medium was replaced with defined medium on day 7 for 22 h, shifted to

treatment medium (defined medium + treatment condition) for the indicated time period. Cultured cells were rinsed with PBS, detached with trypsin, washed with PBS + 1% FBS to inactivate trypsin, washed in staining buffer [Hank's balanced salt solution w/ magnesium chloride and calcium chloride (Life Technologies), supplemented with 1% FBS, 1g/L glucose, and 20 mM Hepes (pH 7.2)] and pelleted by centrifugation. Cells were resuspended in 1 ml staining buffer supplemented with Hoechst (40 µg/ml) and Pyronin Y (1 µg/ml), incubated for 45 min at 37^0C, washed in staining buffer and analyzed using an LSR II flow cytometer (Becton Dickinson [BD]). The percentages of cells with G_0, G_1, and S+G_2/M DNA content was determined with FlowJo software (version 7.5) using published protocols (111). All statistical values were generated using unpaired two-tailed t-tests, and all error bars indicate standard deviation.

Alternatively, for the cyclin D1 knockdown experiments cultured cells were detached with trypsin, washed with PBS, fixed with ice-cold 70% ethanol, and resuspended in propidium iodide (PI) staining mixture as previously described (28, 74) and analyzed using a FACSCalibur flow cytometer (Becton Dickinson). The percentage of cells with G1, S, and G2+M DNA content was determined using the FlowJo (version 7.5) program.

RNA preparation and quantification

Total cellular and ribosome-associated RNA were prepared as described previously (65). In order to assess ribosome recruitment mRNA transcripts, cell homogenates were

overlaid onto a 5 ml sucrose gradient, stratified by ultracentrifugation and fractionated into ten 0.5 ml fractions, numbered 1 (lightest, no ribosomes bound) to 10 (heaviest, most ribosomes bound). These ten fractions of 0.5 ml were collected into tubes containing 50 µl of 10% SDS.

To assess the effect of mifepristone induction on ectopic HA-eIF4E's overall transcript abundance and ribosome recruitment, total cellular RNA and fractions 3 to 10 of ribosome-associated RNA were individually purified using Tri-reagent (Sigma-Aldrich) and reverse transcribed to cDNA using the TaqMan reverse transcriptase kit (Roche). Fractions 1 and 2, containing translationally inactive RNA not bound to ribosomes, were not quantified. Quantitative PCR (Q-PCR) was performed using the Roche Light-Cycler 1.5 with SYBR Green dye (Roche). The primers used were cyclin D1: 5'-GCGTACCCTGACACCAATCT-3' (forward) and 5'-ATCTCCTTCTGCACGCACTT-3' (reverse), cyclin C: 5'- TCTCTGTCTGCTGTACCCTCCGTT-3' (forward) and 5'-TGGAGGTGGTTTTGGTTTCGGCAT-3' (reverse), cytochrome C: 5'-CATCCTGGACCTCCACCTC-3' (forward) and 5'-ACCTGGTGGGAGTGTGCTAC-3' (reverse) and HA-eIF4E: 5'-ACGTTCCAGATTACGCTGCT-3' (forward) and 5'-AGAGTGCCCACCTGTTCTGT-3" (reverse). The reaction products were subjected to gel electrophoresis to confirm the presence of a single PCR product of the appropriate length. Data from total cellular RNA was normalized to a 0 h (baseline) value of 1.0.

shRNA Viral Transduction

Lentiviral constructs (Open Biosystems) expressing small hairpin RNA against mouse cyclin D1 (–NM_007631) and mouse cyclin C (-NM_001122982, NM_016746) were generated from TRC clones for cyclin D1 and a V2LMM clone for cyclin C. The target sequences are:

Clone TRCN0000055233 – 5'-TCTAAGATGAAGGAGACCATT-3'

Clone TRCN0000026883 – 5'-CCACGATTTCATCGAACACTT-3'

Clone TRCN0000026948 – 5'-CCACAGATGTGAAGTTCATTT-3'

Clone V2LMM_52206 – 5'-CTTACAGGATGAATCATAT-3'

Viral production and transduction was performed as follows. Each shRNA construct was transfected along with viral helper plasmids (pMDG & pCMVΔ8.91) into HEK 293 cells using the Fugene6 (Roche) transfection reagent at 1:3 DNA to Fugene6 ratio (w:v). After 48 hours, media containing the virus was collected and filtered through a 0.45 µm filter, mixed (1:1 v/v for cyclin D1 and 1:5 v/v for cyclin C) with fresh growth medium containing 8 µg/ml polybrene (Sigma-Aldrich) and 4E-inducible cells maintained in 6-well dishes which were centrifuged at 2000 rpm for 1 hour. After a 48-66 hour 37°C incubation, the media was replaced with defined media and cultures continued for 24 hours. The media was then replaced with either defined media, induced with

mifepristone, or treated with 1μM PGDF for a treatment period of 0-24 hours. Cells were either processed for flow cytometry analysis, or collected for cyclin D1 immunoblot analysis, or sorted for GFP expression using a FACSAria cell sorter (BD). GFP expressing cells were sorted into negative or greatly positive populations as indicated. Each population was expanded for 4 days, and lysates were collected for qPCR analysis of cyclin C.

Immunoblot analysis

Cells were lysed with NP-40 lysis buffer [1% NP-40, 50 mM Tris pH 7.5, 150 mM NaCl (all Sigma-Aldrich)] supplemented with protease inhibitor (Roche) and protein quantified using a BCA protein assay kit (Pierce). Equal amounts of cell lysate protein per lane were subjected to SDS-PAGE and transferred onto nitrocellulose membranes. Antibodies directed against eIF4E (mouse monoclonal antibody, 1:500, BD Transduction Laboratories), actin (rabbit polyclonal antibody, 1:1500, Sigma-Aldrich), cyclin E (mouse monoclonal antibody, 1:500, Santa Cruz Biotechnology), cyclin D1 (mouse polyclonal antibody, 1:500, BD Pharmingen), p27 (mouse polyclonal antibody, 1:2500, BD Pharmingen), p16 (mouse polyclonal antibody, 1:1000, BD Pharmingen), Rb (mouse polyclonal antibody, 1:1000, BD Pharmingen), Phosphorylated Rb (Ser 780, rabbit polyclonal antibody 1:1000, Cell Signaling), and cdk 4 (mouse polyclonal antibody 1:1000, Cell Signaling) were used to identify these proteins. Lamin (mouse polyclonal

antibody 1:1000, Cell Signaling) served to identify the nuclear fraction after sub-cellular fractionation and actin (mouse polyclonal antibody, 1:500, Sigma) served as a loading control. Signal was detected with secondary antibodies conjugated to horseradish peroxidase (Calbiochem) and developed with chemiluminescent ECL Western Blotting Detection Reagents (GE Healthcare Life Sciences).

Preparation of recombinant adenovirus

Cyclin D1 and β-gal adenovirus were produced as described previously (134).

Sub-cellular fractionation

Protein analysis of cytoplasmic and nuclear compartments was conducted as previously described (40). Following subcellular fractionation, lysates were analyzed for eIF4E (ectopic & endogenous), cyclin D1, cdk4, and actin by immunoblot. Subcellular fractionation for Rb was conducted with the NER-PER® Nuclear and Cytoplasmic Kit (Thermo Scientific) as described in the product's protocol. Nuclear fractions were analyzed by immunoblot for phosphorylated Rb (ser 780) and nuclear Lamin.

Immunoprecipitation

We followed established procedures to conduct a cyclin D1 pull-down assay (149, 150).

Chapter 4 : THESIS CONCLUSION

These are the first studies to systematically examine translation genome-wide across the physiological range of eIF4E activity. We have shown that although increasing eIF4E activity translationally activates cyclin C and D1, neither of these activations are sufficient to fully explain eIF4Es proliferative effect. The genome-wide data further emphasizes this point, as eIF4E selectively and rapidly activates many cell cycle and proliferation-related genes. Although eIF4E pushed quiescent cells out of G_0, most were blocked from synthesizing DNA and completing a cell cycle. Coupled with eIF4Es ability to inhibit apoptosis and encourage survival, this provides these translationally deregulated cells fertile ground for an erroneous response to mitogenic stimulation and the accumulation of DNA-damage induced mutations generated by a partial transit of the cell cycle. The elucidation of the molecular mechanism of this block and the process utilized by pre-malignant cells to overcome it could greatly improve cancer prevention and detection. Our successful characterization of the 3'UTR and 5'UTR structural features of 4E-hypersensitive genes allows us to propose potential mechanisms for the eIF4E-mediated 3'UTR mRNA regulation, cell cycle progression, and oncogenic capability discussed previously in this dissertation.

Therefore the next step is targeted treatment of the translational apparatus in the treatment of many cancers and fibrotic diseases. This thesis outlines a potential

approach for dissecting the translational apparatus in various malignancies with deregulated translational control. The recent development of a repertoire of small molecule inhibitors targeting specific functions of eIF4E, mTOR, eIF4A, eIF4G, Mnks, and other key translational proteins allows a thorough structural and functional characterization of the selection and regulation of specific mRNAs by the translational apparatus. These and other studies provide the foundation for future studies in which precisely targeted reclamation of physiological translational control is utilized as cancer therapy.

Bibliography

References

1. Schwanhausser B, Busse D, Li N, Dittmar G, Schuchhardt J, Wolf J, et al. Global quantification of mammalian gene expression control. Nature. 2011 May 19;473(7347):337-42.

2. Komar AA, Mazumder B, Merrick WC. A new framework for understanding IRES-mediated translation. Gene. 2012 Jul 10;502(2):75-86.

3. Goss DJ, Carberry SE, Dever TE, Merrick WC, Rhoads RE. A fluorescence study of the interaction of protein synthesis initiation factors 4A, 4E, and 4F with mRNA and oligonucleotide analogs. Biochim Biophys Acta. 1990 Aug 27;1050(1-3):163-6.

4. Sonenberg N, Hinnebusch AG. Regulation of translation initiation in eukaryotes: Mechanisms and biological targets. Cell. 2009 Feb 20;136(4):731-45.

5. Culjkovic B, Topisirovic I, Borden KL. Controlling gene expression through RNA regulons: The role of the eukaryotic translation initiation factor eIF4E. Cell Cycle. 2007 Jan 1;6(1):65-9.

6. Holcik M, Sonenberg N. Translational control in stress and apoptosis. Nat Rev Mol Cell Biol. 2005 Apr;6(4):318-27.

7. Liwak U, Faye MD, Holcik M. Translation control in apoptosis. Exp Oncol. 2012 Oct;34(3):218-30.

8. Gingras AC, Raught B, Sonenberg N. eIF4 initiation factors: Effectors of mRNA recruitment to ribosomes and regulators of translation. Annu Rev Biochem. 1999;68:913-63.

9. Duncan R, Milburn SC, Hershey JW. Regulated phosphorylation and low abundance of HeLa cell initiation factor eIF-4F suggest a role in translational control. heat shock effects on eIF-4F. J Biol Chem. 1987 Jan 5;262(1):380-8.

10. Hershey JW. Translational control in mammalian cells. Annu Rev Biochem. 1991;60:717-55.

11. Slepenkov SV, Darzynkiewicz E, Rhoads RE. Stopped-flow kinetic analysis of eIF4E and phosphorylated eIF4E binding to cap analogs and capped oligoribonucleotides: Evidence for a one-step binding mechanism. J Biol Chem. 2006 May 26;281(21):14927-38.

12. Blachut-Okrasinska E, Bojarska E, Stepinski J, Antosiewicz JM. Kinetics of binding the mRNA cap analogues to the translation initiation factor eIF4E under second-order reaction conditions. Biophys Chem. 2007 Sep;129(2-3):289-97.

13. Darzynkiewicz E, Ekiel I, Lassota P, Tahara SM. Inhibition of eukaryotic translation by analogues of messenger RNA 5'-cap: Chemical and biological consequences of 5'-phosphate modifications of 7-methylguanosine 5'-monophosphate. Biochemistry. 1987 Jul 14;26(14):4372-80.

14. Jia Y, Polunovsky V, Bitterman PB, Wagner CR. Cap-dependent translation initiation factor eIF4E: An emerging anticancer drug target. Med Res Rev. 2012 Jul;32(4):786-814.

15. Joshi B, Lee K, Maeder DL, Jagus R. Phylogenetic analysis of eIF4E-family members. BMC Evol Biol. 2005 Sep 28;5:48.

16. Joshi B, Cameron A, Jagus R. Characterization of mammalian eIF4E-family members. Eur J Biochem. 2004 Jun;271(11):2189-203.

17. Osborne MJ, Volpon L, Kornblatt JA, Culjkovic-Kraljacic B, Baguet A, Borden KL. eIF4E3 acts as a tumor suppressor by utilizing an atypical mode of methyl-7-guanosine cap recognition. Proc Natl Acad Sci U S A. 2013 Mar 5;110(10):3877-82.

18. Kubacka D, Kamenska A, Broomhead H, Minshall N, Darzynkiewicz E, Standart N. Investigating the consequences of eIF4E2 (4EHP) interaction with 4E-transporter on its cellular distribution in HeLa cells. PLoS One. 2013 Aug 21;8(8):e72761.

19. Pause A, Methot N, Svitkin Y, Merrick WC, Sonenberg N. Dominant negative mutants of mammalian translation initiation factor eIF-4A define a critical role for eIF-4F in cap-dependent and cap-independent initiation of translation. EMBO J. 1994 Mar 1;13(5):1205-15.

20. Kahvejian A, Svitkin YV, Sukarieh R, M'Boutchou MN, Sonenberg N. Mammalian poly(A)-binding protein is a eukaryotic translation initiation factor, which acts via multiple mechanisms. Genes Dev. 2005 Jan 1;19(1):104-13.

21. Meric F, Hunt KK. Translation initiation in cancer: A novel target for therapy. Mol Cancer Ther. 2002 Sep;1(11):971-9.

22. Kong J, Lasko P. Translational control in cellular and developmental processes. Nat Rev Genet. 2012 Jun;13(6):383-94.

23. Komar AA, Hatzoglou M. Internal ribosome entry sites in cellular mRNAs: Mystery of their existence. J Biol Chem. 2005 Jun 24;280(25):23425-8.

24. Jackson RJ. The current status of vertebrate cellular mRNA IRESs. Cold Spring Harb Perspect Biol. 2013 Feb 1;5(2):10.1101/cshperspect.a011569.

25. Blau L, Knirsh R, Ben-Dror I, Oren S, Kuphal S, Hau P, et al. Aberrant expression of c-jun in glioblastoma by internal ribosome entry site (IRES)-mediated translational activation. Proc Natl Acad Sci U S A. 2012 Oct 16;109(42):E2875-84.

26. Dobson T, Chen J, Krushel LA. Dysregulating IRES-dependent translation contributes to overexpression of oncogenic aurora A kinase. Mol Cancer Res. 2013 Aug;11(8):887-900.

27. Frost P, Berlanger E, Mysore V, Hoang B, Shi Y, Gera J, et al. Mammalian target of rapamycin inhibitors induce tumor cell apoptosis in vivo primarily by inhibiting VEGF expression and angiogenesis. J Oncol. 2013;2013:897025.

28. Polunovsky VA, Rosenwald IB, Tan AT, White J, Chiang L, Sonenberg N, et al. Translational control of programmed cell death: Eukaryotic translation initiation factor 4E blocks apoptosis in growth-factor-restricted fibroblasts with physiologically expressed or deregulated myc. Mol Cell Biol. 1996 Nov;16(11):6573-81.

29. De Benedetti A, Rhoads RE. Overexpression of eukaryotic protein synthesis initiation factor 4E in HeLa cells results in aberrant growth and morphology. Proc Natl Acad Sci U S A. 1990 Nov;87(21):8212-6.

30. Lazaris-Karatzas A, Montine KS, Sonenberg N. Malignant transformation by a eukaryotic initiation factor subunit that binds to mRNA 5' cap. Nature. 1990 Jun 7;345(6275):544-7.

31. Avdulov S, Li S, Michalek V, Burrichter D, Peterson M, Perlman DM, et al. Activation of translation complex eIF4F is essential for the genesis and maintenance of the malignant phenotype in human mammary epithelial cells. Cancer Cell. 2004 Jun;5(6):553-63.

32. Lazaris-Karatzas A, Sonenberg N. The mRNA 5' cap-binding protein, eIF-4E, cooperates with v-myc or E1A in the transformation of primary rodent fibroblasts. Mol Cell Biol. 1992 Mar;12(3):1234-8.

33. Topisirovic I, Svitkin YV, Sonenberg N, Shatkin AJ. Cap and cap-binding proteins in the control of gene expression. Wiley Interdiscip Rev RNA. 2011 Mar-Apr;2(2):277-98.

34. de Andrade JA, Thannickal VJ. Innovative approaches to the therapy of fibrosis. Curr Opin Rheumatol. 2009 Nov;21(6):649-55.

35. Mamane Y, Petroulakis E, Martineau Y, Sato TA, Larsson O, Rajasekhar VK, et al. Epigenetic activation of a subset of mRNAs by eIF4E explains its effects on cell proliferation. PLoS One. 2007 Feb 21;2(2):e242.

36. Koromilas AE, Lazaris-Karatzas A, Sonenberg N. mRNAs containing extensive secondary structure in their 5' non-coding region translate efficiently in cells overexpressing initiation factor eIF-4E. EMBO J. 1992 Nov;11(11):4153-8.

37. van der Velden AW, Thomas AA. The role of the 5' untranslated region of an mRNA in translation regulation during development. Int J Biochem Cell Biol. 1999 Jan;31(1):87-106.

38. Shantz LM, Hu RH, Pegg AE. Regulation of ornithine decarboxylase in a transformed cell line that overexpresses translation initiation factor eIF-4E. Cancer Res. 1996 Jul 15;56(14):3265-9.

39. Fagan RJ, Lazaris-Karatzas A, Sonenberg N, Rozen R. Translational control of ornithine aminotransferase. modulation by initiation factor eIF-4E. J Biol Chem. 1991 Sep 5;266(25):16518-23.

40. Rousseau D, Kaspar R, Rosenwald I, Gehrke L, Sonenberg N. Translation initiation of ornithine decarboxylase and nucleocytoplasmic transport of cyclin D1 mRNA are increased in cells overexpressing eukaryotic initiation factor 4E. Proc Natl Acad Sci U S A. 1996 Feb 6;93(3):1065-70.

41. Buechler RD, Peffley DM. Proto oncogene/eukaryotic translation initiation factor (eIF) 4E attenuates mevalonate-mediated regulation of 3-hydroxy-3-methylglutaryl coenzyme A (HMG-CoA) reductase synthesis. Mol Carcinog. 2004 Sep;41(1):39-53.

42. Abid MR, Li Y, Anthony C, De Benedetti A. Translational regulation of ribonucleotide reductase by eukaryotic initiation factor 4E links protein synthesis to the control of DNA replication. J Biol Chem. 1999 Dec 10;274(50):35991-8.

43. Kevil CG, De Benedetti A, Payne DK, Coe LL, Laroux FS, Alexander JS. Translational regulation of vascular permeability factor by eukaryotic initiation factor 4E: Implications for tumor angiogenesis. Int J Cancer. 1996 Mar 15;65(6):785-90.

44. Pause A, Belsham GJ, Gingras AC, Donze O, Lin TA, Lawrence JC,Jr, et al. Insulin-dependent stimulation of protein synthesis by phosphorylation of a regulator of 5'-cap function. Nature. 1994 Oct 27;371(6500):762-7.

45. Morita M, Gravel SP, Chenard V, Sikstrom K, Zheng L, Alain T, et al. mTORC1 controls mitochondrial activity and biogenesis through 4E-BP-dependent translational regulation. Cell Metab. 2013 Nov 5;18(5):698-711.

46. Zoncu R, Efeyan A, Sabatini DM. mTOR: From growth signal integration to cancer, diabetes and ageing. Nat Rev Mol Cell Biol. 2011 Jan;12(1):21-35.

47. Chen XG, Liu F, Song XF, Wang ZH, Dong ZQ, Hu ZQ, et al. Rapamycin regulates akt and ERK phosphorylation through mTORC1 and mTORC2 signaling pathways. Mol Carcinog. 2010 Jun;49(6):603-10.

48. Cheng H, Walls M, Baxi SM, Yin MJ. Targeting the mTOR pathway in tumor malignancy. Curr Cancer Drug Targets. 2013 Mar;13(3):267-77.

49. Luscher B, Vervoorts J. Regulation of gene transcription by the oncoprotein MYC. Gene. 2012 Feb 25;494(2):145-60.

50. Eilers M, Picard D, Yamamoto KR, Bishop JM. Chimaeras of myc oncoprotein and steroid receptors cause hormone-dependent transformation of cells. Nature. 1989 Jul 6;340(6228):66-8.

51. Jones RM, Branda J, Johnston KA, Polymenis M, Gadd M, Rustgi A, et al. An essential E box in the promoter of the gene encoding the mRNA cap-binding protein (eukaryotic initiation factor 4E) is a target for activation by c-myc. Mol Cell Biol. 1996 Sep;16(9):4754-64.

52. Lin CJ, Cencic R, Mills JR, Robert F, Pelletier J. C-myc and eIF4F are components of a feedforward loop that links transcription and translation. Cancer Res. 2008 Jul 1;68(13):5326-34.

53. De Benedetti A, Joshi B, Graff JR, Zimmer SG. CHO cells transformed by the translation factor eIF4E display increased c-myc expression, but require overexpression of max for tumorigenicity. Mol Cell Differ. 1994;2:347-71.

54. Graff JR, Konicek BW, Vincent TM, Lynch RL, Monteith D, Weir SN, et al. Therapeutic suppression of translation initiation factor eIF4E expression reduces tumor growth without toxicity. J Clin Invest. 2007 Sep;117(9):2638-48.

55. Lin CJ, Malina A, Pelletier J. C-myc and eIF4F constitute a feedforward loop that regulates cell growth: Implications for anticancer therapy. Cancer Res. 2009 Oct 1;69(19):7491-4.

56. Waskiewicz AJ, Flynn A, Proud CG, Cooper JA. Mitogen-activated protein kinases activate the serine/threonine kinases Mnk1 and Mnk2. EMBO J. 1997 Apr 15;16(8):1909-20.

57. Pyronnet S, Imataka H, Gingras AC, Fukunaga R, Hunter T, Sonenberg N. Human eukaryotic translation initiation factor 4G (eIF4G) recruits mnk1 to phosphorylate eIF4E. EMBO J. 1999 Jan 4;18(1):270-9.

58. Scheper GC, Morrice NA, Kleijn M, Proud CG. The mitogen-activated protein kinase signal-integrating kinase Mnk2 is a eukaryotic initiation factor 4E kinase with high levels of basal activity in mammalian cells. Mol Cell Biol. 2001 Feb;21(3):743-54.

59. Stead RL, Proud CG. Rapamycin enhances eIF4E phosphorylation by activating MAP kinase-interacting kinase 2a (Mnk2a). FEBS Lett. 2013 Aug 19;587(16):2623-8.

60. Topisirovic I, Ruiz-Gutierrez M, Borden KL. Phosphorylation of the eukaryotic translation initiation factor eIF4E contributes to its transformation and mRNA transport activities. Cancer Res. 2004 Dec 1;64(23):8639-42.

61. Ueda T, Watanabe-Fukunaga R, Fukuyama H, Nagata S, Fukunaga R. Mnk2 and Mnk1 are essential for constitutive and inducible phosphorylation of eukaryotic initiation factor 4E but not for cell growth or development. Mol Cell Biol. 2004 Aug;24(15):6539-49.

62. Hou J, Lam F, Proud C, Wang S. Targeting mnks for cancer therapy. Oncotarget. 2012 Feb;3(2):118-31.

63. Herdy B, Jaramillo M, Svitkin YV, Rosenfeld AB, Kobayashi M, Walsh D, et al. Translational control of the activation of transcription factor NF-kappaB and production

of type I interferon by phosphorylation of the translation factor eIF4E. Nat Immunol. 2012 Apr 29;13(6):543-50.

64. Larsson O, Tian B, Sonenberg N. Toward a genome-wide landscape of translational control. Cold Spring Harb Perspect Biol. 2013 Jan 1;5(1):a012302.

65. Larsson O, Perlman DM, Fan D, Reilly CS, Peterson M, Dahlgren C, et al. Apoptosis resistance downstream of eIF4E: Posttranscriptional activation of an anti-apoptotic transcript carrying a consensus hairpin structure. Nucleic Acids Res. 2006;34(16):4375-86.

66. Larsson O, Li S, Issaenko OA, Avdulov S, Peterson M, Smith K, et al. Eukaryotic translation initiation factor 4E induced progression of primary human mammary epithelial cells along the cancer pathway is associated with targeted translational deregulation of oncogenic drivers and inhibitors. Cancer Res. 2007 Jul 15;67(14):6814-24.

67. Kim YY, Von Weymarn L, Larsson O, Fan D, Underwood JM, Peterson MS, et al. Eukaryotic initiation factor 4E binding protein family of proteins: Sentinels at a translational control checkpoint in lung tumor defense. Cancer Res. 2009 Nov 1;69(21):8455-62.

68. Mathonnet G, Fabian MR, Svitkin YV, Parsyan A, Huck L, Murata T, et al. MicroRNA inhibition of translation initiation in vitro by targeting the cap-binding complex eIF4F. Science. 2007 Sep 21;317(5845):1764-7.

69. Rosenwald IB, Rhoads DB, Callanan LD, Isselbacher KJ, Schmidt EV. Increased expression of eukaryotic translation initiation factors eIF-4E and eIF-2 alpha in response to growth induction by c-myc. Proc Natl Acad Sci U S A. 1993 Jul 1;90(13):6175-8.

70. Thoreen CC, Chantranupong L, Keys HR, Wang T, Gray NS, Sabatini DM. A unifying model for mTORC1-mediated regulation of mRNA translation. Nature. 2012 May 2;485(7396):109-13.

71. Hsieh AC, Liu Y, Edlind MP, Ingolia NT, Janes MR, Sher A, et al. The translational landscape of mTOR signalling steers cancer initiation and metastasis. Nature. 2012 Feb 22;485(7396):55-61.

72. Kaspar RL, Rychlik W, White MW, Rhoads RE, Morris DR. Simultaneous cytoplasmic redistribution of ribosomal protein L32 mRNA and phosphorylation of eukaryotic

initiation factor 4E after mitogenic stimulation of swiss 3T3 cells. J Biol Chem. 1990 Mar 5;265(7):3619-22.

73. Ghosh B, Benyumov AO, Ghosh P, Jia Y, Avdulov S, Dahlberg PS, et al. Nontoxic chemical interdiction of the epithelial-to-mesenchymal transition by targeting cap-dependent translation. ACS Chem Biol. 2009 May 15;4(5):367-77.

74. Li S, Sonenberg N, Gingras AC, Peterson M, Avdulov S, Polunovsky VA, et al. Translational control of cell fate: Availability of phosphorylation sites on translational repressor 4E-BP1 governs its proapoptotic potency. Mol Cell Biol. 2002 Apr;22(8):2853-61.

75. Li S, Jia Y, Jacobson B, McCauley J, Kratzke R, Bitterman PB, et al. Treatment of breast and lung cancer cells with a N-7 benzyl guanosine monophosphate tryptamine phosphoramidate pronucleotide (4Ei-1) results in chemosensitization to gemcitabine and induced eIF4E proteasomal degradation. Mol Pharm. 2013 Feb 4;10(2):523-31.

76. Lee KS, Tsien RW. Mechanism of calcium channel blockade by verapamil, D600, diltiazem and nitrendipine in single dialysed heart cells. Nature. 1983 Apr 28;302(5911):790-4.

77. Bjur E, Larsson O, Yurchenko E, Zheng L, Gandin V, Topisirovic I, et al. Distinct translational control in CD4(+) T cell subsets. PLoS Genet. 2013 May;9(5):e1003494.

78. Culjkovic B, Topisirovic I, Skrabanek L, Ruiz-Gutierrez M, Borden KL. eIF4E is a central node of an RNA regulon that governs cellular proliferation. J Cell Biol. 2006 Nov 6;175(3):415-26.

79. Khabar KS. Post-transcriptional control during chronic inflammation and cancer: A focus on AU-rich elements. Cell Mol Life Sci. 2010 Sep;67(17):2937-55.

80. Vlasova IA, Tahoe NM, Fan D, Larsson O, Rattenbacher B, Sternjohn JR, et al. Conserved GU-rich elements mediate mRNA decay by binding to CUG-binding protein 1. Mol Cell. 2008 Feb 1;29(2):263-70.

81. Rattenbacher B, Beisang D, Wiesner DL, Jeschke JC, von Hohenberg M, St Louis-Vlasova IA, et al. Analysis of CUGBP1 targets identifies GU-repeat sequences that mediate rapid mRNA decay. Mol Cell Biol. 2010 Aug;30(16):3970-80.

82. Silvera D, Formenti SC, Schneider RJ. Translational control in cancer. Nat Rev Cancer. 2010 Apr;10(4):254-66.

83. Provenzani A, Fronza R, Loreni F, Pascale A, Amadio M, Quattrone A. Global alterations in mRNA polysomal recruitment in a cell model of colorectal cancer progression to metastasis. Carcinogenesis. 2006 Jul;27(7):1323-33.

84. Pestova TV, Kolupaeva VG, Lomakin IB, Pilipenko EV, Shatsky IN, Agol VI, et al. Molecular mechanisms of translation initiation in eukaryotes. Proc Natl Acad Sci U S A. 2001 Jun 19;98(13):7029-36.

85. Cawley A, Warwicker J. eIF4E-binding protein regulation of mRNAs with differential 5'-UTR secondary structure: A polyelectrostatic model for a component of protein-mRNA interactions. Nucleic Acids Res. 2012 Sep;40(16):7666-75.

86. Santhanam AN, Bindewald E, Rajasekhar VK, Larsson O, Sonenberg N, Colburn NH, et al. Role of 3'UTRs in the translation of mRNAs regulated by oncogenic eIF4E--a computational inference. PLoS One. 2009;4(3):e4868.

87. Hamilton TL, Stoneley M, Spriggs KA, Bushell M. TOPs and their regulation. Biochem Soc Trans. 2006 Feb;34(Pt 1):12-6.

88. Ruggero D, Pandolfi PP. Does the ribosome translate cancer? Nat Rev Cancer. 2003 Mar;3(3):179-92.

89. Ferraiuolo MA, Basak S, Dostie J, Murray EL, Schoenberg DR, Sonenberg N. A role for the eIF4E-binding protein 4E-T in P-body formation and mRNA decay. J Cell Biol. 2005 Sep 12;170(6):913-24.

90. Parker R, Sheth U. P bodies and the control of mRNA translation and degradation. Mol Cell. 2007 Mar 9;25(5):635-46.

91. Andrei MA, Ingelfinger D, Heintzmann R, Achsel T, Rivera-Pomar R, Luhrmann R. A role for eIF4E and eIF4E-transporter in targeting mRNPs to mammalian processing bodies. RNA. 2005 May;11(5):717-27.

92. Kedersha N, Tisdale S, Hickman T, Anderson P. Real-time and quantitative imaging of mammalian stress granules and processing bodies. Methods Enzymol. 2008;448:521-52.

93. Sandler H, Kreth J, Timmers HT, Stoecklin G. Not1 mediates recruitment of the deadenylase Caf1 to mRNAs targeted for degradation by tristetraprolin. Nucleic Acids Res. 2011 May;39(10):4373-86.

94. Otulakowski G, Duan W, O'Brodovich H. Global and gene-specific translational regulation in rat lung development. Am J Respir Cell Mol Biol. 2009 May;40(5):555-67.

95. Schwarz KW, Murray MT, Sylora R, Sohn RL, Dulchavsky SA. Augmentation of wound healing with translation initiation factor eIF4E mRNA. J Surg Res. 2002 Apr;103(2):175-82.

96. McKendrick L, Thompson E, Ferreira J, Morley SJ, Lewis JD. Interaction of eukaryotic translation initiation factor 4G with the nuclear cap-binding complex provides a link between nuclear and cytoplasmic functions of the m(7) guanosine cap. Mol Cell Biol. 2001 Jun;21(11):3632-41.

97. Kafasla P, Barrass JD, Thompson E, Fromont-Racine M, Jacquier A, Beggs JD, et al. Interaction of yeast eIF4G with spliceosome components: Implications in pre-mRNA processing events. RNA Biol. 2009 Nov-Dec;6(5):563-74.

98. Wang Y, Yang D, Song L, Li T, Yang J, Zhang X, et al. Mifepristone-inducible caspase-1 expression in mouse embryonic stem cells eliminates tumor formation but spares differentiated cells in vitro and in vivo. Stem Cells. 2012 Feb;30(2):169-79.

99. Pledger WJ, Stiles CD, Antoniades HN, Scher CD. Induction of DNA synthesis in BALB/c 3T3 cells by serum components: Reevaluation of the commitment process. Proc Natl Acad Sci U S A. 1977 Oct;74(10):4481-5.

100. Johnson WE, Li C, Rabinovic A. Adjusting batch effects in microarray expression data using empirical bayes methods. Biostatistics. 2007 Jan;8(1):118-27.

101. Larsson O, Sonenberg N, Nadon R. Identification of differential translation in genome wide studies. Proc Natl Acad Sci U S A. 2010 Dec 14;107(50):21487-92.

102. Larsson O, Sonenberg N, Nadon R. Anota: Analysis of differential translation in genome-wide studies. Bioinformatics. 2011 May 15;27(10):1440-1.

103. Wright GW, Simon RM. A random variance model for detection of differential gene expression in small microarray experiments. Bioinformatics. 2003 Dec 12;19(18):2448-55.

104. Kent WJ, Sugnet CW, Furey TS, Roskin KM, Pringle TH, Zahler AM, et al. The human genome browser at UCSC. Genome Res. 2002 Jun;12(6):996-1006.

105. Meyer LR, Zweig AS, Hinrichs AS, Karolchik D, Kuhn RM, Wong M, et al. The UCSC genome browser database: Extensions and updates 2013. Nucleic Acids Res. 2013 Jan;41(Database issue):D64-9.

106. Carlson M, Pages H, Aboyoun P, Falcon S, Morgan M, Sarkar D, et al. GenomicFeatures: Tools for making and manipulating transcript centric annotations. 2013;R package version 1.10.2.

107. Carlson M. TxDb.mmusculus.UCSC.mm9.knownGene: Annotation package for TranscriptDb object(s). . 2012;R package version 2.8.

108. Lewis BP, Burge CB, Bartel DP. Conserved seed pairing, often flanked by adenosines, indicates that thousands of human genes are microRNA targets. Cell. 2005 Jan 14;120(1):15-20.

109. Halees AS, El-Badrawi R, Khabar KS. ARED organism: Expansion of ARED reveals AU-rich element cluster variations between human and mouse. Nucleic Acids Res. 2008 Jan;36(Database issue):D137-40.

110. Ashburner M, Ball CA, Blake JA, Botstein D, Butler H, Cherry JM, et al. Gene ontology: Tool for the unification of biology. the gene ontology consortium. Nat Genet. 2000 May;25(1):25-9.

111. Ren S, Rollins BJ. Cyclin C/cdk3 promotes rb-dependent G0 exit. Cell. 2004 Apr 16;117(2):239-51.

112. Orford KW, Scadden DT. Deconstructing stem cell self-renewal: Genetic insights into cell-cycle regulation. Nat Rev Genet. 2008 Feb;9(2):115-28.

113. Pyronnet S, Sonenberg N. Cell-cycle-dependent translational control. Curr Opin Genet Dev. 2001 Feb;11(1):13-8.

114. Liu ZJ, Ueda T, Miyazaki T, Tanaka N, Mine S, Tanaka Y, et al. A critical role for cyclin C in promotion of the hematopoietic cell cycle by cooperation with c-myc. Mol Cell Biol. 1998 Jun;18(6):3445-54.

115. Miyata Y, Liu Y, Jankovic V, Sashida G, Lee JM, Shieh JH, et al. Cyclin C regulates human hematopoietic stem/progenitor cell quiescence. Stem Cells. 2010 Feb;28(2):308-17.

116. Rickert P, Seghezzi W, Shanahan F, Cho H, Lees E. Cyclin C/CDK8 is a novel CTD kinase associated with RNA polymerase II. Oncogene. 1996 Jun 20;12(12):2631-40.

117. Sage J, Miller AL, Perez-Mancera PA, Wysocki JM, Jacks T. Acute mutation of retinoblastoma gene function is sufficient for cell cycle re-entry. Nature. 2003 Jul 10;424(6945):223-8.

118. Pardee AB. G1 events and regulation of cell proliferation. Science. 1989 Nov 3;246(4930):603-8.

119. Matsushime H, Quelle DE, Shurtleff SA, Shibuya M, Sherr CJ, Kato JY. D-type cyclin-dependent kinase activity in mammalian cells. Mol Cell Biol. 1994 Mar;14(3):2066-76.

120. Kitagawa M, Higashi H, Jung HK, Suzuki-Takahashi I, Ikeda M, Tamai K, et al. The consensus motif for phosphorylation by cyclin D1-Cdk4 is different from that for phosphorylation by cyclin A/E-Cdk2. EMBO J. 1996 Dec 16;15(24):7060-9.

121. Pontano LL, Diehl JA. Speeding through cell cycle roadblocks: Nuclear cyclin D1-dependent kinase and neoplastic transformation. Cell Div. 2008 Sep 2;3:12.

122. Jayapal SR, Kaldis P. Cyclin E1 regulates hematopoietic stem cell quiescence. Cell Cycle. 2013 Oct 28;12(23).

123. Sun A, Bagella L, Tutton S, Romano G, Giordano A. From G0 to S phase: A view of the roles played by the retinoblastoma (rb) family members in the rb-E2F pathway. J Cell Biochem. 2007 Dec 15;102(6):1400-4.

124. Giacinti C, Giordano A. RB and cell cycle progression. Oncogene. 2006 Aug 28;25(38):5220-7.

125. Nathan CO, Carter P, Liu L, Li BD, Abreo F, Tudor A, et al. Elevated expression of eIF4E and FGF-2 isoforms during vascularization of breast carcinomas. Oncogene. 1997 Aug 28;15(9):1087-94.

126. Wu M, Liu Y, Di X, Kang H, Zeng H, Zhao Y, et al. EIF4E over-expresses and enhances cell proliferation and cell cycle progression in nasopharyngeal carcinoma. Med Oncol. 2013 Mar;30(1):400,012-0400-z. Epub 2013 Jan 1.

127. Cohen N, Sharma M, Kentsis A, Perez JM, Strudwick S, Borden KL. PML RING suppresses oncogenic transformation by reducing the affinity of eIF4E for mRNA. EMBO J. 2001 Aug 15;20(16):4547-59.

128. Culjkovic B, Topisirovic I, Skrabanek L, Ruiz-Gutierrez M, Borden KL. eIF4E promotes nuclear export of cyclin D1 mRNAs via an element in the 3'UTR. J Cell Biol. 2005 Apr 25;169(2):245-56.

129. Oberley TD, Schultz JL, Li N, Oberley LW. Antioxidant enzyme levels as a function of growth state in cell culture. Free Radic Biol Med. 1995 Jul;19(1):53-65.

130. Saxena U, Powell C, Fecko J, Cacioppo R, Chou H, Cooper G, et al. Phosphorylation by cyclin C/cyclin-dependent kinase 2 following mitogenic stimulation of murine fibroblasts inhibits transcriptional activity of LSF during G1 progression. Mol Cell Biol. 2009;9:2335,-45.

131. Rosenwald IB, Lazaris-Karatzas A, Sonenberg N, Schmidt EV. Elevated levels of cyclin D1 protein in response to increased expression of eukaryotic initiation factor 4E. Mol Cell Biol. 1993 Dec;13(12):7358-63.

132. Rousseau D, Gingras AC, Pause A, Sonenberg N. The eIF4E-binding proteins 1 and 2 are negative regulators of cell growth. Oncogene. 1996 Dec 5;13(11):2415-20.

133. Nelsen CJ, Rickheim DG, Timchenko NA, Stanley MW, Albrecht JH. Transient expression of cyclin D1 is sufficient to promote hepatocyte replication and liver growth in vivo. Cancer Res. 2001 Dec 1;61(23):8564-8.

134. Albrecht JH, Hansen LK. Cyclin D1 promotes mitogen-independent cell cycle progression in hepatocytes. Cell Growth Differ. 1999 Jun;10(6):397-404.

135. Carroll M, Borden KL. The oncogene eIF4E: Using biochemical insights to target cancer. J Interferon Cytokine Res. 2013 May;33(5):227-38.

136. DeFatta RJ, Turbat-Herrera EA, Li BD, Anderson W, De Benedetti A. Elevated expression of eIF4E in confined early breast cancer lesions: Possible role of hypoxia. Int J Cancer. 1999 Feb 9;80(4):516-22.

137. Rosenwald IB, Chen JJ, Wang S, Savas L, London IM, Pullman J. Upregulation of protein synthesis initiation factor eIF-4E is an early event during colon carcinogenesis. Oncogene. 1999 Apr 15;18(15):2507-17.

138. Culjkovic B, Borden KL. Understanding and targeting the eukaryotic translation initiation factor eIF4E in head and neck cancer. J Oncol. 2009;2009:981679.

139. Ladha MH, Lee KY, Upton TM, Reed MF, Ewen ME. Regulation of exit from quiescence by p27 and cyclin D1-CDK4. Mol Cell Biol. 1998 Nov;18(11):6605-15.

140. Campaner S, Viale A, De Fazio S, Doni M, De Franco F, D'Artista L, et al. A non-redundant function of cyclin E1 in hematopoietic stem cells. Cell Cycle. 2013 Sep 25;12(23).

141. Evertts AG, Manning AL, Wang X, Dyson NJ, Garcia BA, Coller HA. H4K20 methylation regulates quiescence and chromatin compaction. Mol Biol Cell. 2013 Oct;24(19):3025-37.

142. Li L, Bhatia R. Stem cell quiescence. Clin Cancer Res. 2011 Aug 1;17(15):4936-41.

143. Wang ZM, Yang H, Livingston DM. Endogenous E2F-1 promotes timely G0 exit of resting mouse embryo fibroblasts. Proc Natl Acad Sci U S A. 1998 Dec 22;95(26):15583-6.

144. Wyke AW, Frame MC, Gillespie DA, Chudleigh A, Wyke JA. Mitogenesis by v-src: Fluctuations throughout G1 of classical immediate early AP-1 and mitogen-activated protein kinase responses that parallel the need for the oncoprotein. Cell Growth Differ. 1995 Oct;6(10):1225-34.

145. Yusuf I, Fruman DA. Regulation of quiescence in lymphocytes. Trends Immunol. 2003 Jul;24(7):380-6.

146. Bondi J, Husdal A, Bukholm G, Nesland JM, Bakka A, Bukholm IR. Expression and gene amplification of primary (A, B1, D1, D3, and E) and secondary (C and H) cyclins in colon adenocarcinomas and correlation with patient outcome. J Clin Pathol. 2005 May;58(5):509-14.

147. Keenan SM, Lents NH, Baldassare JJ. Expression of cyclin E renders cyclin D-CDK4 dispensable for inactivation of the retinoblastoma tumor suppressor protein, activation of E2F, and G1-S phase progression. J Biol Chem. 2004 Feb 13;279(7):5387-96.

148. Jacobson BA, Thumma SC, Jay-Dixon J, Patel MR, Dubear Kroening K, Kratzke MG, et al. Targeting eukaryotic translation in mesothelioma cells with an eIF4E-specific antisense oligonucleotide. PLoS One. 2013 Nov 18;8(11):e81669.

149. Tan A, Bitterman P, Sonenberg N, Peterson M, Polunovsky V. Inhibition of myc-dependent apoptosis by eukaryotic translation initiation factor 4E requires cyclin D1. Oncogene. 2000 Mar 9;19(11):1437-47.

150. Zhang T, Liu WD, Saunee NA, Breslin MB, Lan MS. Zinc finger transcription factor INSM1 interrupts cyclin D1 and CDK4 binding and induces cell cycle arrest. J Biol Chem. 2009 Feb 27;284(9):5574-81.